

Matrix product states and projected entangled pair states: Concepts, symmetries, theorems

J. Ignacio Cirac 

*Max-Planck-Institut für Quantenoptik, Hans-Kopfermann-Straße 1,
85748 Garching, Germany
and Munich Center for Quantum Science and Technology,
Schellingstraße 4, 80799 München, Germany*

David Pérez-García 

*Departamento de Análisis Matemático, Universidad Complutense de Madrid,
Plaza de Ciencias 3, 28040 Madrid, Spain
and ICMAT, Nicolas Cabrera, Campus de Cantoblanco,
28049 Madrid, Spain*

Norbert Schuch 

*Max-Planck-Institut für Quantenoptik, Hans-Kopfermann-Straße 1,
85748 Garching, Germany,
Munich Center for Quantum Science and Technology,
Schellingstraße 4, 80799 München, Germany,
University of Vienna, Faculty of Physics, Boltzmannngasse 5, 1090 Wien, Austria,
and University of Vienna, Faculty of Mathematics,
Oskar-Morgenstern-Platz 1, 1090 Wien, Austria*

Frank Verstraete

*Department of Physics and Astronomy, Ghent University,
Krijgslaan 281, S9, 9000 Gent, Belgium*

 (published 17 December 2021)

The theory of entanglement provides a fundamentally new language for describing interactions and correlations in many-body systems. Its vocabulary consists of qubits and entangled pairs, and the syntax is provided by tensor networks. How matrix product states and projected entangled pair states describe many-body wave functions in terms of local tensors is reviewed. These tensors express how the entanglement is routed, act as a novel type of nonlocal order parameter, and the manner in which their symmetries are reflections of the global entanglement patterns in the full system is described. The manner in which tensor networks enable the construction of real-space renormalization group flows and fixed points is discussed, and the entanglement structure of states exhibiting topological quantum order is examined. Finally, a summary of the mathematical results of matrix product states and projected entangled pair states, highlighting the fundamental theorem of matrix product vectors and its applications, is provided.

DOI: [10.1103/RevModPhys.93.045003](https://doi.org/10.1103/RevModPhys.93.045003)

CONTENTS

I. Introduction	2	3. Correlations, entanglement, and the transfer matrix	14
A. Setting	2	a. Matrix product states	14
B. History	4	b. PEPSs	14
C. Outline	6	4. Extension to fermionic, continuous, and infinite tensor networks	15
II. Many-Body Quantum Systems: Entanglement and Tensor Networks	7	a. Fermionic tensor networks	15
A. Entanglement structure in quantum Hamiltonians	7	b. Continuous MPSs	15
1. Local reduced density matrices	8	c. Infinite MPSs	16
2. Area laws for the entanglement entropy	8	5. Tensor networks as quantum circuits: Tree tensor states and MERAs	16
B. Tensor networks	10	C. The ground state manifold of local Hamiltonians	16
1. MPSs and PEPSs	10	1. States to Hamiltonians: Parent Hamiltonians	17
2. MPOs and PEPOs	12	2. Hamiltonians to states	17

a. Area laws and approximability	18	b. Normality, injectivity, and unique ground states	49
b. No low tensor rank ansatz	18	c. Block injectivity, entanglement symmetries, and degenerate ground spaces	51
c. Efficient descriptions in thermal equilibrium	18	d. Converse: MPS ground states for frustration-free Hamiltonians	51
d. Many-body localization	19	2. Gaps	52
3. Manifold of MPSs and the time-dependent variational principle (TDVP)	20	a. The martingale method	52
a. Manifold and the TDVP	20	b. The Knabe bound	52
b. Excitations	20	3. Stability	53
D. Bulk-boundary correspondences	21	a. The LTQO condition	53
1. Entanglement spectrum	22	b. Stability in one dimension	53
2. Boundary theory	22	c. Stability in two dimensions	53
3. Edge theory	23	d. Perturbations of the tensor	53
E. Renormalization and phases of matter	24	4. Alternative Hamiltonians	54
1. Renormalization fixed points in MPSs	24	a. Product vacua with boundary states (PVBS)	54
2. MPDOs	25	b. Uncle Hamiltonians	54
3. Tree tensor states and MERAs	26	V. Conclusions	54
4. RG in higher dimensions	27	Acknowledgments	55
5. The limit to the continuum	28	Appendix: Examples	56
III. Symmetries and Classification of Phases	28	1. One dimension: MPSs	56
A. Symmetries in one dimension: MPSs	28	a. Product states	56
1. Symmetric MPSs	28	b. The GHZ state	56
2. SPT phases and edge modes	30	c. The W state	56
a. Symmetry-protected topological order	30	d. The cluster state	56
b. Entanglement spectrum and edge modes	31	e. The AKLT state	56
c. String order parameters for SPT phases	32	f. The Majumdar-Ghosh model	56
3. Symmetry breaking: Virtual symmetries, Lieb-Schultz-Mattis theorem, Kramers theorem, and topological excitations	32	2. Two dimensions: PEPSs	57
a. Virtual symmetries	32	a. The GHZ state	57
b. SET phases	33	b. The cluster state	57
c. Kramers and Lieb-Schultz-Mattis theorems	33	c. The AKLT model	57
d. Topological excitations: Domain walls and spinons	34	d. The RVB state	57
4. Fermions and the Majorana chain	34	e. The toric code and quantum double models	57
5. Gauge symmetries	35	f. String-net models	57
6. Critical spin systems: MPO symmetries	35	g. PEPSs from classical models	58
a. MPO algebras	35	h. The CZX model	58
b. MPO symmetries	37	3. Fermionic MPSs and PEPSs	58
B. Symmetries in two dimensions: PEPSs	38	a. The Kitaev chain	58
1. Symmetric PEPSs	39	b. Free fermionic and chiral PEPSs	58
a. Injective PEPSs	39	4. MPOs and MPUs	59
b. Noninjective PEPSs: SPT phases	39	a. The CZX MPU	59
c. Virtual symmetries	40	b. The shift MPU	60
d. SET phases	41	c. The MPO for the Fibonacci model	60
e. Chiral phases	41	References	60
2. Entanglement spectrum and edge Modes	42		
a. Entanglement Hamiltonians	42		
b. Edge modes	43		
3. Topological sectors and anyons	43		
a. Topological sectors	43		
b. Anyons	44		
c. Anyon condensation	45		
IV. Formal Results: Fundamental Theorems and Hamiltonians	46		
A. The fundamental theorem of matrix product vectors	46		
1. Overview	46		
2. Canonical form and normal tensors	46		
3. Basis of normal tensors	47		
4. Fundamental theorem of MPVs	48		
B. Fundamental theorems for PEPSs	48		
C. Hamiltonians	49		
1. Parent Hamiltonians and ground space	49		
a. Construction of the parent Hamiltonian	49		

I. INTRODUCTION

A. Setting

The many-body problem has been the central problem in physics over the last 150 years. Starting with the discovery of statistical physics, it was realized that systems with symmetries and many constituents exhibit phase transitions, and that those phase transitions are mathematically described by nonanalyticities in thermodynamic quantities when one takes the limit of the system size to infinity. Quantum mechanics added a new level of complexity to the many-body problem due to the noncommutativity of the different terms in the Hamiltonian, but since the discovery of path integrals it has been realized that the equilibrium quantum many-body problem in d dimensions can be similar to the classical

many-body problem in $d + 1$ dimensions. The quantum many-body problem has been the main driving force in theoretical physics over the past century and led to a comprehensive framework for describing phase transitions in terms of effective field theories and the renormalization group. The central challenge of the many-body problem is to be able to predict the phase diagram for physical classes of microscopic Hamiltonians and to predict the associated relevant thermodynamic quantities, order parameters, and excitation spectra. A further challenge is to predict the associated nonequilibrium behavior in terms of quantities such as the structure factors, transport coefficients, and thermalization rates.

The main difficulty in many-body physics stems from the tensor product structure of the underlying phase space: the number of degrees of freedom scales exponentially in the number of constituents and/or size of the system. A central goal in theoretical physics is to find effective compressed representations of the relevant partition functions or wave functions in such a way that all thermodynamic quantities, including energy, magnetization, and entropy, can efficiently be extracted from that description. A particularly powerful method to achieve this has long since been perturbative quantum field theory: the many-body problem is readily solvable for interaction-free systems in terms of Gaussians, and information about the interactive system can then be obtained by perturbing around the best free approximation of the system. This approach works well for weakly interacting systems but can break down when the system undergoes a phase transition driven by the interactions. The method of choice for describing phase transitions is the renormalization group introduced by Wilson (1975): here one makes an informed guess of an effective field theory describing the system of interest and then performs a renormalization group flow into the space of actions or Hamiltonians by integrating out the high-energy degrees of freedom. In the case of gapped systems, such a procedure leads to a fixed-point structure described by topological quantum field theory. The full power of this method is revealed when applied to gapless critical systems, where it is able to predict universal information such as the possible critical exponents at phase transitions. However, the renormalization group is not well suited to predict the quantitative information needed for simulating a given microscopic Hamiltonian and has severe limitations in the strong coupling regime, where it is not clear how to integrate out the high-energy degrees of freedom without getting a proliferation of unwanted terms. To address those shortcomings, a wide variety of exact and computational methods have been devised.

In the case of two-dimensional classical spin systems and one-dimensional quantum spin systems and field theories, major insights into the interacting many-body problem have been obtained due to the discovery of integrable systems. Integrable systems have an extensive amount of quasilocal conservation laws, and the Bethe ansatz exploits this to construct classes of wave functions that exactly diagonalize the corresponding Hamiltonians or transfer matrices. The solution of those integrable systems was crucial. On the one hand, it showcased the inadequacy of Landau's theory of phase transitions for interacting systems and motivated the

development of the renormalization group. On the other hand, it showed that the collective behavior of many bodies, such as spinons, exhibits interesting emergent phenomena of a completely different nature than the underlying microscopic degrees of freedom. When perturbing Bethe ansatz solutions and moving to higher dimensions, it is *a priori* not clear how much of the underlying structure survives. There are strong similarities between the Bethe ansatz and tensor networks, and tensor networks can in essence be interpreted as a systematic way of extending that framework to generic nonintegrable systems.

Computational methods have also played an important role in unraveling fascinating aspects of the many-body problem. Results of exact diagonalization assisted by finite-size scaling results originating from conformal field theory have allowed simulations of a wide variety of spin systems. However, the exponential wall is prohibitive in scaling up those calculations to reasonably sized systems for all but the simplest systems, especially in higher dimensions. A scalable computational method for classical equilibrium problems is given by Monte Carlo sampling: experience has taught us that typical relevant Gibbs states have special properties that allow one to set up rapidly converging Markov chains to simulate a variety of local thermodynamic quantities of those systems. This is also possible for quantum systems provided that the associated path integral does not have the so-called sign problem. However, this sign problem shows up in many systems of interest, especially in the context of frustrated magnets and systems with fermions. A powerful and scalable solution to overcome this problem is to resort to the variational method: here the goal is to define a low-dimensional manifold in the exponentially large Hilbert space such that the relevant states of the system of interest are well approximated by states in that manifold.

The most well-known variational class of wave functions is given by the class of Slater determinants, and the corresponding variational method is called the Hartree-Fock theory. This method works excessively well for weakly interacting systems, and perturbation theory around the extrema can be done in terms of Feynman diagrams or by coupled cluster theory. Dynamical information can also be obtained by invoking the time-dependent variational principle, which can be understood as a least squares projection of the full Hamiltonian evolution on the variational manifold of Slater determinants. Alternatively, the Hartree-Fock method can be rephrased as a mean field theory, and dynamical mean field theory extends it by modeling the interaction of a cluster with the rest of the system as a set of self-consistent equations of the cluster and a free bath. Although this approach works well in three dimensions, it is not clear how generally applicable it is to lower-dimensional systems. One of the main difficulties for variational methods based on free systems is the fact that the natural basis for free systems is the momentum basis: plane waves diagonalize free Hamiltonians, but the natural basis for systems with strong interactions is the position basis and a phase transition separates both regimes.

This brings us to the concept of tensor networks: tensor networks are a variational class of wave function that allows one to model ground states of strongly interacting systems in position space in a systematic way. As in the case of (post-) Hartree-Fock methods, the starting point is a low-dimensional

variational class in the exponentially large Hilbert space. This manifold seems to capture a rich variety of quantum many-body states that are ground states of local quantum Hamiltonians for both cases of spins, bosons and fermions. The defining character of states that can be represented as tensor networks is the fact that they exhibit an area law for the entanglement entropy. Time-dependent information can be obtained by applying the time-dependent variational principle on the manifold of tensor networks, and spectral information is obtained by projecting the full many-body Hamiltonian on tangent spaces of the manifold. The tensor network description can be understood as a compression of the Euclidean path integral as used in quantum Monte Carlo calculations, but then without a sign problem. Both the coordinate and algebraic Bethe ansatz can be reformulated in terms of tensor networks, and tensor networks allow for a systematic exploration of those methods that are beyond the integrable regime and $1 + 1$ dimensions. Critical properties can be extracted in terms of finite entanglement scaling arguments, and tensor networks allow for a natural formulation of a real-space renormalization group procedure, as originally envisioned by Kadanoff. It also turns out that tensor networks provide representations for ground states of a wide class of Hamiltonians exhibiting topological order, hence being many-body realizations of topological quantum field theories (TQFTs), and provide a natural language for describing the corresponding elementary excitations (anyons) and braiding properties by providing explicit representations of associated tensor fusion algebras.

Tensor networks can hence be understood as a symbiosis of a wide variety of theoretical and computational many-body techniques. From our point of view, the most interesting aspect of this is that it imposes a new way of looking at quantum many-body systems: tensor networks elucidate the need of describing interacting quantum many-body systems in terms of the associated entanglement degrees of freedom, and the essence of classifying phases of matter and understanding their essential differences is encoded in the different symmetries of the tensors that realize that entanglement structure. In many ways, tensor networks provide a constructive implementation of the following vision of Feynman (1988):

“Now, in field theory, what’s going on here and what’s going on over there and all over space is more or less the same. Why do we have to keep track in our functional of all the things that are going on over there while we are looking at the things that are going on over here? [...] It’s really quite insane, actually: we are trying to find the energy by taking the expectation of an operator which is located here and we present ourselves with a functional which is dependent on everything all over the map. That’s something wrong. Maybe there is some way to surround the object, or the region where we want to calculate things, by a surface and describe what things are coming in across the surface. It tells us everything that’s going on outside. [...] I think it should be possible some day to describe field theory in some other way than with the wave functions and amplitudes. It might be something like the density

matrices where you concentrate on quantities in a given locality and in order to start to talk about it you don’t immediately have to talk about what’s going on everywhere else [...]”

Tensor networks precisely associate a tensor product structure to interfaces between different regions in space, and the fact that such an interface is always of a dimension smaller than the original space is a manifestation of the area law for the entanglement entropy. In the case of one-dimensional quantum spin chains and quantum field theories, this virtual Hilbert space is zero dimensional, and the different symmetry-protected topological (SPT) phases of matter can be understood in terms of inequivalent ways in which the symmetries act on that Hilbert space. For two-dimensional systems, the interface is one dimensional and provides an explicit local representation for both the entanglement Hamiltonian and the edge modes as they appear in topological phases of matter.

The central goal of this review is to explain how tensor networks describe many-body systems from this entanglement point of view, and why it is reasonable to do so. Recurring themes are that the manifold of tensor network states parametrizes a wide class of ground states of strongly interacting systems and that all the relevant global information of the wave function is encoded in a single local tensor that connects the physical degrees of freedom to the virtual ones (that is, the entanglement degrees of freedom). This review does not touch upon variational algorithms for optimizing tensor networks, as those topics were covered by Verstraete, Murg, and Cirac (2008), Schollwöck (2011), Orus (2014), Bridgeman and Chubb (2017), and Haegeman and Verstraete (2017). For further reading on the more traditional approaches to the quantum many-body problem, as previously discussed, see Chaikin, Lubensky, and Witten (1995), Wen (2004), Shavitt and Bartlett (2009), Avella and Mancini (2011), Fradkin (2013), Becca and Sorella (2017), Anderson (2018), and Girvin and Yang (2019).

B. History

We start with a review of the historic development of the field of tensor networks. This is complemented by an outlook on ongoing developments and newly evolving directions in Sec. V.

Nishino (2010) traced the history of tensor networks back to the work of Kramers and Wannier (1941). They studied the 2D classical Ising model and introduced the concept of transfer matrices (which are simply matrix product operators in the language of this review) and a variational method for finding the leading eigenvector of it by optimizing over a class of wave functions that can be interpreted as precursors of matrix product states (MPSs). Much later Baxter (1968, 1981, 2007) introduced the formalism of corner transfer matrices and realized that the concept of matrix product states allows one to make perturbative calculations of thermodynamic quantities of classical spin systems to high order; to prove his point, he calculated the hard square entropy constant to 42 digits of precision. Accardi (1981) introduced matrix product states in the realm of quantum mechanics by describing

the wave functions associated with quantum Markov chains. The most well-known matrix product state was introduced by [Affleck *et al.* \(1987\)](#), [the Affleck-Kennedy-Lieb-Tasaki (AKLT) state] in an effort to provide evidence for the Haldane conjecture concerning half integer versus integer spin Heisenberg models. They also wrote a two-dimensional analog of the AKLT state ([Affleck *et al.*, 1988](#)), and provided evidence that it was the ground state of a gapped parent Hamiltonian. Fannes, Nachtergaele, and Werner realized that the 1D AKLT state was part of a much larger class of many-body states, and they introduced a class of finitely correlated states (FCS) that corresponds to injective matrix product states. In a series of groundbreaking papers, they proved that all FCS are unique ground states of local gapped parent Hamiltonians and derived a wealth of interesting properties by exploiting the connection of MPS to quantum Markov chains ([Fannes, Nachtergaele, and Werner, 1989, 1991, 1992a, 1992b, 1994, 1996](#)).

Independent of this work in mathematical physics, [White \(1992, 1993\)](#) discovered a powerful algorithm for simulating quantum spin chains, which he called the density matrix renormalization group (DMRG). DMRG revolutionized the way quantum spin chains can be simulated and provided extremely accurate results for associated ground and excited state energies and order parameters. [Nishino and Okunishi \(1996\)](#) soon discovered interesting parallels between DMRG and the corner transfer matrix method of [Baxter \(1981\)](#). Although it was certainly not envisioned and formulated like that, it turns out that DMRG is a variational algorithm in the set of matrix product states ([Östlund and Rommer, 1995; Dukelsky *et al.*, 1998; Verstraete, Porras, and Cirac, 2004](#)). The reason for the success of DMRG was not understood until much later, when it became clear that ground states of local gapped Hamiltonians exhibit an area law for the entanglement entropy ([Hastings, 2007](#)), and that all states exhibiting such an area law can be faithfully and efficiently represented as matrix product states ([Verstraete and Cirac, 2006](#)). The family of matrix product states was rediscovered multiple times in the community of quantum information theory. [Vidal \(2003\)](#) first devised an efficient algorithm for simulating a quantum computation that produces at most a constant amount of entanglement; it turns out that the same algorithm can be reinterpreted as a time-dependent version of DMRG, thereby opening up an entire new set of applications for DMRG ([Daley *et al.*, 2004; Verstraete, Garcia-Ripoll, and Cirac, 2004; White and Feiguin, 2004; Vidal, 2007a](#)).

From the point of view of entanglement theory, matrix product states were rediscovered in the context of quantum repeaters, where it was understood that degeneracies in the entanglement spectrum such as those occurring in the AKLT model lead to novel length scales in quantum spin systems, as quantified by the localizable entanglement ([Verstraete, Martin-Delgado, and Cirac, 2004; Verstraete, Popp, and Cirac, 2004](#)). A fundamental structure theorem for matrix product states ([Perez-Garcia, Wolf *et al.*, 2008; Cirac *et al.*, 2017a; Molnar, Garre-Rubio *et al.*, 2018](#)) clarified that such degeneracies are the consequence of the presence of projective representations in the manner in which the entanglement degrees of freedom transform under physical symmetries, and this led to the classification of all possible SPT phases for 1D

quantum spin systems ([Chen, Gu, and Wen, 2011a; Schuch, Perez-Garcia, and Cirac, 2011; Pollmann *et al.*, 2012](#)).

Soon after the study of localizable entanglement in matrix product states in 2003, a two-dimensional version of MPS was introduced, and it was realized that the entanglement degrees of freedom can play a fundamental role by demonstrating that measurement-based quantum computation ([Raussendorf and Briegel, 2001](#)) proceeds by effectively implementing a standard quantum circuit on those virtual degrees of freedom ([Verstraete and Cirac, 2004b](#)). Those states were subsequently called projected entangled pair states (PEPSs), and it was quickly understood that the corresponding variational class provides the natural generalization of MPSs to two dimensions in the sense that they parametrize states exhibiting an area law and that there is a systematic way of increasing the bond dimension, i.e., the number of variational parameters ([Verstraete and Cirac, 2004a](#)). Subclasses of PEPSs had been considered previously: the 2D AKLT state was studied by [Affleck *et al.* \(1988\)](#); Richter and Werner ([Richter, 1994](#)) introduced and studied a 2D generalization of FCS based on isometric tensors; [Niggemann, Klümper, and Zittartz \(1997\)](#) studied 2D PEPS where the tensors satisfied the Yang-Baxter equation; and [Sierra and Martin-Delgado \(1998\)](#), [Maeshima *et al.* \(2001\)](#), and [Nishino *et al.* \(2004\)](#) introduced a generalization of MPSs to two dimensions where the tensors could be interpreted as Boltzmann weights of a vertex model.

As in the 1D case, entanglement theory was the key to formulating this ansatz in full generality. This led to the introduction of variational matrix product state algorithms for optimizing PEPSs ([Verstraete and Cirac, 2004a](#)) and infinite versions of them ([Jordan *et al.*, 2008](#)). It was found that PEPSs form a rich class of wave functions, and a plethora of interesting quantum spin liquid states were written in terms of PEPS tensors: the resonating valence bond (RVB) states of Anderson, the toric code state of Kitaev, and any ground state of a local frustration-free commuting quantum Hamiltonian ([Verstraete *et al.*, 2006](#)), such as any ground state of stabilizer Hamiltonians ([Verstraete and Cirac, 2004b](#)) or string nets ([Buerschaper, Aguado, and Vidal, 2009](#)). [Gu, Levin, and Wen \(2008\)](#) and [Gu and Wen \(2009\)](#) realized that the local symmetries of the tensors are of primordial importance for describing long-range topological order, and [Schuch, Perez-Garcia, and Cirac \(2011\)](#) formalized this using the important concept of G -injectivity and later by the more general concept of matrix product operator (MPO) injectivity ([Bultinck, Mariën *et al.*, 2017; Şahinoğlu *et al.*, 2021](#)). This opened the way to simulating systems exhibiting topological quantum order and the associated anyons in terms of tensor networks. Similarly, tensor networks and the associated local symmetries turned out to provide a natural language for describing SPT phases in two dimensions ([Chen *et al.*, 2013; Buerschaper, 2014; Williamson *et al.*, 2016](#)).

In a separate development, [Vidal \(2007b, 2008\)](#) discovered the multiscale entanglement renormalization ansatz (MERA). This generalizes tree tensor networks (TTNs), which represent yet another type of tensor network that naturally arises in the context of real-space renormalization ([Fannes, Nachtergaele, and Werner, 1992c; Shi, Duan, and Vidal, 2006; Murg *et al.*, 2010; Silvi *et al.*, 2010](#)). Unlike MPSs, MERAs and TTNs are meant to describe scale-invariant wave functions, and capture the scale invariance exhibited in conformally invariant

theories by a real-space construction of scale-invariant tensors. The full richness of MERAs is only starting to be explored, but interesting connections with anti-de Sitter/conformal field theory (AdS/CFT) and operator product expansions (Pfeifer, Evenbly, and Vidal, 2009; Evenbly and Vidal, 2016) have been uncovered. We discuss here only a few limited aspects of MERAs in the context of the holographic principle and renormalization; see Evenbly and Vidal (2014) for a full review. Finally, we remark that ideas from renormalization have also led to a range of renormalization-based algorithms for tensor network contraction, such as the tensor renormalization group, the tensor entanglement renormalization group, and tensor network renormalization (Levin and Nave, 2007; Gu, Levin, and Wen, 2008; Jiang, Weng, and Xiang, 2008; Xie *et al.*, 2009, 2012; Zhao *et al.*, 2010; Evenbly and Vidal, 2015; Evenbly, 2017).

C. Outline

There is already an extensive literature on the application of the different kind of tensor networks (TNs) to quantum many-body systems. While there are many reviews on the topic (Schollwöck, 2005, 2011; Hallberg, 2006; Cirac and Verstraete, 2009; Orus, 2014; Bridgeman and Chubb, 2017; Biamonte, 2019), the vast majority focus on the practical aspects of tensor networks, in particular, on how to use them in numerical computations in order to approximate ground, thermal equilibrium, or dynamical states corresponding to Hamiltonians defined on lattices. However, as previously emphasized, tensor networks have also been key to the description, or even the discovery, of a wide variety of physical phenomena, as well as to construct simple examples displaying interesting properties. This was achieved through the development of a theory of tensor networks. We review such a theory here, including both core results and their applications.

We concentrate here on translational-invariant systems in one- and two-dimensional lattices since most of the analytical results have been obtained for such systems. We notice, however, that many of the results covered in this review extend naturally to higher spatial dimensions, other lattice geometries, and also the non-translational-invariant case. This restriction, in the context of TNs, implies that a single tensor A encapsulates the physical properties of the many-body system. As we later see, quantum states as well as operators (such as those characterizing mixed states, Hamiltonians, or dynamics) are constructed in terms of such tensors. For states (operators), the restriction to translationally invariant systems also implies that our focus in this review will be on MPSs (MPOs) and PEPSs (projected entangled pair operators, or PEPOs). The basic questions that we address are as follows: Is this construction unique; that is, can two tensors give rise to the same state or operator? If they do, what is the relation between those tensors? How are the physical properties of the states encoded in the tensor? For instance, how do the local symmetries of the tensors reflect local and/or global symmetries or topological order? Or, vice versa, how are the symmetries in the tensor reflected in the physical properties of the many-body state, or in the dynamics that it describes? There are many other questions about tensor networks that have been resolved in recent years, and it would be impossible

to cover them in detail in this review. We nevertheless go over most of them and give the original references where they can be found. In addition, the interested reader may want to consult Zeng *et al.* (2019), which complements this review in many aspects.

This review is organized in four sections and the [Appendix](#). Section II motivates the use of TNs to describe quantum many-body systems, introduces different TNs, and analyzes some of the most relevant properties. The basic structure of TNs stems from the entanglement structure of the ground states of many-body Hamiltonians fulfilling an area law, which basically dictates that they exhibit little entanglement relative to typical states. Tensor networks provide us with efficient ways of describing systems with small amounts of entanglement, and they are thus ideally suited for parametrizing states satisfying an area law. We introduce the basic notions of MPSs for 1D systems, and their generalization to higher dimensions PEPSs. We also consider the fermionic versions of those TN states, where the physical systems are fermionic modes. While most of the review concerns pure states, we include some analysis of mixed states and evolution operators, and for that purpose we also introduce MPOs and PEPOs. Even though we focus our attention on translational-invariant systems, we do mention some connections between MPSs and MERAs, as they both can be viewed as being created by special quantum circuits. We also argue that, not only do MPSs and PEPSs approximate ground states of local Hamiltonians, but for any of them one can find a special Hamiltonian or set of Hamiltonians, the so-called parent Hamiltonians, that are frustration free and for which they are the exact ground states. In particular, we list the conditions under which the Hamiltonian is degenerate, and also discuss how to describe low-energy excitations. Next we discuss an interesting property of PEPSs, namely, that one can explicitly build a bulk-boundary correspondence with them. That is, for any region of space it is always possible to define a state that encodes all the physical properties of the first but lives in a smaller spatial dimension. This is a version of the holographic principle and enables the use of dimensional reduction, meaning that one can fully characterize the properties of PEPSs by a theory that is defined in the boundary. We finish Sec. II by introducing a powerful technique in the TN context, namely, renormalization. The basic idea is to block tensors into others that can be assigned to blocks of spins, in much the same way as real-space renormalization is used in statistical physics. The fixed point of such a procedure gives rise to a special TN that can be viewed like the ones that appear if one looks at large scales. They have a simple form, so one can easily deal with them and apply them, for instance, to the classification of phases of gapped Hamiltonians. This procedure can be applied to pure or mixed states, as well as unitary operators.

Section III analyzes how the symmetries of the tensor generating a MPS or PEPS can be associated with the symmetries of the states that they generate, or with their topological order. This statement leads to one of the greatest successes of tensor networks, namely, the classification of phases by relating them to the representations of the symmetries of the tensors generating them. In the case of global symmetries, this leads to SPT phases, whereas topological

phases are characterized by purely virtual symmetries. The combination of those results can also be used to characterize symmetry-enriched topological (SET) phases for TN. Attending to the global symmetries of the states with a certain symmetry group, we find that the generating tensor also possess that symmetry, with the same symmetry group but with a representation that is possibly projective. This is why the classification of SPT phases is intimately related to the corresponding cohomology classes. Topological order, however, is related to purely virtual symmetries of the tensor, and we discuss how those virtual symmetries give rise to notions such as topological entanglement entropy and anyons. We also consider local gauge symmetries and ways of gauging a global into a local symmetry within the language of TNs.

Section IV is more mathematical and contains a review of the basic theorems of MPSs and PEPSs. Of particular importance is the so-called fundamental theorem, which lists the conditions under which two tensors generate the same state. This theorem is widely used in many of the analytical results obtained for TNs, such as in the characterization of the fixed points of the renormalization procedure of Sec. II, and in the classification of symmetries and phases in Sec. III. It implies that the same states can be generated by many tensors, so it is useful to find a canonical form, namely, a specific property of the tensor that we can demand such that it is basically uniquely associated with the state. While this is possible for MPSs and a full theory for such a canonical form and fundamental theorem exists, the situation for PEPSs is not yet complete and we discuss the state of the art.

Finally, we collect a number of prototypical examples of MPSs and PEPSs appearing in the context of quantum information and/or condensed matter theory in the Appendix.

II. MANY-BODY QUANTUM SYSTEMS: ENTANGLEMENT AND TENSOR NETWORKS

A. Entanglement structure in quantum Hamiltonians

A central feature of many-body quantum systems is the fact that the dimension of the associated Hilbert space scales exponentially large in the number of modes or particles in the system. The natural way of describing materials, atomic gases, or quantum field theories exhibiting strong quantum correlations is to discretize the continuous Hilbert space by defining a lattice and an associated tensor product structure for the modes that represent localized orbitals such as Wannier modes. Such systems can therefore be described in terms of an effective Hamiltonian acting on a tensor product of these local modes. In the case of bosons, one can typically restrict the local occupation number to be bounded (say, d dimensional), such that we get a Hilbert space of the form $\otimes_{k=1}^N C^d$. In the case of fermions, the tensor product has to be altered to a graded tensor product.

In this review, we mainly consider local translationally invariant quantum spin Hamiltonians defined on a lattice with the geometry of a ring or torus of the form

$$H = \sum_{i=1}^N h_{i,n},$$

where $h_{i,n}$ is a local observable centered at site i and acting nontrivially only on the $n - 1$ closest sites of i . As an example, a nearest-neighbor Hamiltonian such as the Heisenberg model has $n = 2$. As n is finite, it is always possible to block several sites together such that $h_{i,n}$ is acting only on next nearest neighbors according to the underlying lattice. We are mostly interested in the ground state and the lowest energy excitations of such a Hamiltonian in the thermodynamic limit $N \rightarrow \infty$.

The gap Δ plays an important role in such spin systems. It measures the energy difference of the first excited state and the ground state. If it vanishes in the thermodynamic limit $N \rightarrow \infty$, we say that the Hamiltonian is gapless and otherwise gapped. The former occurs for critical systems, whereas the latter implies the existence of a finite correlation length.

As in quantum field theories, the central object of interest in strongly correlated quantum spin systems is the ground state or vacuum, as the quantum features are most pronounced at low temperatures. The vacuum quantum fluctuations hold the key to unraveling the low temperature properties of the material of interest, and the structure of the ground state wave function dictates the features of the elementary excitations or particles that can be observed in experiments. Determining the smallest eigenvector of an exponentially large matrix is in principle an intractable problem. Even a relatively small system, such as a 2D Hubbard model with 12×12 sites, has a Hilbert space of dimension $2^{288} \approx 5 \times 10^{86}$, which is much larger than the number of baryons in the Universe, and hence writing down the ground state wave function as a vector is an impossible feat. The key that allows us to circumvent this impasse is to realize that the matrices corresponding to Hamiltonians of quantum spin systems are sparse due to the fact that they exhibit a tensor product structure and are defined as a sum of local terms with respect to this tensor product. This forces the ground state to have a special structure, and tensor networks are precisely constructed to take advantage of that structure. In addition, the locality of the Hamiltonian forces the other eigenvectors with low energy to be simple local perturbations of the ground state (Haegeman, Pirvu *et al.*, 2012), and this feature is responsible for the existence of localized elementary excitations, which we observe as particles, and hence for the fact that the ground state is such a relevant object even if the system under consideration is not at zero temperature. This has to be contrasted with a generic eigenvalue problem where knowledge of the extremal eigenvector does not give any information about the other eigenvectors, except for the fact that they are orthogonal to it. Without locality, physics would be wild.

The locality and tensor product properties of the Hamiltonians from which we want to determine the extremal eigenvectors are the keys to unraveling the structure of the corresponding wave functions. This tensor product structure and locality also play a central role in the field of quantum information (Nielsen and Chuang, 2000) and entanglement theory (Horodecki *et al.*, 2009), with the original aim of exploiting quantum correlations to perform novel information theoretic tasks. The study of entanglement theory introduced a new way of quantifying quantum correlations in terms of elementary units of entanglement (ebits), and of describing local operations that transform states into one another. A key insight in entanglement theory has been the fact that any pure

bipartite states with an equal amount of entanglement (as measured by the entanglement entropy) can be converted into each other by local quantum operations and classical communication (Bennett *et al.*, 1996). These fundamental facts of the theory of entanglement were the original inspiration for defining tensor networks: ground states of local Hamiltonians turn out to exhibit an area law for the entanglement entropy, just as entangled pairs of particles distributed among nearest neighbors on a lattice have. There should therefore exist local operations that transform the two sets of states into each other. This construction precisely gives rise to the classes of MPSs and PEPSs, which are the main characters of this review.

1. Local reduced density matrices

The energy of a wave function with respect to a local Hamiltonian is completely determined by its marginal or local reduced density matrices $\rho_{i,n}$, which are defined as the density matrix obtained by tracing out all degrees of freedom outside of the region n around site i : $E = \sum_i \text{Tr}[h_{i,n}\rho_{i,n}]$. In the case of a translationally invariant Hamiltonian and a unique ground state, the ground state inherits all symmetries of the Hamiltonian, including the translational invariance. Hence, we can drop the dependence on i and the ground state energy $\text{Tr}[h_n\rho_n]$ is a linear functional in the reduced density matrix ρ_n . Finding ground states is hence equivalent to finding a many-body state whose marginal is extremal with respect to h_n . The set of all possible marginals of translationally invariant quantum many-body states is convex. Any state whose marginal is an extreme point in this convex set must hence be the ground state of a local Hamiltonian defined by the tangent plane on that convex set. The ground state problem is therefore equivalent to characterizing the set of all possible extremal points of local reduced density matrices. The problem would hence be easily solved if such a characterization were possible, but this problem is known as the N -representability problem (Coleman, 1972) and is well known to be intractable for generic systems (Liu, Christandl, and Verstraete, 2007).

The important message, however is that ground states are special: they have extremal local reduced density matrices, and all the global features, such as correlation length, possible topological order, and types of elementary excitations, follow from this local extremality condition. In other words, these global features emerge from the requirement that the local reduced density matrix is an extreme point in the set of all possible reduced density matrices compatible with the symmetries of the system. It will turn out that these extremal points can correspond only to states with little entanglement, and all of them satisfy an area law for the entanglement entropy (Verstraete and Cirac, 2006; Zauner *et al.*, 2016).

It is instructive to consider the example of the Heisenberg spin-1/2 antiferromagnetic Hamiltonian $\sum_{\langle i,j \rangle} \vec{S}_i \cdot \vec{S}_j$, where the sum is restricted to nearest neighbors and $\vec{S} = (S_x, S_y, S_z)$ are the standard spin operators. If we consider only two sites, then the ground state is equal to the spin singlet, which is maximally entangled, and with the associated energy -1 . The case of a chain of N sites is much more complicated: due to the noncommutativity, it is impossible to find a state whose ground state energy is equal to -1 per interaction term.

This noncommutativity leads to frustration: the closer the reduced density matrix of sites 1 and 2 is to a singlet, the further it will have to be from a singlet for the reduced density matrices of sites 2 and 3. This effect can also be understood in terms of the monogamy property of entanglement (Terhal, 2004): a spin 1/2 has the capacity of only 1 ebit of entanglement [with an ebit defined as the amount of entanglement in a maximally entangled state of two spin-1/2 systems (Nielsen and Chuang, 2000)], and if it has to share this 1 ebit with its neighbors, the corresponding reduced density matrices will have at most 1/2 ebit of entanglement. The more neighbors that a spin has, the less entanglement it can share with each individual one. This can be formalized in the quantum de Finetti theorem and is the reason that mean field theory becomes exact in high-dimensional lattices (Raggio and Werner, 1989; Brandao and Harrow, 2016). This is also the reason that 1D and 2D systems exhibit some of the most interesting quantum effects: in general, the marginals of quantum many-body states in 3D lattices are already well approximated by the ones obtained by product or mean field solutions, while this is not the case for low-dimensional systems.

The physics of ground states is completely determined by the competition between translational invariance and extremal local reduced density matrices (for the case of the Heisenberg model, the density matrices will be as close as possible to the singlet). Monogamy of entanglement is precisely the property that gives rise to interesting physics: in the case of classical statistical mechanics, the competition of energy versus entropy gives rise to cooperative phenomena and phase transitions. In the quantum case, the noncommutativity of the different terms in the Hamiltonian leads to monogamy, which plays a similar role and makes such phase transitions possible at zero temperature.

The key to uncovering the structure of ground states of local Hamiltonians is to understand how the entanglement is shared between the different degrees of freedom. Intuitively, for a given spin it is of no use to have strong correlations with faraway spins, as this will only bring marginals farther away from the extremal points. The strongest quantum correlations it needs to have are with those spins that the Hamiltonian forces it to interact with, namely, the nearest neighbors. We can hence imagine that the entanglement between a bipartition of a large system in two regions is proportional to the surface between them, and this area law for entanglement is exactly what is going on in ground states.

In summary, ground states of local Hamiltonians of quantum spin systems are in one-to-one correspondence with states whose reduced density matrices are extremal points within the set of all possible reduced density matrices with a given translational symmetry. This property forces the entanglement to be localized, giving rise to an area law.

2. Area laws for the entanglement entropy

We now consider a quantum spin system with a local quantum Hamiltonian and ground state $|\psi\rangle$ and a bipartition of the quantum spin system into two connected regions A and B , such that ρ_A and ρ_B are the reduced density matrices of the ground state in these regions. The entanglement entropy (Bennett *et al.*, 1996)

$$S(\rho_A) = -\text{Tr}[\rho_A \log(\rho_A)] = S(\rho_B) \quad (1)$$

quantifies the amount of quantum correlations between the two regions and, as argued in the last section, this quantity is expected to be proportional to the surface of the boundary between the two regions ∂A , and hence called the area law for the entanglement entropy (Eisert, Cramer, and Plenio, 2010). This area law should be contrasted with the volume law exhibited by random states in the Hilbert space: quantum states exhibiting an area law for the entanglement entropy are special; such states are hence highly atypical, and it will be possible to represent them using tensor networks.

The origins of the area law can be traced back to studies of the entanglement entropy in free quantum field theories (Holzhey, Larsen, and Wilczek, 1994), where the ensuing area laws were related to the Bekenstein-Hawking black hole entropy (Bekenstein, 1973). Area laws can rigorously be demonstrated for free bosonic (Plenio *et al.*, 2005) and fermionic systems (Giovannelli and Klich, 2006; Wolf, 2006) modulo some logarithmic corrections in the presence of Fermi surfaces. They can also be proven in case the correlations (defined in terms of the mutual information) between two arbitrary regions decay sufficiently quickly with the distance regardless of their sizes (Wolf *et al.*, 2008).

For interacting quantum systems at finite temperature T and described by Gibbs states $\rho \propto \exp(-H/T)$, an area law for the mutual information

$$I(A:B) = S(\rho_A) + S(\rho_B) - S(\rho) \leq c \frac{|\partial A|}{T}$$

was proven by Wolf *et al.* (2008) for any local Hamiltonian in any dimension as long as all terms in the Hamiltonian are bounded from above. Here $|\partial A|$ denotes the number of spins in the boundary ∂A between region A and B . Recently Kuwahara, Alhambra, and Anshu (2021) improved the temperature dependence of this bound to diverge as $1/T^{2/3}$.

It is much harder to prove the area law for ground states of interacting quantum spin systems, although there is plenty of evidence supporting that claim. In the case of gapped quantum spin chains in one dimension, a noteworthy theorem was formulated by Hastings (2007) proving the area law that was later strengthened by Arad *et al.* (2013). Given a local Hamiltonian of a quantum spin chain of N d -dimensional spins whose gap is given by Δ , the entanglement entropy in the ground state is bounded from above by $\mathcal{O}((\log d)^3/\Delta)$ for any bipartite lattice cut into two connected regions; see Kuwahara and Saito (2020) for a generalization to long-range interactions. Note that this means that the entanglement entropy saturates in the thermodynamic limit for the case of a gapped system. In the case of a critical quantum spin chain where the gap vanishes as $\mathcal{O}(1/N)$ or faster, this bound yields a volume law, although it seems that nature is much more economical and, for all critical spin chains described by a conformal field or a Luttinger liquid theory, the actual entanglement entropy is exponentially smaller and scales as $\mathcal{O}(\log(L))$ for a region A of length $L \leq N/2$. When the gap is allowed to vanish must faster as a function of the system size, examples were constructed that saturate the volume law, and

hence give rise to novel phase transitions from bounded to extensive entanglement (Movassagh and Shor, 2016; Zhang, Ahmadain, and Klich, 2017).

Much more precise information about the nature of the entanglement in a system can be obtained by looking at the entanglement spectrum (Li and Haldane, 2008), which is defined as the logarithm of the set of eigenvalues of the reduced density matrix $\lambda_i(\rho_A)$. The Schmidt coefficients are the square roots of these eigenvalues, and the convention is to order them in decreasing order. In the case of gapped integrable spin chains in the thermodynamic limit, these Schmidt coefficients decay as $\exp(-an)$, where $n \in \mathbb{N}$, a is a constant, and a degeneracy $a(n)$ is equal to the number of ways to partition n in sums of unequal integers (Peschel, Kaulke, and Legeza, 1999). Asymptotically, we have $a(n) = \mathcal{O}(\exp(\pi\sqrt{n/3})/n^{3/4})$. This result can be obtained by calculating the eigenvalues of the corner transfer matrix, which is a discrete version of the boost operator H_{Mod} used in quantum field theory to calculate the entanglement entropy. For critical systems described by CFT, the largest Schmidt coefficient seems to encode the information about the full entanglement entropy (Orus *et al.*, 2006).

Alternatively, the Renyi entropies $S_\alpha(\rho) = [1/(1-\alpha)] \log \text{Tr}(\rho^\alpha)$ with $\alpha \geq 0$ can be used to characterize the decay of the Schmidt coefficients. These Renyi entropies are monotonically decreasing as a function of α ; $S_0(\rho)$ measures the rank of ρ , and the ones with $0 \leq \alpha < 1$ will be of particular importance for the description of matrix product states. Improving the results and techniques of Hastings (2007) and Landau, Vazirani, and Vidick (2013), Huang (2014) proved that the ground state α -Renyi entanglement entropy in gapped 1D systems is upper bounded by $\tilde{\mathcal{O}}(\alpha^{-3}/\Delta)$, where $\tilde{\mathcal{O}}$ stands for \mathcal{O} up to logarithmically smaller factors. Specifically, it was demonstrated that the residual probability $\epsilon(D)$, defined as the sum of all eigenvalues of the reduced density matrix smaller than the D th largest one, scales as $\exp\{-c\Delta^{1/3}[\log(D)]^{4/3}\}$ for a general spin chain with gap Δ (Arad *et al.*, 2013). For integrable systems and systems in the scaling regime of a conformal field theory, a faster decay in the form of $\epsilon(D) \simeq \exp\{-c[\log(D)]^2\}$ is obtained (Verstraete and Cirac, 2006; Calabrese and Lefevre, 2008).

For higher-dimensional quantum spin systems, no general proofs of an area law for ground states exist. It is believed that (i) gapped systems always exhibit an area law for the entanglement entropy; (ii) critical systems without a Fermi surface also satisfy an area law but get additive logarithmic corrections; (iii) critical systems with a Fermi surface exhibit an entanglement entropy scaling as $|\partial A| \log |\partial A|$, which is marginally larger than the area law scaling.

In two dimensions, additive corrections also pop up for systems exhibiting topological quantum order. For a region with a perimeter L and ignoring corner effects, the entanglement entropy scales like $cL - \log(\mathcal{D})$, with \mathcal{D} the total quantum dimension of the underlying anyonic theory. As this quantum dimension is always larger than 1, topologically ordered systems have less entanglement than the ones in a trivial phase. This indicates that a topologically ordered system exhibits a certain symmetry that reduces the support of the local reduced density matrix; it will turn out that such

symmetries are naturally described by matrix product operators.

B. Tensor networks

We now define different types of states and operators that can be expressed as tensor networks and analyze their basic properties. Although most of this review focuses on translational-invariant states of spin lattices and thus MPSs and PEPSs are the main actors, we also introduce their extension to fermionic systems and make connections to other sets of states like TTNs and MERAs.

The discussion on local reduced density matrices made it clear that ground states of local quantum Hamiltonians are completely molded by their desire to have extremal local correlations, on the one hand, and to preserve lattice symmetries, on the other hand. The discussion on area laws for the entanglement entropy made it clear that the entanglement between two neighboring regions is concentrated mainly on the interface between the two regions. The same entanglement pattern can be obtained by distributing maximally entangled pairs of D -dimensional spins between all nearest neighbors, then doing a local projection (or a general linear map) on all these local spins to obtain one d -dimensional spin. This projection involves a linear map from a Hilbert space of N_i D -dimensional spins to a d -dimensional spin, with N_i the coordination number of the lattice at site i , and any such linear map can be represented by a tensor $A_{\alpha_1 \alpha_2 \dots \alpha_{N_i}}^i$. Translational invariance is obtained if the lattice has periodic boundary conditions and the same projection is chosen on all lattice sites. This construction, illustrated in Fig. 1, defines the class of PEPSs with bond dimension D , and the different states in that family can be obtained by choosing different projections A . We later give a more precise description of PEPSs and connect them to tensor networks.

This PEPS construction yields quantum many-body states that have strong local correlations, exhibit the translational symmetry of the underlying lattice, and obey an area law for the entanglement entropy with respect to any bipartition. Furthermore, extra symmetries such as global $U(1)$ or $SU(2)$ symmetries can easily be incorporated by defining tensors that transform according to some representation of the corresponding group (Perez-Garcia *et al.*, 2010; Singh, Pfeifer, and Vidal, 2010). All those properties are highly nontrivial, and it is especially hard to write entangled translationally invariant wave functions without using the projected entangled pair construction.

Conceptually, PEPSs present a way of parametrizing interesting many-body wave functions on any lattice with a constant coordination number using a number of parameters

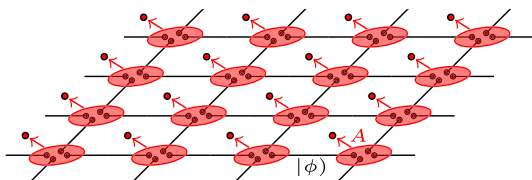


FIG. 1. Construction of projected entangled pair states on a 2D lattice.

that is independent of the system size (at least for translationally invariant states). They hence provide a way of writing a nontrivial wave function in an exponentially large Hilbert space in a compressed form. This comes as no surprise. Both product states and Slater determinants provide ways of writing wave functions in an exponentially large Hilbert space using a few parameters. The main difference, however, is the fact that the PEPS construction can represent a wide variety of ground states of strongly interacting systems. Being able to represent such wave functions has the potential of solving some of the hardest problems in many-body physics.

In the case of 1D spin chains, this PEPS construction defines the class of MPSs. The area law for entanglement allows one to demonstrate that any ground state of a gapped quantum spin chain can be represented efficiently using such a MPS (Arad *et al.*, 2013; Hastings, 2007) and, conversely, that any MPS is the ground state of a local gapped Hamiltonian (Fannes, Nachtergaele, and Werner, 1992b; Perez-Garcia *et al.*, 2007). Similarly, a wide class of correlated many-body systems in higher dimensions can be represented using PEPSs (Verstraete *et al.*, 2006; Buerschaper, Aguado, and Vidal, 2009), and the main topic of this review is to report on the mathematical properties of the manifolds of MPSs and PEPSs and the relevance for the physical properties and classification of strongly correlated systems. In a nutshell, the manifold of MPSs and PEPSs form rich classes of many-body systems and provide a unique window into the physics of strongly correlated quantum many-body systems, from both the theoretical and computational points of view.

1. MPSs and PEPSs

We now introduce PEPSs for an arbitrary lattice and then particularize the definition to one spatial dimension to obtain MPS. We consider a lattice with N vertices, $V = \{1, 2, \dots, N\}$, and a set of edges E connecting them. We consider a spin at each vertex with a corresponding Hilbert space \mathbb{C}^{d_i} of dimension d_i . Our goal is to construct states of these spins, i.e., $|\psi\rangle \in \bigotimes_{i=1}^N \mathbb{C}^{d_i}$.

The elements $e \in E$ are pairs of vertices; for instance, $e = (1, 2)$ represents the edge connecting vertices 1 and 2. We further denote by $S_i \subset V$ the set of vertices that are connected to the vertex i , i.e., $S_i = \{j \in V, \text{ such that } (i, j) \in E\}$, with $z_i = |S_i|$ the coordination number. To construct $|\psi\rangle$, we first assign to each vertex i several auxiliary spins (one for each edge connecting that vertex to another one) that are in a maximally entangled state with their neighbors. More explicitly, for each $i \in V$ and $j \in S_i$ we denote by $a_{i,j}$ the ancilla, which has an associated Hilbert space $\mathbb{C}^{D_{i,j}}$ with dimension $D_{i,j} = D_{j,i} \in \mathbb{N}$. To distinguish states of the auxiliary spin from the physical ones, we use the notation $|\cdot\rangle$ as opposed to the notation $|\cdot\rangle$. The ancillas $a_{i,j}$ and $a_{j,i}$ form a maximally entangled state

$$|\phi\rangle_{i,j} = \sum_{n=1}^{D_{i,j}} |n\rangle_{a_{i,j}} \otimes |n\rangle_{a_{j,i}}, \quad (2)$$

where the $\{|n\rangle\}$ form an orthonormal basis; note that this fixes a preferred basis, making the objects in the construction basis dependent. Thus, the state of the ancillas is

$$|\Phi\rangle = \bigotimes_{e \in E} |\phi\rangle_e. \quad (3)$$

To each vertex i , we next assign a linear map

$$A[i]: \bigotimes_{j \in S_i} \mathbb{C}^{D_{i,j}} \rightarrow \mathbb{C}^{d_i}.$$

We define the PEPS as

$$|\psi\rangle = \bigotimes_{i \in V} A[i]|\Phi\rangle. \quad (4)$$

That is, the state is obtained by a linear map of the entangled pairs of ancillae into the physical spins at each vertex; cf. Fig. 1. The final state will in general be entangled since the entanglement in the ancillae is transferred to the spins through the mapping. This entanglement can lead to long-range correlations, even though the ancillae are entangled only locally. This is a simple consequence of entanglement swapping that allows one to entangle remote particles by a sequence of projections on entangled pairs. Note that the entire state is completely determined by the maps $A[i]$: since each of them is characterized by $p_i = d_i \prod_{j \in S_i} D_{i,j}$ parameters, we need only $\sum_{i \in V} p_i$ parameters to specify the state.

The map $A[i]$ is characterized by the coefficients in a basis as follows:

$$A_{\alpha_1, \dots, \alpha_{z_i}}^s = \langle s | A[i] | \alpha_1, \dots, \alpha_{z_i} \rangle. \quad (5)$$

Thus, the map is also characterized by a tensor (whose entries depend on the basis choice). We indistinguishably call A a map or tensor in the following. A concept that plays a chief role in this review is injectivity and its generalizations: we say that the tensor $A[i]$ is injective if the corresponding map is injective; that is, if there is another map, $A[i]^{-1}: \mathbb{C}^{d_i} \rightarrow \bigotimes_{j \in S_i} \mathbb{C}^{D_{i,j}}$, such that $A[i]^{-1}A[i] = \mathbb{1}$.

There are equivalent ways of defining PEPSs that are used later. One particularly interesting one consists of associating with each vertex $i \in V$ a fiducial state $|\phi_i\rangle$ of the spin and the virtual system (i.e., $|\phi_i\rangle \in \mathbb{C}^{d_i} \otimes_{j \in S_i} \mathbb{C}^{D_{i,j}}$), and defining the PEPS as

$$|\psi\rangle = \langle \Phi | \bigotimes_{i \in V} |\phi_i\rangle. \quad (6)$$

This state coincides with the previous one if we write

$$|\phi_i\rangle = \sum_{s, \alpha_1, \dots, \alpha_{z_i}} A_{\alpha_1, \dots, \alpha_{z_i}}^s |s\rangle \otimes |\alpha_1, \dots, \alpha_{z_i}\rangle \quad (7)$$

and choose as $A_{\alpha_1, \dots, \alpha_{z_i}}^s$ the elements of the map $A[i]$ in the physical ($|s\rangle$) and virtual ($|\alpha_j\rangle$) basis. In this case, the fiducial states $|\phi_i\rangle$ completely determine the many-body state. Finally, yet another equivalent definition is obtained by replacing the state $|\phi\rangle$ of the ancillae in Eqs. (2) and (3) with some tripartite or multipartite local states; such an ansatz is again equivalent to the original construction but can be advantageous in the numerical simulation of frustrated spin systems (Schuch *et al.*, 2012; Xie *et al.*, 2014).

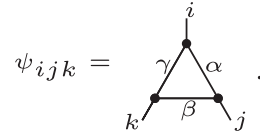
Although this construction applies to any lattice, here we exclusively consider regular lattices with the same coordination number and the same physical dimension at each vertex ($z_i = z$ and $d_i = d$). We call d the physical dimension. We are particularly interested in square lattices in two dimensions, or in 1D lattices, where we recover MPSs. In the first case, we use the convention in the tensors (5) that $\alpha_1, \dots, \alpha_4$ are taken clockwise (top, right, down, left). In the latter, it is useful to define matrices $A^{s_i}[i] \in \mathbb{C}^{D_{i-1,i} \otimes D_{i,i+1}}$ with elements $A_{\alpha\beta}^{s_i}[i]$, and the previous expression is equivalent to

$$\langle s_1, s_2, \dots | \psi \rangle = \text{Tr}[A^{s_1}[1]A^{s_2}[2] \cdots A^{s_N}[N]]. \quad (8)$$

Every probability amplitude is given by the trace of a product of N matrices: hence the name matrix product state.

In regular lattices, translationally invariant (also named *uniform*) states are obtained by choosing the same map at every site $A[i] = A$, and thus $D_{i,j} = D$, the bond dimension. By construction, it is clear that the PEPS is invariant under translations. For any lattice size, the state is completely determined by a single map A or, equivalently, a single tensor. We say in the review that the tensor A generates the state $|\psi(A)\rangle$. Thus, we can associate with any tensor A a set of states $|\psi(A)_N\rangle$ corresponding to each lattice size. This map from a tensor to a set of states is not one to one, a notion that forms the basis for many of the features of MPS and PEPS descriptions. Also note that all the physical properties (criticality, symmetries, topological order, etc.) of the states are completely determined by A and thus are somehow encoded in that tensor. A main goal of the theory of tensor networks is to obtain such properties directly from the tensor.

Instead of working with the notation in Eq. (5) and the corresponding proliferation of indices, it turns out to be much more useful to work with a graphical tensor notation, and to represent MPSs and PEPSs as a tensor network. A tensor network consists of vertices and edges that have the same geometry as the lattice. Every vertex represents a tensor with a number of legs equal to the number of edges. An edge with an open end represents an open index, while an edge that is sandwiched between two vertices is to be contracted and hence summed over. For example, the tensor $\psi_{ijk} = \sum_{\alpha\beta\gamma} A_{\alpha\beta}^i A_{\beta\gamma}^j A_{\gamma\alpha}^k$ is represented by three vertices, three open lines, and three closed lines as



With this tensor network notation, we can readily represent any MPS or PEPS, examples of which are shown for a spin chain and a square lattice in Fig. 2. The marginal or reduced density matrix of a MPS or PEPS can be obtained by summing over or contracting the physical indices. Similarly, we can represent local expectation values in the form of a tensor network contraction.

An important practical consideration is that of the computational complexity of contracting such tensor networks. Generally, contracting a generic PEPS network is as hard

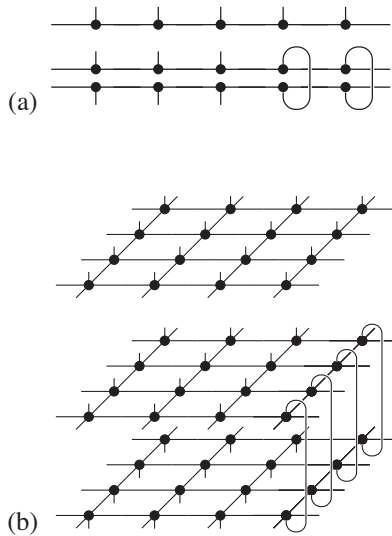


FIG. 2. Tensor network description of (a) a MPS, (b) a PEPS on a square lattice, and their corresponding marginals.

as calculating the partition function of a spin glass and can hence be #P hard in the number of tensors (Verstraete *et al.*, 2006; Schuch *et al.*, 2007; Haferkamp *et al.*, 2020). In practice, however, PEPS tensor networks have a high degree of homogeneity (e.g., translational invariance), and powerful algorithms are being developed to contract them. Contracting tensor networks made of matrix product states is much cheaper, as the cost of calculating any expectation value scales linearly in the number of sites and as a cube in the bond dimension ($\sim ND^3$): one can contract the tensor network starting at one end and progress to the other end while contracting all tensors along the way. This difference in complexity of contracting 1D versus higher-dimensional tensor networks is responsible for the large discrepancy in accuracy that currently exists between simulations for 1D spin chains using DMRG and those for 2D systems using PEPSs. It is, however, an active area of research to determine how to speed up these higher-dimensional tensor contractions. For state-of-the-art algorithms, see Corboz (2016), Vanderstraeten *et al.* (2016), and Liao *et al.* (2019).

Another important consideration is the fact that MPS and PEPS representations are not unique: as we mentioned before, two tensors may generate the same set of states. This fact will play a central role in understanding how symmetries are represented in tensor networks, in the classification of different phases of matter, and in the process of devising efficient numerical methods for dealing with tensor networks. We now consider the case of MPSs and define a translationally invariant MPS $|\psi(A)\rangle$ with periodic boundary conditions generated by the tensor A ; due to the cyclic nature of the trace, it is clear that $|\psi(A)\rangle = |\psi(B)\rangle$ if B^i is related to A^i by a “gauge transform” X as follows:

$$B^i = X A^i X^{-1}, \tag{9}$$

where X is any invertible $D \times D$ matrix. This is a specific instance of the fundamental theorem of MPSs (Perez-Garcia *et al.*, 2007; Perez-Garcia, Wolf *et al.*, 2008), which is

reviewed in Sec. IV, and which basically states that this is the only possibility as long as the tensors are expressed in some canonical form.

Many familiar states in the context of quantum information and condensed matter theory have simple descriptions in terms of MPSs and PEPSs. One can also construct PEPSs that are closely connected to classical Gibbs distributions: that is, for any classical spin system with short-range interactions, one can build a quantum state such that the expectation values of the operators diagonal in the computational basis coincide with those of the classical distribution (Verstraete *et al.*, 2006).

2. MPOs and PEPOs

An important generalization of the class of MPSs and PEPSs are MPOs and PEPOs. They are readily defined by the tensor network depicted in Fig. 3. When the operators that they represent are translationally invariant, they are fully characterized by a single tensor, just like PEPSs, but now with two physical indices: one corresponding to the bra and the other to the ket of the local action of the operator. Analogously to their pure state counterparts, they allow us to encode relevant many-body operators in an economical way. In particular, matrix product operators (Verstraete, Garcia-Ripoll, and Cirac, 2004; Zwoleak and Vidal, 2004) describe mixed states (like those corresponding to thermal equilibrium or open quantum systems), Hamiltonians (McCulloch, 2007; Crosswhite and Bacon, 2008; Pirvu *et al.*, 2010), or unitary evolution (Cirac *et al.*, 2017b; Şahinoğlu *et al.*, 2018).

MPOs and PEPOs relate to other operators appearing in the context of statistical physics. They appear as transfer matrices in 2D and 3D classical statistical mechanical models, where the free energy can be inferred from its leading eigenvalue. The exact diagonalization of such transfer matrices in the former case is the main aim of the field of integrable models, and intricate algebraic structures in integrable systems have been uncovered by invoking the Bethe ansatz and the associated Yang-Baxter relations. Similarly, MPOs are obtained as the transfer matrix in the path integral formulation of 1D quantum spin systems. They also appear in the description of cellular automata and as transfer matrices in nonequilibrium statistical physics in the realm of percolation theory and the asymmetric exclusion process. See the review given by Haegeman and Verstraete (2017) for a detailed exposition of these connections.

MPOs are widely used in different scenarios in the field of tensor networks. Although all these roles can be extended to higher dimensions using PEPOs, we discuss them here in the context of MPOs.

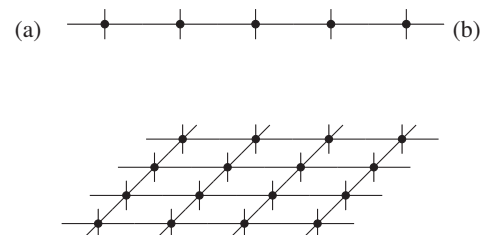


FIG. 3. Definitions of (a) matrix product operators (MPOs) and (b) projected entangled pair operators (PEPOs).

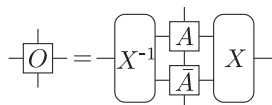


FIG. 4. Sufficient condition for a translationally invariant MPO ρ to be positive.

We first focus on MPOs as density matrices, that is, mixed state analogs of a pure MPS. In this case they are called matrix product density operators (MPDOs). From the computational point of view, they arise in simulations at finite temperature or in the presence of dissipation. A sufficient local condition for a MPO represented by the four-leg tensor O to be a global positive operator (in the semidefinite sense, hence representing a density matrix) is the existence of a four-leg tensor A (the “purification”) and a three-leg tensor X (the gauge transform) such that the property depicted in Fig. 4 is satisfied. Note that this condition is only sufficient, but not necessary, to ensure positivity. Indeed, it has been shown that there can be an arbitrary trade-off in the bond dimension of the purification (De las Cuevas *et al.*, 2013), and that there are translationally invariant MPDOs that do not possess MPO purifications (as in Fig. 4) and are valid for all system sizes (De las Cuevas *et al.*, 2016).

Second, MPOs can also describe the dynamics of a quantum many-body system. In that case they are called matrix product unitaries (MPUs) (Cirac *et al.*, 2017b), as they generate a unitary operator U fulfilling $UU^\dagger = 1$. As in the case of MPDOs, this extra condition imposes a restriction on the tensor generating U . For this case, it is possible to fully characterize them. In fact, by blocking at most D^4 spins, the resulting tensors have a simple structure (Fig. 5). The MPU can thus be viewed as a quantum circuit with two layers of unitary operators acting on nearest neighbors. In fact, MPUs can be shown to be equivalent to 1D quantum cellular automata, that is, unitary operators that transform local operators into local operators, where by local we mean acting nontrivially in a finite region only. That is, any MPU possesses that property and any quantum cellular automaton can be written as a MPU with finite bond dimension. Furthermore, an evolution operator generated by a local Hamiltonian in finite time can be approximated by a MPU since the Lieb-Robinson

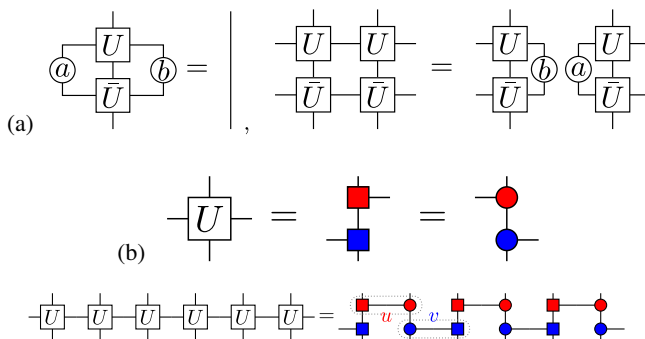


FIG. 5. (a) Tensors generating a MPU after blocking. (b) The MPU can be described as a quantum circuit, with alternating layers of unitary operators u and v acting on nearest neighbors with even-odd indices and odd-even indices, respectively.

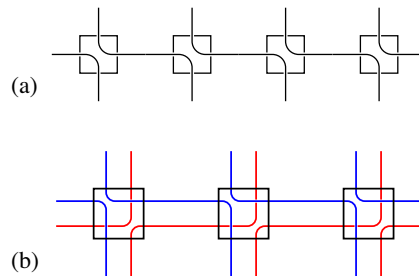


FIG. 6. (a) MPU representation of the left-moving shift operator. (b) MPU made of two shift operators, one right moving and another left moving.

bound for the propagation of correlations ensures that it behaves as a quantum cellular automaton, and thus as a MPU, up to some small corrections. There are also some MPUs that cannot be approximated by a local time-evolution operator. An example is the shift operator sketched in Fig. 6(a) (see Appendix A.4), which in each application translates the state by one site to the left. The fact that this operator cannot be obtained (or even approximated) by the evolution of a local Hamiltonian is a direct consequence of the index theorem, originally proven for 1D quantum cellular automata (Gross *et al.*, 2012), which states that MPUs can be classified in terms of an index, where the equivalence relation is that the tensors generating the MPU can be continuously transformed into one another. The index measures how quantum information is transported to the right (positive index) or to the left (negative index), and can take only discrete values. The dynamics generated by local Hamiltonians has zero index, whereas the one of the shift operator is ± 1 . In Fig. 6(b) we give an example of a MPU where the local Hilbert space has dimension 4 (and thus, it acts on pairs of qubits), with zero index as it moves the same information to the left as to the right.

Third, MPOs play a fundamental role in describing symmetries of PEPSs (Chen, Liu, and Wen, 2011; Bultinck, Marien *et al.*, 2017; Şahinoğlu *et al.*, 2021). In particular, the generalization of Eq. (9) to PEPSs is the pulling through equation depicted in Fig. 7. It gives a sufficient condition for two tensors to generate the same PEPS. In the case of systems exhibiting topological quantum order, similar pulling through equations characterize the symmetries of the underlying tensors; these symmetries form an algebra and provide an explicit representation of tensor categories describing the topological phase and its emerging anyons; see Sec. III.B.

Finally, MPOs are also key in the bulk-boundary correspondence (Cirac *et al.*, 2011), where the physical properties of PEPSs in two dimensions can be mapped onto those of a theory defined at the boundary by a MPO. As we later show, the classification of the renormalization fixed points of MPOs

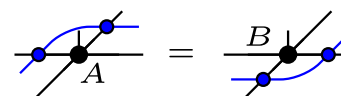


FIG. 7. A sufficient condition for two PEPSs to be equal to each other is the existence of a MPO satisfying the pulling through equation.

thus allow us to characterize the topological order of 2D systems (Cirac *et al.*, 2017a).

3. Correlations, entanglement, and the transfer matrix

a. Matrix product states

All matrix product states satisfy an area law for the entanglement entropy. This follows directly from the projected entangled pair construction, where the MPS was obtained by applying a local map on a tensor product of D -dimensional maximally entangled states; see Fig. 1. We now take a region of contiguous spins in the chain. Before the map, it is clear that only the two pairs that are at the boundary contribute to the entanglement entropy. In fact, the rank of the reduced state in that region is equal to D^2 . Since the map does not change the rank of the reduced state, it follows that the entropy is at most $2 \log(D)$. For a generic infinite translationally invariant MPS, it is possible to calculate all eigenvalues of this reduced density matrix exactly. This density matrix can be represented by the tensor network depicted in Fig. 8. Before we show how to determine this spectrum, some basic algebraic properties of MPSs have to be introduced.

A central object for a MPS is its corresponding transfer matrix E , which is defined as $E_{\alpha\alpha',\beta\beta'} = \sum_i A_{\alpha\beta}^i \bar{A}_{\alpha'\beta'}^i$. It is called the transfer matrix, as it plays a role similar to the transfer matrix in classical 1D statistical mechanics models. The eigenvalues and eigenvectors of this transfer matrix are of importance, as we see in several places in this review. The eigenvalues can be complex, as E is not necessarily Hermitian and it may have some Jordan blocks. For a generic MPS, however, the largest eigenvalue in magnitude is unique and there are no Jordan blocks associated with it. We assume this to be the case for the time being. We find it convenient to write the corresponding right and left eigenvectors $|\rho^{R,L}\rangle$ as operators $\rho^{R,L}$ so that $(\rho^{R,L})_{\alpha,\alpha'} = \langle \alpha, \alpha' | \rho^{R,L} \rangle$. The quantum Perron-Frobenius theorem (Albeverio and Høegh-Krohn, 1978; Wolf, 2012) then guarantees that this largest eigenvalue is positive, as the eigenvalue equation can be written in the form of a completely positive (CP) map (the quantum version of a stochastic matrix) as follows: $\sum_i A^i \rho^R A^{i\dagger} = \lambda_1 \rho^R$ and

$\sum_i A^{i\dagger} \rho^L A^i = \lambda_1 \rho^L$. Note that the left eigenvector and right eigenvector do not have to be equal, but Perron-Frobenius theory guarantees that both ρ^L and ρ^R can be chosen to be positive semidefinite. As we see in Sec. IV, the MPS fulfilling the requirements that the largest eigenvalue (in magnitude) of the transfer matrix is unique and that both ρ^L and ρ^R are positive definite is called *normal*. It is not difficult to show that, by blocking a finite number of sites, any normal MPS becomes injective; see Sec. IV for a discussion.

In the case of an injective MPS with periodic boundary conditions, the Euclidean norm of the MPS is given by $\text{Tr} E^N$ and hence scales as λ_1^N with N the number of sites. In the limit of large N , this norm should be equal to 1, and we rescale the tensors $A^i \rightarrow A^i / \sqrt{\lambda_1}$ to achieve this. We henceforth assume that $\lambda_1 = 1$. The second largest eigenvalue λ_2 of the transfer matrix defines the correlation length of the state: $\xi = -1 / \log(|\lambda_2|)$. For a general connected correlation function $C(X, Y) := \langle XY \rangle - \langle X \rangle \langle Y \rangle$ of two operators X and Y with a distance n between them, the expectation value will be of the form $\sum_{i \geq 2} c_{XY}(i) \lambda_i^n$ and is hence a sum of $D^2 - 1$ pure exponentials, with D the bond dimension. MPSs can henceforth not reproduce algebraic correlations at long distances, as a sum of exponentials cannot reproduce the tail of an algebraic function. For a finite system with N sites, however, it is enough to choose D as a polynomial in N to reproduce all correlation functions faithfully (Verstraete and Cirac, 2006). Similarly, Ornstein-Zernike-type corrections of the form $\exp(-n/\xi) / \sqrt{n}$ can be taken into account by taking a large enough D (Rams *et al.*, 2015; Zauner *et al.*, 2015).

We now return to the calculation of the eigenvalues of a reduced density matrix of n sites of an injective MPS; see Fig. 8. Using the basic fact in linear algebra that the eigenvalues of the matrix AB are equal to the eigenvalues of the matrix BA , the problem reduces to finding the eigenvalues of the $D^2 \times D^2$ matrix $F_{\alpha\beta,\alpha'\beta'} = \sum_{\alpha''\beta''} \rho_{\alpha\alpha''}^L \rho_{\beta''\beta'}^R (E^n)_{\alpha''\beta'',\alpha'\beta'}$. In the limit of large n , E^n factorizes in $|\rho^R\rangle\langle\rho^L|$ and we see that the eigenvalues of the reduced density matrix are given by the eigenvalues of $(\rho^L \cdot \rho^R)^{\otimes 2}$; in other words, the contribution from the left and right sides of the block disentangle for distances larger than the correlation length. The eigenvalues of the matrix $\rho^L \rho^R$ are the squares of the Schmidt coefficients of an injective MPS with open boundary conditions. The entanglement spectrum is defined as the logarithm of these eigenvalues.

b. PEPSs

PEPSs automatically fulfill the area law, as one can argue in the same way that we did with MPSs. In this case, the entanglement entropy of an $L \times L$ block on a square lattice is upper bounded by $4L \log(D)$.

Calculating correlation functions and the entanglement spectrum of a PEPS is much more involved than the MPS case. This follows from the fact that the contracted tensor network looks much like the partition function of a classical statistical mechanical model, but then with two layers and complex numbers. The calculation of the leading eigenvector of this transfer matrix corresponds to finding fixed points of completely positive maps acting on an infinite spin chain. The entanglement spectrum is then obtained by the eigenvalues of

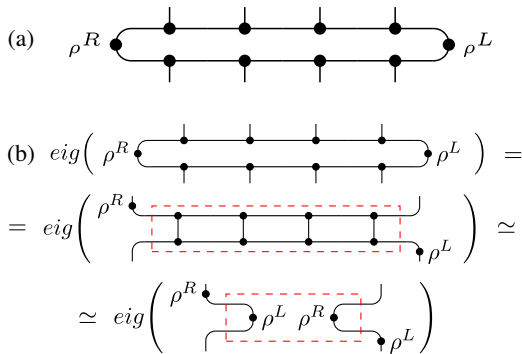


FIG. 8. (a) Tensor network description of the reduced density matrix of n spins in an infinite translationally invariant MPS. $|\rho^{R,L}\rangle$ correspond to the right and left fixed points, respectively, of the transfer matrix; see the main text. (b) Argument showing that the eigenvalues of the reduced density matrix of n sites in a MPS coincide with those of $(\rho^L \rho^R)^{\otimes 2}$ in the limit of large n .

the corresponding fixed-point density matrix. Note that for topological states of matter, an additive negative correction to this entanglement entropy emerges (Kitaev and Preskill, 2006; Levin and Wen, 2006); this is called topological quantum entanglement entropy and is a signature of the fact that the PEPS tensors exhibit nontrivial symmetries by which they do not have full support on the physical Hilbert space. This is discussed in Sec. III.B.

Unlike in the 1D case, correlation functions can in principle decay following a power law, for example, in the case of the so-called Ising PEPS tuned at criticality (Verstraete *et al.*, 2006), which is discussed in the Appendix.

4. Extension to fermionic, continuous, and infinite tensor networks

Tensor networks have also been defined for fermionic systems (Barthel, Pineda, and Eisert, 2009; Corboz *et al.*, 2010; Kraus *et al.*, 2010; Bultinck, Williamson *et al.*, 2017) and have been formulated directly in the continuum (Verstraete and Cirac, 2010), and nontrivial MPSs with infinite bond dimension have been constructed using vertex operators of conformal field theories (Cirac and Sierra, 2010).

a. Fermionic tensor networks

Defining tensor networks for fermionic systems presents two new difficulties. First, the tensor product structure is altered due to the anticommutation relations of the creation and annihilation operators and, second, a new superselection rule emerges in the form of parity conservation. The projected entangled pair construction can, however, be readily extended as follows to the fermionic case by considering virtual maximally entangled modes of fermions as opposed to maximally entangled D -level systems: $|I\rangle = \sum_{\alpha} a_{\alpha}^{\dagger} b_{\alpha}^{\dagger} |\Omega\rangle$. The parity constraint can be enforced by choosing the projection operator $\hat{A}^i = \sum_{\alpha\beta\gamma\dots} A_{\alpha\beta\gamma\dots}^i a_{\alpha} b_{\beta} c_{\gamma} \dots$ to have a fixed parity. This parity constraint ensures that the locality of the tensor network will be conserved, which makes it possible to contract tensor networks built from such tensors efficiently. Alternatively, the construction can be made using Majorana modes, and this will be useful for constructing fermionic PEPSs with a chiral character.

From the mathematical point of view, working with fermions amounts to changing the convention of working in vector spaces with a tensor product structure to working in supervector spaces with a \mathbb{Z}_2 graded tensor product. In essence, the Hilbert space is split into a direct sum of two vector spaces, $V_0 \oplus V_1$, and every vector $|i\rangle$ in the Hilbert space has to be fully supported in one of these spaces and therefore has a parity $|i\rangle$ associated with it. Given that the graded tensor product of two vectors $|i\rangle \otimes_g |j\rangle$, swapping the vectors amounts to the relation $|i\rangle \otimes |j\rangle \rightarrow (-1)^{|i||j|} |j\rangle \otimes |i\rangle$. Matrix product states can now be defined in this supervector space (Bultinck, Williamson *et al.*, 2017) in the form of $\hat{A} = \sum_{i\alpha\beta} A_{\alpha\beta}^i |\alpha\rangle \otimes_g \langle i| \otimes_g \langle \beta|$ and, using the sign rules of grading when moving vectors around each other so as to contract the virtual indices, any bosonic tensor network can be readily fermionized.

The notion of injectivity has to be altered in fermionic tensor networks since the parity superselection rule cannot be broken. As a consequence, different boundary conditions have to be chosen to construct translationally invariant states with an even or an odd parity. These two distinct possibilities relate to the fact that there are two distinct types of \mathbb{Z}_2 graded tensor algebras, and these are characterized by the absence or presence of Majorana edge modes. The prime example of a fermionic spin chain with Majorana edge modes is the Kitaev wire (Kitaev, 2001). When putting the Kitaev wire on a ring with periodic boundary conditions (hence making it translationally invariant), one gets a system with odd parity and the MPS description is given by

$$|\psi\rangle = \sum_{i_1 \dots i_N} \text{Tr}[Y A^{i_1} A^{i_2} \dots A^{i_N}] |i_1\rangle \otimes_g |i_2\rangle \otimes_g \dots, \quad (10)$$

with

$$A^0 = \begin{pmatrix} 1 & 0 \\ 0 & 1 \end{pmatrix}, \quad A^1 = \begin{pmatrix} 0 & 1 \\ -1 & 0 \end{pmatrix} = Y.$$

Contrary to the bosonic case, this MPS description is irreducible and hence injective. By considering more copies of this Kitaev chain, it is possible to study the entanglement spectrum of all states in the Z_8 classification of gapped fermionic spin chains (Fidkowski and Kitaev, 2011; Bultinck, Williamson *et al.*, 2017). This construction has been extended to fermionic MPUs (Piroli *et al.*, 2020), which include all quantum cellular automata in one dimension.

b. Continuous MPSs

Continuous matrix product states (Verstraete and Cirac, 2010; Haegeman, Cirac *et al.*, 2013) can be defined by taking the limit of the lattice spacing going to zero while rescaling the matrix product tensors in an appropriate way. This enables one to write wave functions for quantum field theories without a reference to an underlying lattice discretization, and this is useful for doing numerical simulations of cold atoms and quantum field theories.

We now consider a bosonic system on a ring of length L and with creation and annihilation operators of type α satisfying $[\psi_x^{\alpha}, \psi_y^{\beta\dagger}] = \delta_{\alpha\beta} \delta(x-y)$. The continuous MPS (cMPS) wave function of bond dimension D is defined as

$$|\psi\rangle = \text{Tr} \left\{ \mathcal{P} \exp \left[\int_{-L/2}^{L/2} \left(Q(x) + \sum_{\alpha} R^{\alpha}(x) \psi_x^{\dagger}(\alpha) \right) dx \right] \right\} |\Omega\rangle, \quad (11)$$

where $Q(x), R^{\alpha}(x) \in \mathbb{C}^{D \times D}$, \mathcal{P} denotes a path ordered exponential, and $[R^{\alpha}(x), R^{\beta}(x)] = 0$. The path ordered exponential is the continuous limit of a MPS with tensors given by $A^0[i] = 1 + \epsilon Q[i]$ and $A^{\alpha}[i] = \sqrt{\epsilon} R^{\alpha}[i]$, with ϵ the lattice parameter. Fermionic cMPSs are defined by replacing the commutation with anticommutation conditions.

A translationally invariant cMPS is obtained by choosing the Q, R^{α} independent of x and choosing $L \rightarrow \infty$. An interesting property exhibited by these cMPSs is the fact that

the diagonal elements of the one-particle reduced density matrix in momentum space $n(k)$ decay as $\mathcal{O}(1/k^4)$. This implies that they are sufficiently smooth such as to not suffer from UV divergencies and can therefore be used as variational wave functions without suffering the UV catastrophe occurring in other variational methods (Haegeman *et al.*, 2010).

c. Infinite MPSs

Instead of taking the continuum limit in the space direction, it is possible to consider matrices A^i as operators in a general infinite-dimensional Hilbert space, as opposed to a finite-dimensional one (as in the case of MPSs). A particularly interesting choice in the case of spin-1/2 systems is to define those operators in terms of normal ordered vertex operators appearing in conformal field theory as follows (Cirac and Sierra, 2010; Nielsen, Cirac, and Sierra, 2012; Nielsen, Sierra, and Cirac, 2013; Tu *et al.*, 2014):

$$A^{s_i} = :e^{i\sqrt{4\alpha} s_i \phi(z_n)}:,$$

where $\alpha > 0$ is a free parameter, $s_i = \pm 1/2$, and $\phi(z_n)$ is the field of a free massless boson located on position $z_n = x + i \cdot y$ of the lattice. For a spin chain with N sites with periodic boundary condition, we can choose $z_n = L \cdot \exp(2\pi i \cdot n/N)$, but it is also possible to parametrize 2D wave functions in this form. By taking the expectation value of the virtual bosonic fields with respect to the vacuum, the MPS wave function is then equivalent to

$$\psi_{s_1 s_2 \dots s_n} = \delta_{\sum_i s_i} \prod_i \chi_{i, s_i} \prod_{i < j} (z_i - z_j)^{4\alpha s_i \cdot s_j}.$$

These wave functions are effectively lattice versions of the Laughlin state, and a wealth of interesting critical and chiral states such as the ground state of the Haldane-Shastry-type or Kalmeyer-Laughlin-type wave functions can be constructed in this form. Additionally, it is possible to define the corresponding parent Hamiltonians and to calculate exact expressions for the entanglement entropy.

A similar construction allows one to study ground states of the fractional quantum Hall effect on a cylinder by using different CFTs, and such a systematic program of variational calculations for quantum Hall systems was pursued by Zaletel and Mong (2012), Estienne *et al.* (2013), Zaletel, Mong, and Pollmann (2013), and Zaletel *et al.* (2015).

5. Tensor networks as quantum circuits: Tree tensor states and MERAs

Thus far, we have advocated for the viewpoint that MPSs and PEPSs parametrize the quantum correlations in the corresponding many-body wave functions, and therefore that the virtual D -level systems represent the entanglement degrees of freedom. In the case of a MPS with open boundary conditions, there is, however, an alternative way of interpreting the wave function in terms of a quantum circuit acting on a product state and assisted by a D -level ancillary system [Fig. 9(a)]. The unitaries (or rather isometries) building up the

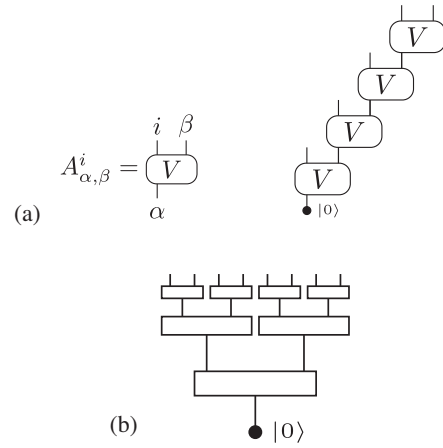


FIG. 9. (a) Staircase quantum circuit representing a MPS. (b) Tree tensor network.

circuit are obtained by bringing the MPSs into canonical form by appropriate gauge transformations (Schön *et al.*, 2005).

Instead of using a circuit in the form of a staircase, one could envision using a circuit in the form of a tree [Fig. 9(b)]. Although translational invariance is lost in this construction, it is possible to parametrize quantum states using this construction with an entanglement entropy that scales logarithmically in certain bipartitions (Fannes, Nachtergaele, and Werner, 1992c; Shi, Duan, and Vidal, 2006; Murg *et al.*, 2010; Silvi *et al.*, 2010). This makes this ansatz particularly well suited for simulating critical 1D systems. Expectation values can still be calculated efficiently, as one can always choose a contraction sequence for which there is no proliferation of indices.

A more powerful and sophisticated ansatz can be made by allowing for loops in the quantum circuit of the tree tensor network, but at the same time ensuring that the circuit is efficiently contractable. This gives rise to the concept of the multiscale entanglement renormalization ansatz (Vidal, 2007b, 2008). See Evenbly and Vidal (2014) for an authoritative review.

C. The ground state manifold of local Hamiltonians

Matrix product states and PEPSs form a low-dimensional manifold in an exponentially large Hilbert space. More precisely, the set of uniform MPSs forms a Kähler manifold (Haegeman *et al.*, 2014). The question addressed in this section regards how this manifold is related to ground states of local quantum spin Hamiltonians. It is shown that the manifold of MPSs is in one-to-one correspondence with ground states of local gapped Hamiltonians. This is a strong justification for using this manifold for variational calculations. Using concepts of differential geometry, it is then possible to relate the linear Schrödinger equation on the exponentially large Hilbert space to nonlinear differential equations on the compressed MPS manifold, as implemented in DMRG algorithms. Additionally, the concept of the tangent plane of the MPS manifold leads to a clear characterization of the elementary excitations on top of the ground state vacuum.

1. States to Hamiltonians: Parent Hamiltonians

As argued in Sec. II.B, MPSs and PEPSs were explicitly constructed so as to mimic the entanglement structure of ground states of local quantum Hamiltonians: they have strong local correlations, possess all the symmetries of the problem, and obey an area law. Conversely, to every MPS and PEPS there exists a local frustration-free quantum spin Hamiltonian for which the MPS or PEPS is the ground state, called the parent Hamiltonian. (Here frustration-free refers to the fact that the ground state minimizes the energy of each Hamiltonian term locally.) In the case of injective MPSs and PEPSs it is, furthermore, the unique ground state, and in the case of MPSs the parent Hamiltonian can be proven to be gapped; see Sec. IV.

The existence of such a parent Hamiltonian is a consequence of the fact that the rank of the reduced density matrix in a contiguous region B scales as $D^{|\partial A|}$, with $|\partial A|$ the length of the boundary of that region, as shown in Sec. II.B.3 (in the case of 1D systems, $|\partial A| = 2$). The total dimension of the Hilbert space spanned by all spins in the region B scales as d^V , with V the volume of that region (in the 1D case, this is the length of the block L). On any regular lattice, there is a size and shape of the block for which $D^A < d^V$, regardless of the lattice size, and this region is the support of one local term of the parent Hamiltonian that is defined as the projector orthogonal to the support of the local reduced density matrix in that region. The full parent Hamiltonian is then obtained by summing up all these projectors over all possible regions. This Hamiltonian is a sum of positive semidefinite terms, and every term in the Hamiltonian annihilates the tensor network state under consideration. It is therefore frustration free. We further elaborate on the properties of this parent Hamiltonian in Sec. IV.

Conceptually it is interesting that any MPS or PEPS is the ground state of a local frustration-free Hamiltonian. However, these states are also approximate ground states of completely different frustrated Hamiltonians. How would all those different Hamiltonians be related to each other? From the linear algebra point of view, it indeed seems that knowledge about one extremal eigenvector does not provide much information about the other ones, let alone about the spectrum of the full Hamiltonian. However, the locality of the Hamiltonian puts stringent constraints on the possible elementary excitations or eigenvectors with eigenvalues close to the ground state energy. The excitation spectrum is indeed completely reflected into the correlation functions in the ground state. If the quantum states under consideration would exhibit Lorentz invariance, this would be an obvious statement, but it is not obvious that this argument survives for lattice systems. It has indeed been observed (Haegeman *et al.*, 2015; Zauner *et al.*, 2015) that the logarithms of the eigenvalues of the transfer matrix reproduce the dispersion relations of the full quantum Hamiltonian. This is a clear indication of the fact that it is enough to understand the ground state to deduce all low-energy physics of a full quantum Hamiltonian: all information is encoded in the ground state.

An even stronger argument can be made in the case of topologically ordered systems and the associated anyonic excitations. In that case, the full fusion and braiding statistics of the anyons can be deduced from studying the symmetries of

the PEPS tensors representing the ground states. No knowledge of the Hamiltonian is needed, as the algebraic features of the excitations follow from the entanglement structure present in the ground state. This is discussed in Sec. III.B.

2. Hamiltonians to states

From the traditional point of view of quantum many-body physics, the central question of interest concerning tensor networks is whether any ground state of a local quantum Hamiltonian can be well approximated with a MPS or PEPS. From a practical point of view, the main challenge is to understand how large the bond dimension D has to be chosen such that a MPS or PEPS exists that provides a faithful approximation to the true ground state. Given a ground state $|\psi_N\rangle$ of a quantum spin system on N sites, the question is how large the bond dimension $D \equiv D(N, \epsilon)$ has to be chosen as a function of N and error measure ϵ such that there exists a MPS or PEPS $|\psi(A)\rangle$ for which the fidelity or overlap with the exact ground state $|\langle\psi(A)|\psi_N\rangle| \geq 1 - \epsilon$. For the tensor network description to be useful, the dependency on N and $1/\epsilon$ should be polynomial (note that simple strategies based on an exact diagonalization of small blocks yields an exponential scaling).

We later discuss several approaches toward solving this problem, as each approach highlights a complementary aspect of this issue. In summary, the results for the case of spin chains and MPSs are as follows:

- If the Renyi entropy S_α , $\alpha < 1$, with respect to any bipartition is bounded from above by $c \log(N)$, then an efficient polynomial approximation of the ground state exists in terms of a MPS. Note that this includes the case of critical systems (Verstraete and Cirac, 2006; Schuch *et al.*, 2008).
- If the quantum spin chain is gapped and has a unique ground state, then an efficient polynomial approximation of the ground state exists in terms of a MPS (Hastings, 2007; Arad *et al.*, 2013).
- If the state to be approximated has exponential decay of correlation functions with respect to every pair of observables (with potentially unbounded support), then an efficient polynomial approximation exists in terms of a MPS (Brandao and Horodecki, 2013).

The fact that MPSs are powerful enough to represent ground states does not mean that there is an efficient algorithm to find them. Examples of quantum Hamiltonians can indeed be constructed for which the exact ground state is a MPS, but for which it is NP hard to find it (Schuch, Cirac, and Verstraete, 2008); the catch is that such Hamiltonians have a small gap scaling as $1/\text{poly}(N)$. Provided that the system under consideration has a gap that does not scale with the system size, it was proven by Landau, Vazirani, and Vidick (2013) that an efficient algorithm scaling as a polynomial in the system size can be constructed to find an approximate MPS ground state. This result was extended by Arad *et al.* (2017) to the case in which the Hamiltonian has a small density of low-energy states. However, the question as to whether such an algorithm is possible for all critical systems with a gap scaling as $\mathcal{O}(1/N)$ is still open.

In the case of 2D PEPSs, the strongest approximation result is weaker but still certifies that we can simulate quantum spin

systems efficiently: a Gibbs state $\exp(-\beta H)$ can be approximated by a PEPO with bond dimension $D = (N/\epsilon)^{O(\beta)}$ (Hastings, 2006; Molnar *et al.*, 2015). If, however, the Hamiltonian consists of terms that all commute, as in the case of stabilizer Hamiltonians and all string nets, an exact representation of the ground states can be found in terms of a PEPS with a bond dimension that depends only on the size of the support of the local terms in the Hamiltonian terms and not on the system size (Verstraete *et al.*, 2006).

a. Area laws and approximability

Using arguments related to the decay of the Schmidt coefficients in 1D spin chains, it has been proven that an efficient approximation of the ground state for a finite spin chain with L sites can be obtained whenever the Renyi entanglement entropy of half a chain of length N is bounded by $S_\alpha(N) \leq c \log(N)$ for an $\alpha < 1$.

To show this, consider an exact ground state $|\psi_N\rangle$ defined on a spin chain with N sites and open boundary conditions, and assume that its Schmidt spectrum or eigenvalues of the reduced density matrix across a cut between sites i and $i + 1$ are given by $\{\mu_x(i)\}$. The main idea lies in the fact that for ground states these Schmidt coefficients decay fast, and therefore only a small error is made when one cuts the Schmidt decomposition after the D largest Schmidt coefficients. We define the residual probability $\epsilon_i(D) = \sum_{x=D+1}^\infty \mu_x(i)$ and $\epsilon_{\text{total}}(D) = \sum_{i=1}^N \epsilon_i(D)$. Verstraete and Cirac (2006) showed that a MPS with bond dimension D is guaranteed to exist for which the fidelity $|\langle \psi(A) | \psi_N \rangle| \geq 1 - \epsilon_{\text{total}}(D)$. If the Renyi entanglement entropy S_α with $\alpha < 1$ for a system of size N maximized over all bipartitions of the spin chain is given by $S_\alpha(N)$, there is a MPS with bond dimension D for which

$$\frac{\epsilon_{\text{total}}(D)}{N} \leq \left(\frac{D}{1-\alpha}\right)^{-(1-\alpha)/\alpha} \exp\left(\frac{1-\alpha}{\alpha} S_\alpha(N)\right). \quad (12)$$

This proves that the scaling of D to achieve a fidelity $1 - \epsilon$ is polynomial in $1/\epsilon$ and N provided that the Renyi entropy of half a chain satisfies $S_\alpha(N) \leq c \log N$. As shown in Sec. II.A.2, this is indeed the case for all gapped quantum spin systems, and also for all integrable critical spin chains with a logarithmic term. A MPS description therefore provides an exponential compression for a wide variety of ground states of quantum spin systems, including critical ones.

The fact that Renyi entropies with $\alpha < 1$ had to be used stems from the fact that they are more susceptible to the tails of the distribution of Schmidt values. Conversely, it holds that a state with an entanglement entropy satisfying a volume law for the von Neumann entropy cannot be approximated faithfully using MPSs, but this problem is undetermined for the $\alpha < 1$ Renyi entropies (Schuch *et al.*, 2008).

b. No low tensor rank ansatz

It has been argued that the MPS manifold is in one-to-one correspondence with the set of ground states of local gapped Hamiltonians. One may question whether it is possible to

obtain a similar identification with a simpler ansatz, such as linear combinations of polynomially many product states, as is the case in the examples given by De Lathauwer, De Moor, and Vandewalle (2000), Beylkin and Mohlenkamp (2002), Kolda and Bader (2009), and Hackbusch (2012). We now prove that this is not possible, since one can show that any injective MPS has an exponentially small overlap with any product state.

Indeed, consider an injective MPS in canonical form such that the right (left) fixed point of the associated transfer operator, seen as a completely positive map, is the identity matrix [a positive definite full matrix Λ with $\text{Tr}(\Lambda) = 1$]. See Sec. IV for more details. This implies that the operator norm $\|\Lambda\|_{\text{op}} < 1$. Consider $\epsilon = (1/2)(1 - \|\Lambda\|_{\text{op}})$. Then block the tensors until the transfer operator E is, in operator norm, ϵ close to the rank-1 projector $|\mathbb{1}\rangle\langle\mathbb{1}|$.

We denote the corresponding blocked tensor by A , and the maximum of the operator norm of the $D \times D$ matrices $A^w = \langle w|A$ by λ , where $\|w\| \leq 1$ in the Hilbert norm. λ can be rewritten as the maximum of $|(u|A^w|v)|$, where u , v , and w are again normalized in the Hilbert norm.

By the Cauchy-Schwarz inequality and the hypothesis on the transfer operator,

$$\begin{aligned} |(u|A^w|v)| &\leq |(u|(\bar{u}|E|v)|\bar{v})| \leq (u|u)(v|\Lambda|v) + \epsilon \\ &\leq \|\Lambda\|_{\text{op}} + \epsilon < 1, \end{aligned}$$

which implies that $\lambda < 1$ (by a standard compactness argument that holds due to the fact that the physical and bond dimensions are both finite).

Therefore, we can conclude [see Eq. (8)] that

$$\begin{aligned} |\langle w_1 w_2 \cdots w_N | \psi(A) \rangle| &= |\text{Tr} A^{w_1} A^{w_2} \cdots A^{w_N}| \\ &\leq D \prod_{j=1}^N \max_w \|A^w\|_{\text{op}} = D \lambda^N. \end{aligned}$$

c. Efficient descriptions in thermal equilibrium

The ground state of a gapped Hamiltonian can be well approximated by evolving the Euclidean path integral $\exp(-tH)|0\rangle$ for a time $t \simeq 1/\Delta$, with Δ the gap of the system and $|0\rangle$ a state with nonzero overlap with the ground state. If the Hamiltonian is frustration free and consists only of commuting terms, this expression is equal to the product of the exponentials of the local terms acting on the state $|0\rangle$, even in the limit of $t \rightarrow \infty$, and therefore automatically produces a MPS or PEPS with a bond dimension related to the size of the local support of the individual commuting terms. This implies that the ground states of all local stabilizer Hamiltonians and string nets have a simple exact description in terms of PEPSs with a bond dimension independent of the system size.

One can extend this result to the noncommutative case by using a Trotter expansion of $\exp(-tH) \approx [\prod_k \exp(-\beta h_k/M)]^M$ (with $H = \sum h_k$ the local terms in the Hamiltonian), with M sufficiently large. Each term $\exp(-\beta h_k/M)$ can be written as a local tensor network with a constant bond dimension. However,

when put together naively this construction yields a tensor network with a bond dimension that scales exponentially in M . Since each $\exp(-\beta h_k/M) \approx 1 - \beta h_k/M$ is close to the identity, it is possible to compress this representation by choosing a suitable subset of terms in the full expansion of $[\prod(1 - \beta h_k)]^M$. This way, one obtains a PEPO σ_D with bond dimension D that approximates the Gibbs state $\rho_\beta = e^{-\beta H}/Z$ up to error $\epsilon := \|\sigma_D - \rho_\beta\|_1$ in trace norm with a bond dimension $D = \exp\{O[\log^2(N/\epsilon)]\}$, as long as $\beta \leq O(\log N)$ (Molnar *et al.*, 2015), regardless of the spatial dimension. To obtain a polynomial scaling in N for fixed temperature, one instead starts from the Taylor series $e^{-\beta H} = \sum (-\beta)^\ell (\sum h_k)^\ell / \ell!$, expands $(\sum h_k)^\ell$, and finds that only clustering terms in this expansion are relevant. This way, one arrives at a PEPO approximation of the Gibbs state for which $D = (N/\epsilon)^{O(\beta)}$ for a fixed temperature (Hastings, 2006; Molnar *et al.*, 2015) [for a practical implementation, see Vanhecke, Van Damme *et al.* (2019)]; using a refined approximation of the Taylor series, an improved scaling of $D \sim \exp[O(\sqrt{\beta \log(n/\epsilon)})]$ was recently shown by Kuwahara, Alhambra, and Anshu (2021). From there one can construct a PEPS approximation for ground states by applying $e^{-\beta H}$ to a suitable initial product state at a temperature $\beta = O(\log N)$, which yields sufficient overlap with the ground state as long as the density of states scales at most as $N^c E$ for some constant c , that is, the polynomial in N (Hastings, 2006), which is the case for gapped systems with particlelike excitations. The reverse direction was analyzed by Chen, Kato, and Brandão (2020), who showed that generic MPDOs can be well approximated by Gibbs states of (quasi)local Hamiltonians.

A different approach can be taken if, instead of assuming a low density of low-energy states, one restricts to Hamiltonians that belong to a phase with a zero-correlation renormalization fixed point, as is the case for all known nonchiral topological phases in two dimensions. As derived by Coser and Perez-Garcia (2018) following an idea of Osborne (2007), the quasiadiabatic theorem (Hastings and Wen, 2005; Bachmann *et al.*, 2012) gives a finite depth quantum circuit whose gates act on $\log^{2+\delta} N$ neighboring sites ($\delta > 0$ but arbitrarily small). When applied on the renormalization fixed-point state (which is an exact PEPS with a finite bond dimension), the circuit gives an approximation of the ground state of the target Hamiltonian with an error that goes to zero with N faster than any polynomial. This approximation is a PEPS with bond dimension scaling as $e^{O(\log^{2+\delta}(N/\epsilon))}$. Moreover, it keeps all the virtual symmetries present on the initial renormalization fixed-point PEPS, and hence also the information about the topological phase that it belongs to; see Sec. III. A similar argument was used by Huang (2020) to propose quasipolynomial algorithms to compute local observables in systems belonging to the trivial phase.

In the case of gapped 1D systems, the strongest results along these lines have been obtained by randomizing the path integral and invoking a Chebyshev-based approximate ground space projector (Arad *et al.*, 2013, 2017; Huang, 2014). Given an infinite chain of d -level systems with $r \leq \text{poly}(n)$ -fold degenerate ground space and gap Δ and considering one cut in an infinite spin chain, one finds that

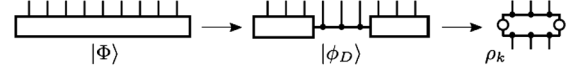


FIG. 10. Construction of a translation invariant MPO approximation to infinite translation invariant ground states by truncating the bond dimension in an intermediate region (Schuch and Verstraete, 2017). The resulting MPO ρ_k for k sites is then patched together and superimposed with its translations.

$$\log[\epsilon(D)] = -\frac{\Delta^{1/3} \tilde{\Omega}[\log(D/r)^{4/3}]}{(\log d)^{4/3}} + \frac{(\log d)^{8/3}}{\Delta}, \quad (13)$$

where $\epsilon(D)$ is as previously defined, that is, the sum of the square of all but the first D Schmidt coefficients on that cut, and $g = \tilde{\Omega}(h)$ exactly if $h = \tilde{O}(g) \equiv O[g \log(g)^k]$ for some k . In other words, the truncation error $\epsilon(D)$ decreases super-polynomially with the number of Schmidt coefficients kept, i.e., the bond dimension.

A corollary of this result is the existence of efficient translationally invariant MPO descriptions for infinite translationally invariant gapped quantum spin chains, in the sense that any local expectation values of the MPO approximation are ϵ close to those of the exact ground state. A direct proof was formulated by Schuch and Verstraete (2017) and we sketch it here; building on it, similar results were obtained for pure uniform MPSs (Dalzell and Brandao, 2019; Huang, 2019). The construction is as follows: define a MPO ρ_k on k sites by cutting the exact ground state $k+1$ times and then tracing the outer spins (Fig. 10). This yields a MPO with bond dimension D^2 such that the trace distance to the true ground state reduced density matrix σ_k is $\|\rho_k - \sigma_k\|_1 \leq 2\sqrt{2\epsilon(D)(k+1)}$. To obtain a translationally invariant MPO for the infinite chain, take an infinite tensor product of this MPO with itself and sum over all k translations. The resulting MPO has bond dimension kD^2 and its reduced state on ℓ contiguous sites approximates σ_ℓ up to error

$$\epsilon \leq 2\sqrt{2k\epsilon(D)} + \frac{2(\ell-1)}{k}.$$

Choosing an appropriate k and using Eq. (13), one gets the result that the bond dimension required to give an ϵ approximation on ℓ sites scales as $D \leq \ell/\epsilon$. This result demonstrates that the MPS compression is still faithful in the thermodynamic limit, and hence provides clear evidence for the falling of the exponential many-body wall.

Finally, approximation results of thermal states by MPOs can also be obtained from area laws for thermal states; see Kuwahara, Alhambra, and Anshu (2021) and Jarkovsky *et al.* (2020).

d. Many-body localization

Matrix product states also pop up for the description of eigenstates of quantum spin systems subject to randomness. It has been argued that all eigenstates, not just the ground state, of many-body localized (MBL) Hamiltonians exhibit an area law for the entanglement entropy, and furthermore that all have an efficient description in terms of matrix product states (Bauer and Nayak, 2013; Nandkishore and Huse, 2015; Wahl, Pal, and

Simon, 2017). This follows from a result of Imbrie (2016) proving that there is a low-depth quantum circuit that completely diagonalizes any MBL Hamiltonian.

3. Manifold of MPSs and the time-dependent variational principle (TDVP)

a. Manifold and the TDVP

As previously demonstrated, ground states of local gapped quantum spin chains can efficiently be parametrized as matrix product states, and furthermore any such MPS is the ground state of a local Hamiltonian. This implies that the manifold of a MPS is in one-to-one correspondence to all possible ground states, and this opens up a large number of perspectives, including the classification of all phases of matter of 1D spin chains.

The manifold of infinite uniform matrix product states was studied in detail by Haegeman *et al.* (2014). MPSs have the mathematical structure of a principal fiber bundle; this follows from the parameter redundancy corresponding to the gauge transforms. The total bundle space corresponds to the parameter space, i.e., the space of tensors associated with a physical site. The base manifold is embedded in the Hilbert space and can be given the structure of a Kähler manifold by inducing the Hilbert space metric. A similar construction holds in the finite case of MPSs with open boundary conditions. The metric is governed by the Schmidt numbers and is singular when the MPS is not normal or injective.

Given a specific MPS on the manifold, we can associate a linear subspace with it, namely, the tangent space on the manifold (Haegeman *et al.*, 2011; Vanderstraeten, Haegeman, and Verstraete, 2018). The dimension of that space is $(d - 1)D^2$ and is spanned by the vectors

$$|\psi_{\alpha\beta i}(A)\rangle = \frac{\partial}{\partial A_{\alpha\beta}^i} |\psi(A)\rangle.$$

Owing to the product rule of differentiation, these vectors correspond to plane waves and are hence normalized as delta functions. D^2 of these are linearly dependent due to the gauge freedom. These degrees of freedom can be used to make the Gram matrix or metric $g_{xy} = \langle \psi_x(A) | \psi_y(A) \rangle$ locally Euclidean ($g_{xy} = \delta_{xy}$); the gauge transformations needed to achieve this are precisely those that bring the MPSs into left and right canonical form. As shown in Fig. 11, the projector on the tangent space $P_{T(A)}$ in a specific point $|\psi(A)\rangle$ can be constructed in terms of a sum of matrix product operators that are expressed in terms of the tensors in left (A_L) and right (A_R) canonical form.

This expression is of great practical interest, as it allows one to write evolution equations within the manifold of MPSs. Assume that we aim to simulate the time evolution generated by a Hamiltonian H of a quantum state $|\psi(A)\rangle$ that is initially a MPS. The evolution described by the Schrödinger equation $i\partial_t |\psi\rangle = H|\psi\rangle$ will take the state outside of the manifold and hence seemingly make the problem intractable. The projector on the tangent plane, however, allows one to pull the state back on the manifold in a way that maximizes the overlap to any state on the manifold as follows:

$$[A_L^s]_{\alpha,\beta} = \alpha \begin{array}{c} \nearrow \\ s \\ \searrow \end{array} \beta \quad [A_R^s]_{\alpha,\beta} = \alpha \begin{array}{c} \nwarrow \\ s \\ \nearrow \end{array} \beta$$

$$\begin{array}{c} \left(\begin{array}{c} \leftarrow \\ \rightarrow \end{array} \right) = \left(\begin{array}{c} \leftarrow \\ \rightarrow \end{array} \right) = \end{array}$$

$$P_{T(A)} = \sum_{i=1}^n \begin{array}{c} \leftarrow \leftarrow \leftarrow \leftarrow \leftarrow \\ \leftarrow \leftarrow \leftarrow \leftarrow \leftarrow \end{array} \Big| \begin{array}{c} \leftarrow \leftarrow \leftarrow \leftarrow \leftarrow \\ \leftarrow \leftarrow \leftarrow \leftarrow \leftarrow \end{array} \\ - \sum_{i=1}^n \begin{array}{c} \leftarrow \leftarrow \leftarrow \leftarrow \leftarrow \\ \leftarrow \leftarrow \leftarrow \leftarrow \leftarrow \end{array} \Big| \begin{array}{c} \leftarrow \leftarrow \leftarrow \leftarrow \leftarrow \\ \leftarrow \leftarrow \leftarrow \leftarrow \leftarrow \end{array}$$

FIG. 11. For a given MPS, one considers the two possible canonical forms, given by tensors A_L and A_R , where the right and left fixed points of the transfer operator, respectively, are the identities; see Sec. IV for more details. They are distinguished by the direction of the triangle. They allow one to express the tangent space projector $P_{T(A)}$ as a sum of MPOs. The variable i in the sum corresponds to the position of the central (blue) index.

$$i \frac{\partial}{\partial t} |\psi(A)\rangle = P_{T(A)} H |\psi(A)\rangle.$$

The corresponding equations are the MPS equivalents of the following TDVP as originally derived in the context of Hartree-Fock theory (Dirac, 1930):

$$\partial_t A_{\alpha\beta}^i = F(A_{\alpha\beta}^i).$$

This equation is nonlinear due to the fact that the projector $P_{T(A)}$ itself depends on A . It conserves the energy and all symmetries that can be represented within the tangent plane, and it is possible to associate symplectic structure with a Poisson bracket to it (Haegeman *et al.*, 2011). MPS therefore yields novel semiclassical descriptions of the dynamics of quantum spin chains.

There are many methods to solve these differential equations in practice, and the most interesting case consists of evolving the equations in imaginary time so as to converge to the ground state. The DMRG method (White, 1993) can be understood in terms of splitting the differential equation into the $2N - 1$ MPO terms and then evolving each one of them for an infinitely large imaginary time step (Haegeman *et al.*, 2016). Increasing the bond dimension can be understood in terms of a projection on the two-site tangent plane, and time-dependent DMRG can be completely formulated within the time-dependent variational principle. See the review by Vanderstraeten, Haegeman, and Verstraete (2018) on tangent space methods for MPSs.

b. Excitations

The tangent plane of a MPS representing the ground state of a quantum spin system reveals another interesting aspect of MPSs, namely, the fact that the projection of the full many-body Hamiltonian on its linear subspace gives rise to an effective Hamiltonian whose spectrum reveals the dispersion relations of the true elementary excitations of the many-body Hamiltonian (Rommer and Östlund, 1997; Porras, Verstraete, and Cirac, 2006; Haegeman, Pirvu *et al.*, 2012; Pirvu,

Haegeman, and Verstraete, 2012). More precisely, the tangent plane yields a method for parametrizing plane waves of the form $|\psi_k(A, B)\rangle =$

$$|\psi_k(A, B)\rangle = \frac{1}{\sqrt{N}} \sum_x e^{2\pi i k x} \text{Tr}[A^{i_1} \dots A^{i_{x-1}} B^{i_x} A^{i_{x+1}} \dots] |i_1\rangle |i_2\rangle \dots,$$

which correspond to Bloch wavelike excitations; the tensors $B_{\alpha\beta}^i$ can be easily determined by solving a linear eigenvalue problem of the effective Hamiltonian. While making use of Lieb-Robinson techniques (Hastings, 2004b; Bravyi, Hastings, and Verstraete, 2006; Hastings and Koma, 2006; Nachtergaele and Sims, 2010), it was proven by Haegeman, Michalakis *et al.* (2013) that such an ansatz provides a faithful representation of the exact excitations in the system if these are part of an isolated band with a gap $\Delta(k)$ above it in the momentum sector k ; by allowing the tensor B to act on l sites, the fidelity to the exact excited state is lower bounded by $1 - p(l) \exp[-\Delta(k)l/2v_{LR}]$, with $p(l)$ a polynomial in l and v_{LR} the Lieb-Robinson velocity.

This is a strong manifestation of the fact that ground state correlations reveal plenty of information about the excitation spectrum. In fact, as previously commented, the spectrum of the transfer matrix E of the MPS itself already contains this information: the correlation length can be extracted from the gap in eigenvalues of E , and the phases of all eigenvalues reveal information about the full dispersion relation (Zauner *et al.*, 2015).

D. Bulk-boundary correspondences

One of the most interesting consequences of tensor network descriptions is the fact that single tensors can represent entire many-body states if translational invariance is imposed. Once we know the geometry of the lattice, which tells us how to contract the local tensor with copies of itself, the entire state is completely determined. Thus, all physical properties (i.e., expectation values of observables) are contained in the tensor A , as they are all functions of the coefficients of that tensor. In a sense, one could establish a map between all physical properties of many-body states (given a certain geometry in d spatial dimensions) and the space of tensors corresponding to that geometry. However, this map is highly nonlinear, as the expectation values of observables in Hilbert space will be complex functions of the tensor.

The special form of the MPS or PEPS allows one to establish other maps that are linear. In particular, if the PEPS is defined in a Hilbert space \mathcal{H}_d corresponding to a certain geometry in d spatial dimensions, it is possible to map all physical properties to those of a different space \mathcal{H}_{d-1} corresponding to $d-1$ spatial dimensions (Cirac *et al.*, 2011). Furthermore, the map takes the form of a linear isometry. More explicitly, given a region R it is possible to find an isometry \mathcal{U}_R that maps the reduced state, and all operators acting on that region, to a state and operators acting on its boundary ∂R so that the expectation values computed in R coincide with those computed in ∂R .

The existence of this holographic principle is not surprising, at least for ground states of local Hamiltonians fulfilling the

area law; see Sec. II.A.2. In fact, the area law states that the entropy of the reduced state in a region R scales with the number of particles at its boundary. As the entropy counts degrees of freedom, this intuitively means that one can map the reduced state to a space that lives in the boundary ∂R . What is special about tensor networks is that the Hilbert space of this boundary is dictated by the bond dimension of the tensors, and one can thus talk about geometrical notions there too. For instance, the state in the boundary may be a mixed state that can be described as the Gibbs state of a local Hamiltonian, where the notion of locality refers to that geometry. All this becomes clearer when we later show how to explicitly construct the bulk-boundary correspondence.

There is another way to construct a bulk-boundary correspondence that may be more “physical” (Yang *et al.*, 2014). The previously mentioned method relates the physical properties in a region of the bulk to those of another theory living in the boundary of such a region, but in thermal equilibrium. The boundary Hamiltonian characterizing such a Gibbs state in the boundary does not have a dynamical meaning (i.e., does not generate the evolution), but instead simply a statistical one. In contrast, it is possible to derive a Hamiltonian that describes the dynamics of the physical boundary (i.e., the edges) of a many-body system with respect to perturbations in the bulk. One can build an isometry to map this Hamiltonian to one that acts on the auxiliary indices associated with the edges of the system. Thus, one can describe the dynamics in the bulk by simply transferring the dynamics to these auxiliary indices by using the isometry. For PEPSs with a finite correlation length, this isometry will affect only those lattice sites that are close to the physical boundary, and thus will be describing edge excitations. All this is reminiscent of the physics of the quantum Hall effect in two dimensions, where there is a 1D Hamiltonian that describes the dynamics of the edge states. What we later discuss is that something similar occurs with generic PEPSs.

Recently the kind of bulk-boundary relations appearing in tensor networks have been used to construct toy models of the AdS/CFT correspondence (Maldacena, 1999), as it appears in holographic principles proposed in the context of high-energy physics and string theory. The construction of MERAs (and TTNs) can be associated with a coarse tessellation of an anti-de Sitter geometry, where the renormalization direction coincides with the radial coordinate (Evenbly and Vidal, 2011; Swingle, 2012). The 1D MERA construction can be interpreted as a quantum circuit that implements a conformal mapping between the physical Hilbert space and the renormalized one in scale space (Czech *et al.*, 2016); the entanglement spectrum of the MERA can be identified with that of a MPO representing a thermal state, hence relating the bond dimension of the MERA approximation to the bond dimension needed to represent thermal states using MPOs (Van Acoleyen *et al.*, 2020). For MERAs in 1D it is straightforward to show that they display a logarithmic correction to the area law associated with CFTs by simply finding the shortest path in the MERA embracing the region in which one is interested (Vidal, 2008) [on the other hand, 2D MERAs can be embedded in PEPSs and thus obey an area law (Barthel, Kliesch, and Eisert, 2010)]. Swingle pointed out an interesting connection between this way of determining the entropy and

the Ryu-Takayanagi formula relating the entropy of the ground state of a CFT and the geometry of AdS space (Swingle, 2012). This indicated that MERAs could define geometries through that formula, and thus in a sense relate the entanglement properties of many-body states with geometries appearing in gravitational physics. It was later realized that, by adding a physical index to the MERA tensors, one could build a linear correspondence (an isometry) between these physical indices and the auxiliary ones living in the boundary (Pastawski *et al.*, 2015). This is closely related to the previously mentioned bulk-boundary correspondence. In fact, if one builds PEPS in a tessellated hyperbolic geometry using the quantum circuit construction, they are equivalent. In recent works (Hayden *et al.*, 2016; Kohler and Cubitt, 2019; Qi and Yang, 2018; Qi, Yang, and You, 2017), it was shown that, by appropriately choosing the tensors that build the tensor network state, one can ensure certain desired properties of the AdS/CFT correspondence and, in this way, explicitly build toy models displaying such properties.

1. Entanglement spectrum

We now consider a many-body state $|\Psi\rangle$ in d dimensions and its reduced state ρ_R in a region R . The entanglement spectrum σ_Ψ of the state with respect to region R is defined as the spectrum of $H_R = -\log(\rho_R)$. These dimensionless numbers are related to the entanglement of region R and its complement \bar{R} . In fact, we can always write the Schmidt decomposition of $|\Psi\rangle$ as

$$|\Psi\rangle = \sum_{n=1}^{d_R} \lambda_n |\varphi_n\rangle_R \otimes |\psi_n\rangle_{\bar{R}}, \quad (14)$$

where φ_n and ψ_n are orthonormal sets in \mathcal{H}_R and $\mathcal{H}_{\bar{R}}$, respectively. These are the Hilbert spaces corresponding to the lattice sites in regions R and \bar{R} and have dimensions $d^{|\bar{R}|}$ and $d^{|R|}$, respectively, where as usual $|R|$ denotes the number of lattice sites in R . $\lambda_n \in [0, 1]$ are the Schmidt coefficients and completely characterize the entanglement of state Ψ with respect to regions R and \bar{R} . As any Schmidt decomposition, the number of coefficients is $d_R \leq \min(d^{|\bar{R}|}, d^{|R|})$. Given the normalization of $|\Psi\rangle$, their squares add up to 1. By definition,

$$\sigma_\Psi = \{-\log(\lambda_n^2)\}_{n=1}^{d_R}, \quad (15)$$

which indicates that the entanglement spectrum is simply the Schmidt coefficients, which thus fully characterize the entanglement. The operator H_R is usually referred to as the entanglement Hamiltonian.

Li and Haldane (2008) argued that for quantum Hall states (integer or fractional) the low-lying part of the entanglement spectrum coincides (up to a proportionality constant) with the Hamiltonian corresponding to the CFT associated with its topological order. This has been verified for other states with topological order and proven for more general states whose wave function can be written in terms of correlators of a CFT under certain assumptions; see Dubail, Read, and Rezayi (2012), Qi, Katsura, and Ludwig (2012), the references therein, and Sec. III.B.2). In models without topological order

in $d = 2$ dimensions it has also been found that the lower sector of the entanglement spectrum resembles that of local theories in $d = 1$ dimensions (Cirac *et al.*, 2011; Lou *et al.*, 2011). For instance, for the AKLT state in a square lattice it was found that the entanglement spectrum also resembles that of a Wess-Zumino-Witten $SU(2)_1$ theory. We discuss this in more detail in Sec. II.D.2.

2. Boundary theory

Both the existence of an area law and the numerical results displaying a 1D-like spectrum in ground states of 2D theories indicate that it should be possible to compress the degrees of freedom corresponding to any region R from $|R|$ to $|\partial R|$. More specifically, one could always find a P_R such that $\tilde{\rho}_R = P_R \rho_R P_R \approx \rho_R$, where P_R is a projector onto a subspace of \mathcal{H}_R with dimensions $d_b^{|\partial R|}$, where d_b is a constant integer. Note that this hints to an area law given the fact that the von Neumann entropy of a mixed state is upper bounded by the logarithm of the dimension of the Hilbert space on which it is supported; in this case, $S(\tilde{\rho}_R) \leq |\partial R| \log(d_b)$. Furthermore, there should be a Hamiltonian $H_{\partial R}$ acting on a different space corresponding to $d - 1$ spatial dimensions such that the lowest part of the entanglement spectrum coincides with the spectrum of $H_{\partial R}$. The latter should somehow be local (note that otherwise it does not make as much sense to talk about the spatial dimensions).

For PEPSs it is possible to make the previous conclusions rigorous (Cirac *et al.*, 2011). The projector P_R comes automatically from the theory of tensor networks and, in fact, $\tilde{\rho}_R = \rho_R$, where $d_b = D$ (the bond dimension). Furthermore, for any region R there is an isometry

$$U_R: \mathcal{H}_R \rightarrow \mathcal{H}_{\partial R} \quad (16)$$

with $U_R^\dagger U_R = \mathbb{1}_{\partial R}$ and $U_R U_R^\dagger = P_R$ such that

$$\rho_R = P_R \rho_R P_R = U_R^\dagger \sigma_{\partial R} U_R, \quad (17)$$

where

$$\sigma_R = U_R \rho_R U_R^\dagger \quad (18)$$

is an operator defined on the auxiliary indices at ∂R (coming out of region R ; see Fig. 12). In fact, for any observable X_R acting on \mathcal{H}_R we can define $X_{\partial R} = U_R X_R U_R^\dagger$ such that

$$\langle \Psi_R | X_R | \Psi_R \rangle = \text{tr}_R(X_R \rho_R) = \text{tr}_{\partial R}(X_{\partial R} \sigma_{\partial R}). \quad (19)$$

Equation (19) expresses the fact that one can compute all physical properties of the bulk (in R) in terms of a state living in the boundary $\sigma_{\partial R}$ and defines the bulk-boundary correspondence. Furthermore, we can identify the entanglement Hamiltonian $H_{\partial R} = -\log(\sigma_{\partial R})$ or, equivalently, write

$$\sigma_{\partial R} = e^{-H_{\partial R}}. \quad (20)$$

The isometric character of U_R ensures that the entanglement spectrum $\sigma(H_R) = \sigma(H_{\partial R})$.

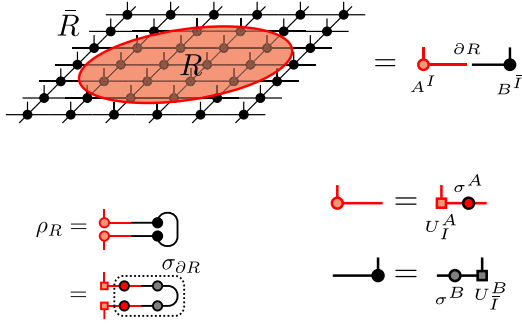


FIG. 12. Bulk-boundary correspondence. For any given region R , ρ_R can be isometrically mapped to a density operator $\sigma_{\partial R}$ that is defined in the auxiliary indices of the boundary of R via a polar decomposition; see the main text.

The derivation of the previous statements is straightforward, and we reproduce it here. For that, we consider the PEPS $|\psi\rangle$ and denote by A_i^I the tensor corresponding to the contraction of all the auxiliary indices in region R , where we have combined all the physical indices of region R into a single index I , and all the auxiliary indices that have not been contracted (and thus stick out of region R) into an index i . We do the same with region \bar{R} and denote the corresponding tensor by $B_i^{\bar{I}}$. Note that the auxiliary indices connect R and \bar{R} , and thus the auxiliary legs are characterized by the same combined index i . Thus, we can write the coefficients of $|\psi\rangle$ as

$$\Psi_{I\bar{I}} \equiv \langle I, \bar{I} | \psi \rangle = \sum_{i=1}^{D^{|\partial R|}} A_i^I B_i^{\bar{I}}. \quad (21)$$

Considered as matrices, A and B can be expressed in terms of their polar decomposition

$$A_i^I = \sum_{r=1}^{D^{|\partial R|}} U_{I,r}^A \sigma_{r,i}^A, \quad (22)$$

$$B_i^{\bar{I}} = \sum_{r=1}^{D^{|\partial R|}} U_{I,r}^B \sigma_{r,i}^B. \quad (23)$$

Here $U^{A,B}$ are isometries and $\sigma^{A,B}$ positive semidefinite operators. From here, one directly obtains Eq. (18), where $U_R = U^A$ and $\sigma_{\partial R} = \sigma^A (\overline{\sigma^B})^2 \sigma^A$.

The possibility of explicitly building this bulk-boundary correspondence for PEPSs is a direct consequence of its TN structure. Indeed, in this case there is a natural identification of the degrees of freedom of the boundary with these corresponding to the auxiliary indices. The boundary state, as well as the Hamiltonian $\mathcal{H}_{\partial R}$, acts on that space. However, there is nothing that guarantees that this Hamiltonian is in any way local. In numerical studies, however, it has been always found that if the state $|\psi\rangle$ has a finite correlation length, then the boundary Hamiltonian is quasilocal (Cirac *et al.*, 2011). With a suitable treatment of sectors, this also holds for symmetry-breaking (Rispler, Duivenvoorden, and Schuch, 2015; Rispler, Duivenvoorden, and Schuch, 2017) and topological (Schuch *et al.*, 2013) phases. More specifically, we can always expand it as

$$H_{\partial R} = \sum_{r=1}^{|\partial R|} h_r, \quad (24)$$

where h_r combines operators with nontrivial support on exactly r consecutive sites. In the studied examples, there is clear evidence that $\|h_r\|$ decays exponentially with r . Furthermore, in some cases where the many-body state is changed as a function of a parameter $\Psi(g)$ and the corresponding correlation length $\xi(g)$ diverges at some $g = g_c$, this exponential decay disappears, so the boundary Hamiltonian displays long-range couplings. A first rigorous proof in this direction was provided by Kastoryano, Lucia, and Perez-Garcia (2019) and Perez-Garcia and Pérez-Hernández (2020): If the boundary Hamiltonian is sufficiently local, then the parent Hamiltonian of $|\Psi\rangle$ is gapped (and hence $|\Psi\rangle$ has a finite correlation length).

As explained in Sec. III, if $|\Psi\rangle$ displays topological order and corresponds to a specific sector, $\sigma_{\partial R}$ itself is supported on a subspace of the boundary. In the presence of a finite correlation length, the boundary Hamiltonian is also expected to be local (Schuch *et al.*, 2013; Haegeman *et al.*, 2015) and the nonlocal projector related to the topological order can be understood as a superselection sector.

A key point in the construction is that global symmetries in the bulk wave function $|\Psi\rangle$ will show up as global symmetries of the boundary state $\sigma_{\partial R}$ with specific representations, and correspondingly as symmetries of the entanglement Hamiltonian $H_{\partial R}$, which (together with locality) can significantly restrict the possible form of $H_{\partial R} = \sum h_r$. This is further discussed in Sec. III.B.2.

3. Edge theory

We now consider a PEPS $|\Psi\rangle$, defined on a 2D torus, with translational invariance along both directions. As previously explained, it is always possible to find a frustration-free parent Hamiltonian H for which $|\Psi\rangle$ is the ground state (possibly not unique). This Hamiltonian is itself translationally invariant, and thus can be written as a sum of translations of a projector H_r acting on few sites that also annihilate $|\Psi\rangle$. Now, following Yang *et al.* (2014), we consider the same problem but with open boundary conditions. That is, we take the same Hamiltonian H_R but consider only the terms acting on some region R . The ground state of that Hamiltonian is now highly degenerate. In fact, by defining the tensor A as in Eq. (22), for any

$$|\varphi_r\rangle = \sum_I A_r^I |I\rangle \quad (25)$$

we have

$$H_R |\varphi_r\rangle = 0. \quad (26)$$

We denote by $\mathcal{H}_0 \subseteq H_{\partial R}$ the subspace of the auxiliary indices spanned by all vectors A_r^I , with $I = 1, \dots, d^{|\partial R|}$. In the generic case in which $|\Psi\rangle$ is injective, all $|\varphi_r\rangle$ will be linearly independent and $\mathcal{H}_0 = H_{\partial R}$. If $|\Psi\rangle$ has topological order, $\mathcal{H}_0 \subsetneq H_{\partial R}$ will be the support of a MPO projector; see Sec. III. In both cases, $|\varphi_r\rangle$ will span the entire ground space

of H_R by construction. We denote by P_R the projector onto that subspace.

We assume that H_R is gapped, i.e., that there is a $\gamma > 0$ such that, for any size N , the gap Δ_N above the ground state subspace is $\Delta_N \geq \gamma > 0$. If we add a small local perturbation to H_R such that the new Hamiltonian reads

$$H'_R = H_R + \epsilon V_R, \quad (27)$$

where V_R is a sum of translations of a local operator acting on a few neighboring sites, the degeneracy of the ground state subspace will be lifted. Assuming that ϵ is small enough that perturbation theory applies, the effect of V_R on the low-energy sector can be determined with the help of degenerate perturbation theory, which yields the following effective Hamiltonian:

$$H''_R = \epsilon P_R V_R P_R. \quad (28)$$

Using the bulk-boundary correspondence of Sec. II.D.2, we can map this Hamiltonian as follows to the auxiliary indices at the edge of the system:

$$h_{\partial R} = \epsilon U_R V_R U_R^\dagger. \quad (29)$$

We can now use Eq. (29), which acts on the auxiliary indices corresponding to the edges of our system, to determine the low-energy dynamics generated by the perturbation and then map it back to the bulk. Note that, in contrast to the scenario in Sec. II.D.2, where the boundary Hamiltonian had a merely statistical mechanics role, in the current scenario the edge Hamiltonian (29) describes the real low-energy dynamics in the system.

In summary, we see that the isometry U_R defined by the PEPS can be considered a mapping between a theory that lives in the bulk and another one that lives in the boundary and allows one to relate the physics of the two.

As before, in practice the edge Hamiltonian turns out to be quasilocal for systems with a finite correlation length. When mapping back the dynamical action of $H_{\partial R}$ from the boundary, only regions close to the edge (at a distance of about the correlation length) will be affected, so perturbations give rise only to excitations at the edge. This is reminiscent of the quantum Hall effect, where the low-energy excitations occur at the edge. Furthermore, the global symmetries of $|\Psi\rangle$ (and thus of H) will be inherited by $H_{\partial R}$; see Sec. III. In addition, by changing parameters in V_R , one can drive phase transitions in $H_{\partial R}$: This illustrates that it is possible to have phase transitions in the edge of a system, and in fact realize a range of different phases, without changing the phase of the gapped bulk (Yang *et al.*, 2014). Finally, as we later discuss, the existence of topological order in $|\Psi\rangle$ is reflected by the fact that any $H_{\partial R}$ (resulting from a perturbation) has to commute with a nonlocal MPO projector, which thus plays the role of a superselection rule at the boundary. Indeed, this is how the topological anomaly is revealed in this setup.

E. Renormalization and phases of matter

As previously discussed, tensor networks give efficient representations of ground states, thermal states, and elementary excitations in gapped locally interacting systems. Therefore, if one is interested in classifying the different possible features appearing in the low-energy sector of gapped strongly correlated lattice models, one can restrict the attention to MPSs and PEPSs.

In this review we focus on properties that are global (or topological), in the sense that they are stable under renormalization steps. Since its conception by Kadanoff, Fisher, and Wilson, the renormalization group (RG) has played a central role in many-body physics. From the conceptual point of view, the RG has clarified how simple toy Hamiltonians of spin systems can nevertheless exhibit the full spectrum of features of realistic Hamiltonians, as the universal properties of both theories at long length scales can be identified. In essence, RG provides a systematic method for integrating out UV degrees of freedom, thereby mapping a Hamiltonian to one for which the length scale is reduced. The correlation length of the ground state of a Hamiltonian which is a fixed point of a RG flow should hence be 0 or ∞ , with the former corresponding to trivial or topological phases and the latter to critical systems.

Formally, a renormalization step can be understood as the composition of two processes: blocking several sites, which coarse grain the lattice, and acting with a reversible operation in the blocks that rearranges the local entanglement pattern. Reversibility is crucial since we want to guarantee an exact renormalization process without discarding any relevant degrees of freedom.

As we are interested in the topological content of a phase, arguably the best way to capture it is to restrict the attention to renormalization fixed points (RGFPs), where all local entanglement is integrated out and only the topological content remains. It is, however, difficult to characterize such fixed points without a description of all possible renormalization flows. To circumvent this problem, we define RGFPs in tensor networks intrinsically, from first principles, without referring to a concrete flow. For that we identify some key properties that any RGFP of a gapped phase must have and conclude from there that there is indeed a renormalization flow for which the given state is a fixed point, together with a structural characterization of the tensor networks that are RGFPs.

We first analyze the case of MPSs, following Verstraete *et al.* (2005) and Cirac *et al.* (2017a), and comment on the implications for the classification of 1D phases. We then analyze the case of MPOs, following Cirac *et al.* (2017a), and show how a fusion category emerges from the RGFP conditions that sheds light on the classification of 2D phases via the bulk-boundary correspondence analyzed in Sec. III.B.2. We also comment on RGFPs in higher dimensions and concrete renormalization flows in tensor networks.

1. Renormalization fixed points in MPSs

As just discussed, we should identify properties that any RGFP MPS must have. For that, given the ground state subspace S of a local Hamiltonian H , we say that it has *zero correlation length* if connected correlation functions vanish.

That is, for any state $\Psi \in S$ and any two observables A and B acting on non-neighboring regions (i.e., those not directly connected by the action of H),

$$\langle \Psi | AB | \Psi \rangle - \langle \Psi | AP_S B | \Psi \rangle = 0, \quad (30)$$

where P_S is the projector onto S . Note that, according to this definition, a Greenberger-Horne-Zeilinger (GHZ) state has zero correlation length.

As normal MPSs have a finite correlation length and general MPSs can be expressed as superpositions of normal MPSs, it should happen that as we block the correlation length decreases. Thus, the RGFP must have zero correlation length. We then say that a MPS is a RGFP if it has zero correlation length. Since the transfer matrix E of a MPS is the operator that mediates the correlations in the system (Sec. II.B.3), zero correlation length is equivalent to the following condition:

$$E^2 = E. \quad (31)$$

There are other notions that are clearly connected to RGFPs that can also be shown to be equivalent to zero correlation length in MPSs (Cirac *et al.*, 2017a) and can then be taken as alternative (but equivalent) definitions of RGFPs for MPSs. The first is the fact that the parent Hamiltonian can be written as sums of local terms that mutually commute. It was recently shown by Kastoryano and Lucia (2018) that if the parent Hamiltonian of a PEPS is gapped, then the norm of the commutator of the associated terms goes to zero as we coarse grain the system; see Sec. IV. One can then expect that RGFP PEPSs (and particularly RGFP MPSs) have commuting parent Hamiltonians. This property is indeed equivalent to the RGFP, as shown by Cirac *et al.* (2017a).

The second equivalent notion is the *saturation of the area law*. Strong subadditivity of the von Neumann entropy (Lieb and Ruskai, 1973) implies that for a spin chain of size N and a region of size $L < N/2$, $S_{L+1}^{(N)} \geq S_L^{(N)}$, where $S_L^{(N)}$ denotes the entanglement entropy of that region. Since MPSs fulfill the area law (i.e., $S_L^{(N)}$ is upper bounded by a constant that is independent of L and N), it follows that $\lim_{L \rightarrow \infty} S_L^\infty = c < \infty$. This implies that RGFPs must satisfy $S_L^{(N)} = c$ for all L and thus, in particular, for $L = 1$. That is, they must saturate the area law. As previously stated, the converse is also true.

We now focus on property (31) and see what can be concluded from it.

First, since different Kraus representations of a completely positive map must be related by an isometry (Stinespring, 1955; Wolf, 2012), a tensor A corresponds to a MPS RGFP if and only if (Verstraete *et al.*, 2005)

$$A^{i_1} A^{i_2} = \sum_{i_1, i_2} U_{(i_1, i_2), j} A^j \quad (32)$$

for some isometry U . Graphically, we have

$$\begin{array}{c} \text{---} \square A \text{---} \square A \text{---} \\ \text{---} \square A \text{---} \end{array} = \begin{array}{c} \text{---} \square A \text{---} \\ \text{---} \square U \text{---} \end{array} . \quad (33)$$

That is, the MPS given by A is the renormalization fixed point of a particular type of flow that is obtained by acting with an isometry on the physical degrees of freedom.

Such a flow has a natural interpretation in light of the usual definition of topological phases in quantum systems. Two ground states, particularly two PEPSs, are said to be in the same topological phase precisely if there is a low-depth local quantum circuit converting one state into the other. Via the quasiadiabatic theorem (Hastings and Wen, 2005; Bachmann *et al.*, 2012), this corresponds to the existence of a continuous gapped path of Hamiltonians connecting the two systems. The intuition behind this definition is that, in order to proceed to a different phase, one needs to generate global (topological) correlations, which requires a time (i.e., circuit depth) that scales with the system size.

The flow described in Eq. (33) keeps a state in the same phase. If the unitary implemented in the renormalization flow aims to disentangle the left and right ends of a block, one expects only either nearest-neighbor or purely global entanglement to remain in the limit. Indeed, if the tensors are normal, the RGFP condition $E^2 = E$ implies that E is a rank-1 projector, and (using the isometric relation between Kraus representations) we can then split each spin at a given site n into a left and a right system n_ℓ and n_r , such that the structure of the RGFP state up to local isometry is of the form

$$|\Phi\rangle = \otimes_{n=1}^N |\varphi\rangle_{(n-1)_r, n_\ell}, \quad (34)$$

where $|\varphi\rangle$ is an entangled state defined on the right and left parts of neighboring spins. If the state is not normal, then one has a direct sum of states of the form of Eq. (34), where the terms in the sum are locally orthogonal (meaning that the corresponding $|\varphi\rangle$ are supported on orthogonal subspaces for each of the spins).

These states provide representatives for all possible phases of matter for closed 1D systems; see Sec. III.A.2.

2. MPDOs

For the case of mixed states we follow a similar approach. As with Eq. (31), in this context we say that a MPDO associated with tensor M has zero correlation length if

$$\begin{array}{c} \text{---} \square M \text{---} \square M \text{---} \\ \text{---} \square M \text{---} \end{array} = \begin{array}{c} \text{---} \square M \text{---} \end{array} . \quad (35)$$

Unlike in the pure state case, this is not enough to guarantee that a given MPDO has no length scale associated with it. In particular, this does not necessarily imply that the MPDO fulfills a property analogous to the saturation of the area law. As previously mentioned, in the context of mixed states the notion of an area law refers to the mutual information, not the entanglement entropy (Wolf *et al.*, 2008). That is, a system is said to satisfy an area law for the mutual information if the mutual information between a region R and its complement \bar{R} , $I(R:\bar{R}) = S(\rho_R) + S(\rho_{\bar{R}}) - S(\rho_{R\bar{R}})$, can be bounded by the number of spins at the boundary of R (up to a multiplicative constant). It has been shown that thermal states of short-range Hamiltonians (Wolf *et al.*, 2008), as well as fixed points of fast-mixing Lindbladians (Brandao *et al.*, 2015), fulfill an area

law for the mutual information, which therefore characterizes the relevant corner of the Hilbert space for equilibrium states in analogy to the area law for the entanglement entropy for ground states.

As in the case of a MPS, in any MPDO the mutual information between a region R and its complement is upper bounded by a constant that depends only on the bond dimension, not the system size or the size of R . Moreover, an analogous argument based on strong subadditivity implies that the mutual information increases monotonically with the size of the region R . Hence, just as before, we expect MPDO RGFPs to saturate the area law for the mutual information. As shown by Cirac *et al.* (2017a), this condition is, however, not equivalent to zero correlation length. To characterize RGFPs in MPDOs, we therefore need to impose both conditions independently: We therefore say that a MPDO is a RGFP if it has both zero correlation length and saturation of the area law for mutual information.

It can be proven that RGFP MPDOs are characterized (up to a technical condition) by the existence of two trace-preserving completely positive maps (quantum channels) \mathcal{T} and \mathcal{S} such that

$$\begin{array}{c} \text{---} \boxed{M} \text{---} \boxed{M} \text{---} \\ \text{---} \boxed{M} \text{---} \end{array} \quad (36)$$

One can immediately see that taking traces in Eq. (36) implies zero correlation length. Moreover, since Eq. (36) allows one to grow or reduce a region by acting locally on it, it also implies saturation of the area law. On the other hand, the fact that the two conditions together imply Eq. (36) is far less obvious (Cirac *et al.*, 2017a). We thus see that, in analogy to the case of a MPS, imposing RGFP conditions related to the absence of length scales gives rise to a particular type of RG flow for which the given MPDO is a fixed point. Here the flow consists of blocking a finite number of sites and implementing a renormalizing quantum channel on the blocks whose action can be inverted. One can use this type of RG flow to define phases for mixed states in analogy to the previously discussed MPS case: Two mixed states are said to be in the same phase if there exists a low-depth circuit of quantum channels that can map one state onto the other (Coser and Perez-Garcia, 2018).

As in the MPS case, there is also a result that characterizes the structure of RGFP MPDOs. Namely, it turns out that RGFP MPDOs generate a finite-dimensional algebra of matrix product operators, in the following sense: Consider a MPDO generated by a tensor M (obtained by contracting the tensors horizontally, as in Fig. 3), and consider the MPO

$$O_L(M) = \begin{array}{c} \text{---} \boxed{M} \text{---} \\ \vdots \\ \text{---} \boxed{M} \text{---} \end{array}, \quad (37)$$

which was generated by M by contracting the same tensors vertically on a ring of length L . Assume without loss of generality (w.l.o.g.) that this MPO is in canonical form, i.e.,

$$M = \bigoplus_{\alpha} \mu_{\alpha} M_{\alpha}, \quad (38)$$

where M_{α} are the different injective blocks [we do not include the case of multiple blocks, which can be treated in a similar way; see Cirac *et al.* (2017a)]. The given MPDO is then a RGFP if and only if there is a set of diagonal matrices $\chi_{\alpha,\beta,\gamma}$ with positive entries such that, for each L , the operators $O_L(M_{\alpha})$ linearly span an algebra with structure coefficient $c_{\alpha,\beta,\gamma}^{(L)} = \text{tr}(\chi_{\alpha,\beta,\gamma}^L)$, i.e.,

$$O_L(M_{\alpha})O_L(M_{\beta}) = \sum_{\gamma} c_{\alpha,\beta,\gamma}^{(L)} O_L(M_{\gamma}) \quad (39)$$

and

$$\mu_{\gamma} = \sum_{\alpha,\beta} c_{\alpha,\beta,\gamma}^{(1)} \mu_{\alpha} \mu_{\beta}. \quad (40)$$

That is, the vector $(\mu_{\alpha})_{\alpha}$ is an idempotent for the “multiplication” induced by $c^{(1)}$.

If the structure coefficients $c_{\alpha,\beta,\gamma}^{(L)} = \text{tr}(\chi_{\alpha,\beta,\gamma}^L)$ are independent of L , one can easily show that $\chi_{\alpha,\beta,\gamma,k} \in \{0, 1\}$, and therefore $c_{\alpha,\beta,\gamma}^{(L)} \in \mathbb{N}$. In this case, one can further show that the RGFP MPDOs generated by M can be written as

$$\rho^{(N)}(M) = \sum_{i=1}^d \lambda_i P_i^{(N)} e^{-H_N}, \quad (41)$$

where d is the local Hilbert dimension of a single site, $P_i^{(N)}$ are projectors, $H_N = \sum_{i=1}^N h_{i,i+1}$ is translationally invariant, nearest neighbor, and commuting ($[h_{i-1,i}, h_{i,i+1}] = 0$), and $[P_i, e^{-H}] = 0$ for all i .

This result establishes a connection with the boundary theories of topological PEPSs in two dimensions, rigorously proving the desired structure for the boundary theory for RGFP (see Sec. II.D): a global projector selecting the topological sector and a local boundary Hamiltonian commuting with it. At the same time, it concludes (based only on a natural RGFP condition) the existence of an algebra of MPOs that, as explained in Sec. III.B, is the starting point to obtain the most general class of nonchiral topological models in two dimensions.

3. Tree tensor states and MERAs

For a general quantum state describing a spin chain, it is possible to devise a multitude of renormalization processes. The simplest one is the real-space renormalization, in which one joins a block of spins and truncates the corresponding Hilbert space to build a new one. It is straightforward to check to see that the concatenation of this procedure gives rise to a TTN, where each layer is characterized by the truncation map; see Sec. II.B.5. As previously explained, it is possible to choose these maps as isometries. The renormalization flow can be interpreted as the sequence of isometries corresponding to each level of the renormalization. The sequence may converge, so one could define these TTNs where all the isometries are the same as fixed points of the RG flow. These

states give rise to a logarithmic violation of the area law and have averaged correlation functions that in general decay as a power law.

A much more sophisticated and comprehensive way of performing such a renormalization consists of including unitary operators (“disentangler”) acting on neighboring spins before each step of the previous procedure. The resulting states are the MERAs (Vidal, 2008), which include more correlations than TTNs, as the tensor network now contains loops; see Sec. II.B.5. Furthermore, the procedure can be applied to higher spatial dimensions with an area law scaling of the entanglement, something that is not possible with TTNs.

The renormalization procedure in terms of MERAs was introduced by Vidal (2008), who interpreted the unitaries and isometries as ways of disentangling neighboring spins at each step. In fact, by reading the MERA or the TTN the other way round, one can see that each can be generated out of a product state by applying unitary operators.

Compared to previous procedures, MERA and TTN are more appropriate for describing critical states, where the correlation length diverges. In fact, given their structure one can extract properties of the conformal field theory describing the critical behavior of the state, such as the form of the primary fields or their scaling dimensions (Giovannetti, Montangero, and Fazio, 2008; Pfeifer, Evenbly, and Vidal, 2009; Milsted and Vidal, 2017; Zou, Milsted, and Vidal, 2018).

4. RG in higher dimensions

The previously reviewed renormalization procedures can be extended to higher dimensions using PEPSs. In principle, one can look for unitary operators acting on blocks of spins (in plaquettes, for instance) that disentangle some of them locally. This procedure will not work as well for PEPSs as it does for MPSs since in a spatial dimension larger than 1 blocking increases the bond dimension, as a direct reflection of the area law. Thus, one might want to choose a different approach.

The most natural one is to truncate the states by replacing the unitary operator with an isometry to obtain a tree tensor network or adding disentangling unitaries to obtain a MERA (Evenbly and Vidal, 2009). If one considers tensor networks without physical degrees of freedom such as classical partition functions, another approach consists of replacing several tensors corresponding to neighboring spins with a single tensor but making sure that the tensor in some way generates a tensor network that is close to the original one (Gu, Levin, and Wen, 2008; Evenbly and Vidal, 2015; Bal *et al.*, 2017; Yang, Gu, and Wen, 2017). Although these procedures may be useful as numerical tools, the state obtained at the end will in general not be the same as the original one.

A way around this is to look for fixed points of such types of renormalization procedures. The corresponding nontrivial fixed points turn out to form representative states for phases exhibiting topological quantum order (Wen, 2017). As pioneered by Dennis *et al.* (2002), qubits in the toric code (Kitaev, 2003) can be disentangled with local unitaries, and therefore the corresponding fixed-point topological states can be represented in terms of a quantum circuit of isometries and unitaries. Essentially the same construction was used by Aguado and Vidal (2008) and König, Reichardt, and Vidal

(2009) to represent all quantum doubles (Kitaev, 2003) and string nets (Levin and Wen, 2005) as fixed points of renormalization flows in the form of a MERA. All those models have zero correlation length and are the ground states of frustration-free Hamiltonians with local commuting terms. The ground states of those models can hence be obtained by projecting a product state on the ground subspaces of all those local Hamiltonian terms; such a construction generates a simple PEPS description for the ground states of such fixed-point Hamiltonians (Verstraete *et al.*, 2006). This PEPS representation was worked out for string nets by Gu and Wen (2009), and its emerging MPO symmetries were studied by Schuch, Cirac, and Perez-Garcia (2010) and Şahinoğlu *et al.* (2021) and are presented in Sec. III.B.

From a more general perspective, one can consider renormalization fixed-point equations for PEPSs, such as those shown in Fig. 13, and write the corresponding nonlinear stationary equations that fully characterize these PEPS, which can be considered RGFPs with respect to that property. Realizing such a program would involve nontrivial results from algebraic geometry but has not yet been realized in full generality.

An alternative method in two spatial dimensions consists of using the bulk-boundary correspondence reviewed in Sec. II.D.2. Using this correspondence, the physical properties of a PEPS are characterized by a density operator that lives at the boundary. We next consider a PEPS on a cylinder. In the course of renormalizing the PEPS using any RG procedure, the boundary state itself will be renormalized as well and, as the RG fixed point is reached, one expects to obtain a RGFP MPDO (Cirac *et al.*, 2017a) (cf. Sec. II.E.2) at the boundary as well. This RGFP condition at the boundary leads to an emerging algebra of MPOs. We discuss in Sec. III.B.2 how, from the existence of such an algebra, one recovers in a direct way all known 2D nonchiral topologically ordered phases together with a description of their anyon excitations. The point of view of the characterization of renormalization group fixed point in terms of boundary density operators is therefore equivalent to the one in terms of disentangling circuits acting on the bulk, and both give rise to quantum double models and string nets.

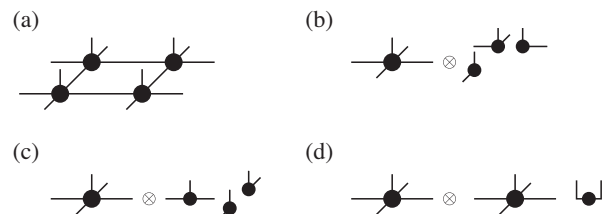


FIG. 13. Examples of different possibilities for RGFPs in a 2D square configuration, where (a) a unitary operation is applied to the physical indices of four spins and invertible operations are applied to the auxiliary ones. (b) One can disentangle several spins, i.e., obtain the original tensor and other ones as product states. (c) One can obtain the original tensor and other generating MPSs. (d) One can obtain two copies of the original tensor.

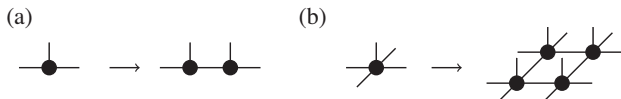


FIG. 14. Inverse renormalization procedure. (a) For MPSs, if E is divisible, one can rewrite the tensor in terms of two tensors of the same bond dimension and iterate the procedure. (b) For PEPSs in two dimensions, the same step would imply that the bond dimension of the new tensor has to be square rooted.

5. The limit to the continuum

A natural question is whether one can also implement a process inverse to renormalization in the context of tensor networks. That is, instead of coarse graining the lattice to distill the global entanglement pattern, fine graining it to obtain a meaningful continuum limit.

We first discuss this for one dimension, following Verstraete and Cirac (2010) and De las Cuevas *et al.* (2018). As seen in Sec. II.B.3, MPSs are characterized by a quantum channel E (their transfer operator) up to a local basis change. A blocking step of r sites simply corresponds to taking the transfer operator to the r th power E^r , as used in Sec. II.E.1. A fine-graining step would therefore correspond to taking integer roots of E . However, this is subtle, as there are quantum channels T that cannot be divided (Wolf and Cirac, 2008), in the sense that there are not any other quantum channels R such that $R^2 = T$. To guarantee a well-defined continuum limit, one needs to require that the transfer operator is *infinitely divisible*, meaning that all possible integer roots exist (De las Cuevas *et al.*, 2018). This in turn is equivalent, up to a projector P commuting with a given channel E , to the existence of an infinitesimal generator \mathcal{L} that generates a semigroup $e^{t\mathcal{L}}$, $t \geq 0$, that interpolates the initial E (which corresponds to $t = 1$) all the way back to $t = 0$ (Kholevo, 1987; Denisov, 1989). The state obtained by taking $t \rightarrow 0$ in this fine-graining process is precisely the cMPS discussed in Sec. II.B.4.

This procedure cannot be easily extended to higher dimensions. The reason is that the inverse renormalization process should produce tensors with noninteger bond dimensions (as bond dimensions multiply when blocking), which is impossible. For instance, in two dimensions one should progress from bond dimension D to tensors of bond dimension \sqrt{D} ; see Fig. 14. At some point of the iteration, the square root will not be an integer, so the procedure cannot work. The only way around it is if in some sense $D = \infty$. In fact, continuous PEPSs can be defined in this way, for instance, in terms of path integrals where the discrete auxiliary indices of the tensors are replaced by functions that are integrated over when they are contracted (Jennings *et al.*, 2015; Tilloy and Cirac, 2019).

III. SYMMETRIES AND CLASSIFICATION OF PHASES

Symmetries are a main guiding principle in quantum many-body physics, and the situation is no different for tensor networks. In fact, one of the main reasons for the success of tensor networks is precisely the fact that they make the role of

symmetries in many-body systems so explicit: a quantum state described by a MPS or PEPS $|\psi_N\rangle$ will be invariant under a global symmetry $U^{\otimes N}|\psi_N\rangle$ if and only if all local tensors transform trivially under that symmetry. As a consequence, any global symmetry, including symmetries associated with topological order, will be reflected in the local symmetries of the tensors describing the many-body states. Phrased differently, the entanglement spectrum acts like a signature of those symmetries. This yields a unifying principle for describing distinct gapped phases of matter, including topological ones for which there is no distinct local order parameter in the sense of Landau (1937): distinct phases of matter can be distinguished by the different ways in which the local tensors transform under the global symmetries. The local tensors hence provide a nontrivial generalization of the notion of a local order parameter and reduce the problem of classifying different gapped phases of matter to a problem in the representation theory of groups and algebras. It is a well-known fact that there are certain topological obstructions to convert tensors, which transform according to different representations of the same group, into each other continuously. Those obstructions are precisely the ones responsible for the existence of topological quantum order.

One of the noteworthy success stories of many-body physics has certainly been the realization that global symmetries can be lifted to local ones by introducing new “gauge” degrees of freedom. Such a procedure can also be carried out in the language of tensor networks and gives rise to tensors with an increased intrinsic symmetry action on the entanglement degrees of freedom. The ensuing gauge theories exhibit fascinating properties such as excitations with anyonic statistics and nontrivial edge modes, and the fact that such features directly follow from the symmetry properties of the local tensors makes tensor networks a natural framework for describing and exploring quantum topological order. In fact, it can be argued that tensor networks implement the representation theory of braided fusion categories, which form the foundation of both topological and conformal field theories.

This section is divided into two parts. Section III.A discusses symmetries of matrix product states and is hence concerned with the classification of phases of quantum spin chains. Section III.B discusses symmetries of projected entangled pair states, including the case of quantum topological order. In both cases, we limit the discussion to uniform translationally invariant systems.

A. Symmetries in one dimension: MPSs

1. Symmetric MPSs

Normal (and injective) uniform matrix product states exhibit the noteworthy property that two states $|\psi(A)\rangle$ and $|\psi(B)\rangle$ are equal to each other if and only if there is a gauge transform X and a phase χ for which $A^i = e^{i\chi} X^{-1} B^i X$ (Perez-Garcia, Wolf *et al.*, 2008). If both A^i and B^i are in canonical form, then X is guaranteed to be unitary due to the uniqueness of the fixed point. This is a consequence of the fundamental theorem of MPSs and is discussed in Sec. IV. A useful feature is the following property of a normal MPS:

$$X^{-1}A^iX = e^{ix}Y^{-1}A^iY \Rightarrow \chi = 0 \wedge \exists \phi: X = e^{i\phi}Y. \quad (42)$$

Furthermore, any translationally invariant normal MPS has a uniform representation, i.e., the tensors A^i do not depend on the site label. This property has strong consequences for MPSs that are invariant under global on-site, reflection, and time-reversal symmetries. This implies that the tensors building up a MPS with global symmetries must themselves transform trivially up to a phase under that symmetry. To illustrate this, we consider the case of a MPS in canonical form that is invariant under a global on-site symmetry group $G: U(g)^{\otimes N}|\psi_N\rangle \simeq |\psi_N\rangle$. It follows from Eq. (42) that

$$\sum_j U_{ij}(g)A^j = e^{i\phi(g)}X^\dagger(g)A^iX(g). \quad (43)$$

In other words, the three-leg MPS tensor A^i written as a vector in a vector space of dimension $d \cdot D^2$ transforms trivially under the action of $e^{-i\phi(g)}U(g) \otimes X(g) \otimes \bar{X}(g)$, with $\bar{X}(g)$ the conjugate. This implies that the tensor A^i can be written in terms of Clebsch-Gordan coefficients of irreducible representations of the group G , and that the variational degrees of freedom can be incorporated by adding multiplicities (White, 1993; McCulloch and Gulácsi, 2002; Sanz *et al.*, 2009; Singh, Pfeifer, and Vidal, 2010; Weichselbaum, 2012). Such decompositions have been used for a long time and with great success in the context of DMRG. There are two nontrivial facts that one can deduce as a result.

First, the condition of injectivity in conjunction with translational invariance imposes constraints on the types of symmetries that can be realized in a MPS. This is best illustrated with an example. Consider a spin-1/2 system with $SU(2)$ symmetry. As the physical spin transforms according to a half-integer representation, the Clebsch-Gordan coefficients impose that the virtual irreducible representations (irreps) alternate between integer and half-integer representations (Sanz *et al.*, 2009). By blocking two sites, the MPS matrices A^i therefore exhibit two invariant subspaces, and hence the MPS cannot be normal, which shows that no uniform normal or injective MPS can exhibit such a symmetry. As we later discuss, this is the tensor network manifestation of the Lieb-Schultz-Mattis theorem.

Second, there is no need for the irreps on the virtual degrees of freedom to form representations of the group G : it is perfectly fine if they transform according to projective representations, that is, representations up to a phase

$$X_gX_h = e^{i\omega(g,h)}X_{gh}, \quad (44)$$

as such phases leave $e^{i\phi(g)}U(g) \otimes X(g) \otimes \bar{X}(g)$ invariant (Pollmann *et al.*, 2010; Chen, Gu, and Wen, 2011a; Schuch, Perez-Garcia, and Cirac, 2011). As an authoritative example, if the physical system transforms according to $SO(3)$, the virtual systems can both transform according to either half-integer or integer representations of $SU(2)$, as readily determined from the Clebsch-Gordan coefficients. The half-integer representations of $SU(2)$ form a projective representation of $SO(3)$, with phases $\omega(g, h) = 0$ or π .

For a given group G , it is a relatively easy task to find all possible projective representations, as the associativity of matrix multiplication heavily constrains the possible $\omega(g, h)$. If the group is finite, this can be achieved by using the Smith normal form, which is similar to the Schmidt decomposition but with integer arithmetic. The following picture emerges (Chen *et al.*, 2013). For a given group G , the various projective representations fall into equivalence classes, whereas in a given equivalence class the projective representations are related to each other by simple phases as follows: $X_g = \exp[i\phi(g)]\tilde{X}_g$. These phases are irrelevant from the point of view of MPSs, as they cancel, and hence only the equivalence classes count. Those classes are classified according to the second cohomology group $H_a^2(G, U(1))$ with group action α (this action is nontrivial in the case of time-reversal and reflection symmetries) and are classified according to the solutions of

$$\alpha_g(\omega(h, l)) - \omega(g \cdot h, l) + \omega(g, h \cdot l) - \omega(g, h) = 0 \pmod{2\pi}, \quad (45)$$

which is obtained by imposing associativity relations on the projective representations. The action α is a homomorphism from G to the automorphism group Z_2 of $U(1)$, and hence consists of \pm . In the case of global symmetries excluding reflection and time reversal, this is simply the following identity map: $\alpha_g(x) = x$ for all $g \in G$. As follows from the Smith normal form, there are only a finite number of such equivalence classes for a finite group, and these are labeled by integer and hence topological indices.

In the case of a continuous semisimple Lie group G , irreducible projective representations are in one-to-one correspondence to irreducible linear representations of its universal covering group C , from which G is then obtained by modding out a subgroup Z_s of its center Z , $G = C/Z_s$. Note that the previously discussed relation between $SU(2)$ and $SO(3)$ is precisely of this form. In the previous example, half-integer representations of $SU(2)$ correspond to projective nonlinear representations of $SO(3)$. For compact groups such as $SO(3)$, this also yields a finite number of different inequivalent classes of projective representations (i.e., the second cohomology group is finite).

Before studying the significant physical implications of those projective representations, we generalize the discussion to include time-reversal and/or reflection symmetries. A symmetry \mathcal{G} of the system can be labeled by a subset of the tuples $x = (g, t, r) \in G \times Z_2^T \times Z_2^R$, where g denotes the physical group action and $t, r \in 0, 1$ denotes the linear representation of time-reversal and reflection. From now on we consider \mathcal{G} to be of the form $G \rtimes H$, with H a subgroup of $Z_2^T \times Z_2^R$.

We start by discussing a normal MPS in canonical form that is invariant under pure time-reversal symmetry represented by the tuple $x = (1, 1, 0)$ corresponding to the morphism $S_x(A^i) = \bar{A}^i$: it is elementwise conjugation. As this is a symmetry of the system, the fundamental theorem imposes that there is a X_x and $\phi(x)$ such that $\bar{A}^i = e^{i\phi(x)}X_x^\dagger A^i X_x$. As conjugating a tensor twice yields the original tensor, we must have $A^i = S_x(S_x(A^i)) =$

$S_x(e^{i\phi(x)}X_x^\dagger A^i X_x) = e^{-i\phi(x)}\bar{X}_x^\dagger \bar{A}^i \bar{X}_x = (X_x \bar{X}_x)^\dagger A^i (X_x \bar{X}_x)$. Per Eq. (42), this is possible only for $X_x \bar{X}_x = \pm 1$ and, as discussed in Sec. III.A.2, ± 1 is a topological index. Note that if we had defined time-reversal symmetry in the form $x = (\sigma_y, 1, 0)$, as encountered in Wigner’s discussion on time reversal in spin-1/2 systems, we would have obtained $A^i = S_x(S_x(A^i)) = (X_x \bar{X}_x)^\dagger A^i (X_x \bar{X}_x) = \sigma_y \cdot \overline{\sigma_y A^i} = -A^i$, which is in violation with Eq. (42). This implies that ground states of systems exhibiting such a symmetry cannot be represented by a normal or injective MPS or, phrased differently, cannot be unique ground states of a local gapped Hamiltonian. This turns out to be the tensor network analog of the Kramers theorem on time reversal. From the mathematics point of view, the obstruction follows from the fact that the physical symmetry σ_y acts as a projective representation under time reversal.

As has become clear, to discuss global symmetries labeled by $x_i = (g_i, t_i, r_i)$ and $x_3 = x_1 \circ x_2$, we need to define the actions of the symmetries on MPS tensors in the form $S_x(e^{i\phi} X^\dagger A^i X) = e^{i\chi_x^1(\phi)} \chi_x^2(X)^\dagger A^i \chi_x^2(X)$. Here we introduced the functions $\chi_x^1(\phi)$ as the morphism on the phase ϕ and $\chi_x^2(X)$ as the morphism on the gauge X induced by element x . As previously discussed, if $x = (g, 1, 0)$ involves time reversal, then $\chi_x^1(\phi) = -\phi + \phi(x)$ and $\chi_x^2(X) = X_x \cdot \bar{X}$, with $\phi(x)$ and the gauge tensor X_x depending only on the group element x . Similarly, a reflection $x = (g, 0, 1)$ in terms of the MPS is implemented by taking the transpose of the matrices involved: $S_x(e^{i\phi} X^\dagger A^i X) = e^{i\phi} X^T (A^i)^T \bar{X} = e^{i[\phi + \phi(x)]} X^T X_x^\dagger A^i X_x \bar{X}$. Hence, in this case $\chi_x^1(\phi) = \phi + \phi(x)$ and $\chi_x^2(X) = X_x \cdot \bar{X}$. If a group element involves simultaneous time reversal and reflection $x = (g, 1, 1)$, then $\chi_x^1(\phi) = -\phi + \phi(x)$ and $\chi_x^2(X) = X_x \cdot X$. The fundamental theorem of MPSs imposes the condition that χ_x^1 must form a linear representation of the group $\chi_{x_1}^1 \circ \chi_{x_2}^1 = \chi_{x_1 \cdot x_2}^1$. This imposes the following nontrivial constraint on the phases $\phi(x)$:

$$(-1)^{t_1} \cdot \phi(x_2) - \phi(x_1 \cdot x_2) + \phi(x_1) = 0 \pmod{2\pi},$$

with $t_1 = 1$ if and only if x_1 involves time reversal. This is precisely the defining equation for a 1-cocycle of the first cohomology group $H_\beta^1(\mathcal{G}, U(1))$ with group action $\beta_x(\phi) = (-1)^{t(x)} \cdot \phi$. For finite groups and compact semisimple Lie groups, there are only a finite number of distinct cocycle solutions of this equation modulo the trivial coboundary solutions. Indeed, the equivalence class of a cocycle is obtained by adding a coboundary to it, $\phi(x) \rightarrow \phi(x) + [\beta_x(c) - c]$ for any constant c , and all such solutions are indistinguishable from the point of view of MPSs.

Similarly, the fundamental theorem implies that the morphism $\chi_x^2(\cdot)$ must form a projective representation of \mathcal{G} , that is, $\chi_{x_1}^2 \circ \chi_{x_2}^2 = \exp[i\omega(x_1, x_2)] \chi_{x_1 \cdot x_2}^2$. Imposing associativity in the form $\chi_{x_1}^2 \{ \exp[i\omega(x_2, x_3)] \chi_{x_2 \cdot x_3}^2(X) \} = \exp[i\omega(x_1, x_2)] \chi_{x_1 \cdot x_2}^2 \times [\chi_{x_3}^2(X)]$ leads to the following condition on the phases $\omega(x_1, x_2)$:

$$\begin{aligned} (-1)^{(t_1+t_2)} \omega(x_2, x_3) - \omega(x_1 \cdot x_2, x_3) + \omega(x_1, x_2 \cdot x_3) \\ - \omega(x_1, x_2) = 0 \pmod{2\pi}. \end{aligned}$$

This is precisely the defining equation for a 2-cocycle of the second cohomology group $H_\alpha^2(\mathcal{G}, U(1))$ with group action $\alpha_x(\phi) = (-1)^{[t(x)+r(x)]} \phi$. Given a finite group G , the finite number of equivalence classes of this equation can again be found explicitly by making use of the Smith normal form. In this case, the coboundaries correspond to $\omega(x, y) \rightarrow \omega(x, y) + \alpha_x(\xi(y)) - \xi(x \cdot y) + \xi(x)$ for any function $\xi(x)$. $H_\alpha^2(\mathcal{G}, U(1))$, as is also the case for $H_\beta^1(\mathcal{G}, U(1))$, is itself an Abelian group and hence is of the form $Z_n \times Z_m \times \dots$.

In summary, we have seen that all global symmetries of uniform normal (or injective) MPS wave functions are reflected in the local tensors A^i of the MPS; these symmetries can be represented projectively on the virtual level, and the classification of all possible ways in which this can occur can be obtained by solving the integer linear algebra problem of finding all 1- and 2-cocycles of the group of interest.

2. SPT phases and edge modes

a. Symmetry-protected topological order

The way global symmetries are reflected on the local MPS tensors has strong implications for the classification and description of phases of matter of 1D spin systems. The fundamental idea underlying this classification is the fact that the unique ground state of any local gapped quantum spin chain has an efficient representation in terms of a normal (or injective) MPS. This implies that the classification of gapped phases can be done on the level of MPSs as opposed to Hamiltonians, which is a significant simplification.

Given two translationally invariant normal MPSs parametrized by tensors A^i and B^i , it turns out that there is always an interpolation between them (even if they have different bond dimensions) for which all intermediate MPSs are also injective. There is no topological obstruction for constructing such a path, and hence there is only one phase for gapped quantum spin systems (Chen, Gu, and Wen, 2011a; Schuch, Perez-Garcia, and Cirac, 2011) (note that the situation changes in the case of fermions, as we discuss in Sec. III.A.4). This problem is equivalent to constructing an interpolating path $A^i(t)$ for which the transfer matrix $E = \sum_i A^i(t) \otimes \bar{A}^i(t)$ has a unique largest eigenvalue (which is guaranteed to be real). As demonstrated by Schuch, Perez-Garcia, and Cirac (2011), this can be achieved in three steps. First, we block different sites until the tensor $A^i A^i \dots$ is injective, then apply a filtering operation to bring this blocked MPS into the form of a renormalization group fixed point while keeping the unique largest eigenvalue property. Second, we can readily interpolate between any two of such dimer-type wave functions by a local quantum circuit without closing the gap. In the third step, we apply another filtering operation to obtain the tensor B^i . The corresponding parent Hamiltonian $H(t)$ is guaranteed to be gapped along the path, demonstrating that any two injective MPSs are in the same phase. For a generalization of this theorem without the blocking step, see Szehr and Wolf (2016).

The situation changes drastically when symmetry constraints are imposed on the adiabatic path, and hence on the MPS: a much smaller dimensional manifold can then be traversed during the interpolation, and topological obstructions might occur. Colloquially speaking, the submanifold of

all normal MPSs with a given symmetry decomposes into disconnected components. As a consequence, any symmetry-preserving interpolating path between two states living on different components has to pass through a phase transition, and at this point the interpolating MPS will not be injective anymore (Chen, Gu, and Wen, 2011a; Schuch, Perez-Garcia, and Cirac, 2011). These different components correspond to different SPT phases. They are protected by translational invariance, on-site symmetries, time-reversal symmetry, and/or reflection invariance.

The necessary mathematical framework for demonstrating this was developed in Sec. III.A.1. By studying how a MPS A^i transformed under one or a combination of the previous symmetries $S_x(A^i) = \exp[i\phi(x)]X_x^\dagger A^i X_x$, it was shown that $\phi(x)$ had to be a 1-cocycle of $H_\beta^1(\mathcal{G}, U(1))$ and that we could associate with the gauge matrices X_x a map (morphism) $\chi_x^2(X) = X_x \cdot X$ or $\chi_x^2(X) = X_x \cdot \bar{X}$ (depending on whether time reversal, reflection invariance, or both are involved), which itself forms a projective representation of the physical symmetry group: $\chi_{x_1}^2 \cdot [\chi_{x_2}^2(\cdot)] = \exp[i\omega(x_1, x_2)]\chi_{x_1 x_2}^2(\cdot)$. The corresponding phases are characterized by the topologically distinct 2-cocycles $\omega(x_1, x_2)$ of the second cohomology group $H_\alpha^2(\mathcal{G}, U(1))$.

A noteworthy point is that the opposite is also true: whenever two injective MPSs A^i and B^i exhibit equivalent 1- and 2-cocycles ϕ and ω when transformed under the group involving on-site, time-reversal, and/or reflection symmetry, then there is an adiabatic path of injective MPSs that interpolates between them. The proof of this is basically equivalent to the one sketched when no symmetries are involved. Within each of these phases, a representative MPS with zero correlation length can be constructed starting from any solution of the 1- and 2-cocycle condition. The translationally invariant SPT phases of gapped spin systems for a given symmetry group G are therefore completely classified by $H_\alpha^2(\mathcal{G}, U(1)) \times H_\beta^1(\mathcal{G}, U(1))$ (Chen *et al.*, 2013). The H^2 part has a strong influence on the entanglement spectrum. The H^1 part is related to the translational invariance of the system and is not stable under blocking (note that the first cohomology group indeed plays a central role in the description of the space groups).

We now explicitly construct the RG fixed-point MPS that transforms according to a given 1- and 2-cocycle ϕ and ω . The local physical Hilbert space will have the dimension squared of the number of elements in the symmetry group and can be parametrized as a tensor product (a, b) , while the virtual indices are labeled by the group elements. The MPS is defined as

$$A_{xy}^{ab} = \begin{cases} e^{i\alpha(a \cdot x) \cdot \omega(a, x) + i\beta(b) \cdot \phi(b)} & \text{if } y = a \cdot x, \\ 0 & \text{otherwise,} \end{cases}$$

and the corresponding gauge matrices are of the form

$$(X_g)_{xy} = \begin{cases} e^{i\alpha(x) \cdot \omega(x, g)} & \text{if } y = x \cdot g, \\ 0 & \text{otherwise.} \end{cases}$$

This works since the condition $S_q(A^{ab}) = \exp[i\phi(q)]X_q^\dagger A^{ab} X_q$ is equivalent to the 2-cocycle equation.

This MPS has zero correlation length (which follows from the fact that the transfer matrix is a rank-1 projector) and hence represents the renormalization group fixed point in its corresponding phase. In the particular case of an on-site $Z_2 \times Z_2$ symmetry, the simplest group exhibiting nontrivial 2-cocycles, this construction precisely yields the 1D cluster state (see the Appendix) when blocking pairs of adjacent sites.

The prime example of a MPS in a nontrivial SPT phase is the AKLT state (Affleck *et al.*, 1988), which is specified by the Pauli matrices $A^i = \sigma^i$, $i = x, y, z$. Its SPT character can be protected by multiple distinct physical symmetries: on-site $SO(3)$ (with virtual symmetry given by a spin-1/2 representation), on-site $Z_2 \times Z_2$ [the smallest subgroup of $SO(3)$ still exhibiting a nontrivial 2-cocycle], time-reversal, or reflection symmetry. In all these cases, the AKLT MPS tensor transforms projectively.

By making use of the Smith normal form, it is easy to solve for all cocycle conditions and determine the number of possible different SPT phases by combining those symmetries. If we consider the symmetries of the AKLT state (on-site $Z_2 \times Z_2$, time-reversal Z_2^T , and reflection Z_2^R symmetries), we obtain the following classification: $H_\alpha^2(Z_2 \times Z_2 \times Z_2^T \times Z_2^R, U(1)) = Z_2^{*7}$, while $H_\beta^1(Z_2 \times Z_2 \times Z_2^T \times Z_2^R, U(1)) = Z_2^{*3}$. This means that there are 1024 distinct topological phases protected by this large symmetry group (Chen, Gu, and Wen, 2011b). A simpler example is obtained when considering an on-site Z_2 symmetry in combination with time reversal, leading to $H_\alpha^2(Z_2 \times Z_2^T, U(1)) = Z_2^{*2}$ and $H_\beta^1(Z_2 \times Z_2^T, U(1)) = Z_2$. Similarly, $H_\alpha^2(Z_2 \times Z_2^R, U(1)) = Z_2^{*2}$, $H_\alpha^2(Z_2^T \times Z_2^R, U(1)) = Z_2^{*2}$, and $H_\alpha^2(Z_2 \times Z_2 \times Z_2^T, U(1)) = Z_2^{*4}$. The submanifolds of normal MPSs subject to global symmetries clearly exhibit a rich structure.

b. Entanglement spectrum and edge modes

In Sec. II.D, we saw how PEPSs provide a natural way to access the entanglement spectrum, compute boundary Hamiltonians, and determine the edge physics of quantum many-body systems. In the context of nontrivial SPT phases, all of these exhibit characteristic fingerprints of the phase, which we discuss in the following.

A distinct feature of normal MPS belonging to a nontrivial SPT phase is the fact that their entanglement spectrum exhibits a clear pattern of degeneracies. The fact that topological order is reflected in the entanglement spectrum was first observed by Li and Haldane (2008). Pollmann *et al.* (2012) connected these ideas to the dangling spin-1/2 edge modes in the AKLT chain, and by making use of the fundamental theorem of MPS they realized that these edge modes were protected. The consecutive work of Chen *et al.* (2013) revealed that the appropriate mathematical formalism to deal with this phenomenon is cohomology theory.

The degeneracy of the entanglement spectrum and the existence of edge modes follows from the following property of projective representations X_g : they cannot be Abelian and cannot be reduced to one-dimensional representations, and hence are only reducible to matrices of dimension strictly larger than 1. We first consider the case of on-site group

symmetries. If a given injective MPS is in canonical form and exhibits nontrivial SPT order, its entanglement spectrum is obtained by looking at the leading eigenvector of its transfer matrix $\sum_i A^i \otimes \bar{A}^i |\rho\rangle = |\rho\rangle$. Because of the uniqueness of the corresponding eigenvalue, ρ has to inherit all symmetries of the MPS and will hence be invariant under the transformation $X_g \rho X_g^\dagger = \rho$. As X_g has no one-dimensional invariant subspaces, ρ must necessarily have a spectrum in which all eigenvalues have a degenerate multiplicity. For the case of time-reversal and/or reflection symmetries, the situation is slightly more complicated. The virtual degrees of freedom of the MPS in the nontrivial SPT phase then transform according to an antisymmetric gauge transform $X = -X^T$ if the MPS is in canonical form. The entanglement spectrum is then determined by the eigenvalues of the matrix $\rho = X \bar{\rho} X^\dagger$, with ρ the leading eigenvector of the transfer matrix. All eigenvalues of ρ are guaranteed to be degenerate: given a right eigenvector $|x\rangle$ with real eigenvalue λ , $\langle \bar{x} | X^{-1}$ is guaranteed to be a left eigenvector with the same eigenvalue. But $\langle \bar{x} | X^{-1} | x \rangle = 0$, as it is the trace of a product of a symmetric with an antisymmetric matrix; this implies that $\langle \bar{x} | X^{-1}$ is the left eigenvector corresponding to a different right eigenvector, thus implying a twofold degeneracy.

Exactly the same feature is responsible for the fact that nontrivial SPT phases exhibit edge modes when defined on systems with open boundary conditions: the ground state degeneracy of a MPS with respect to its parent Hamiltonian with open boundary conditions will be at least the dimension of the irrep space squared, as we can define boundary vectors on both sides, which will transform nontrivially under X_g and will not change the energy. An attractive feature of MPSs is the fact that these gapless edge modes can actually be constructed by lifting operators acting on the virtual level to the physical level (which is always possible when the MPS is normal). For the case of the AKLT model, this indeed leads to a fourfold degeneracy. There is, however, only one state in this four-dimensional space that will be in the spin-0 sector, and that state will exhibit long-range entanglement between the two edges. This is a general feature of SPT phases.

c. String order parameters for SPT phases

Symmetry-breaking phases can be distinguished by their local order parameters. Since SPT phases do not break any symmetries, we will need nonlocal observables to distinguish them. Such nonlocal order parameters have long been used to study the AKLT model under the name string order parameters (den Nijs and Rommelse, 1989; Kennedy and Tasaki, 1992). In general, if we consider a gapped quantum spin system with a unique ground state exhibiting a physical symmetry group U_g , we can construct a family of observables acting on $L + 2$ sites of the form

$$S_{\alpha,g}(L) := R_{\bar{\alpha}} \otimes U_g^{\otimes L} \otimes R_{\alpha},$$

where R_{α} is an observable that transforms according to a nontrivial linear representation $\alpha(g)$ of G : $U_g^\dagger R_{\alpha} U_g = \exp[i\alpha(g)] R_{\alpha}$ (the nontriviality ensures that the local expectation value of R_{α} is zero), whereas $R_{\bar{\alpha}}$ transforms according to

$-\alpha(g)$. We say that a spin system exhibits string order if and only if for some R_{α} , $R_{\bar{\alpha}}$, and g the limit $\langle S_{\alpha,g} \rangle := \lim_{L \rightarrow \infty} \langle \psi | S_{\alpha,g}(L) | \psi \rangle \neq 0$. Using the language of MPSs, we can readily prove that the existence of such a string order implies the fact that the system is in a nontrivial SPT phase when the group under consideration is Abelian (Pollmann and Turner, 2012). This can most easily be shown by demonstrating the fact that it has to be equal to zero in the trivial phase, i.e., in a phase in which the virtual symmetries X_g form a group representation of G . As U_g represents a physical symmetry, the expectation value $\langle S_{\alpha,g} \rangle$ (in the thermodynamic limit) is

We denote the left diagram by $D_{\alpha,g}^L$. By inserting $\mathbb{1} = U_h^\dagger U_h$ between A and $R_{\bar{\alpha}}$, a simple manipulation yields $D_{\alpha,g}^L = e^{i\alpha(h)} D_{\alpha,hgh^{-1}}^L$. As we assumed the group to be Abelian and the one-dimensional irrep $\alpha(h)$ to be nontrivial, this implies that the expectation value of the string order parameter has to be equal to zero.

The expectation value of the string order parameter can certainly be nonzero in the case of a nontrivial SPT phase; in that case (and again assuming an Abelian group), we obtain $D_{\alpha,g}^L = e^{i\alpha(h) + \omega(h,g) + \omega(h,g,h^{-1})} D_{\alpha,hgh^{-1}}^L$. As the group is Abelian, $\omega(h \cdot g, h^{-1}) = -\omega(g, h)$, and hence the expectation value does not have to vanish if $\alpha(h) = \omega(g, h) - \omega(h, g)$. This is precisely what happens in the case of the AKLT chain when considering the string order parameter for the $Z_2 \times Z_2$ symmetry. Note that not all SPT phases are detectable using this idea (Pollmann and Turner, 2012); this happens when all the commuting pairs of elements g_1 and g_2 also commute in the projective representation.

A related idea that directly measures an observable targeting the commutator $\exp\{i[\omega(g, h) - \omega(h, g)]\} \simeq \text{Tr}(X_g X_h X_g^\dagger X_h^\dagger)$ can be defined in terms of swaps between distant regions; see Haegeman, Perez-Garcia *et al.* (2012) for details.

3. Symmetry breaking: Virtual symmetries, Lieb-Schultz-Mattis theorem, Kramers theorem, and topological excitations

a. Virtual symmetries

We now consider the case of a noninjective MPS that is invariant under a global symmetry. After blocking, the tensor A^i corresponding to a noninjective MPS can always be written as a direct sum of injective MPS blocks $A^i = \bigoplus_{\alpha} A_{\alpha}^i$. The full MPS is hence a sum of these injective ones: $|\psi(A^i)\rangle = \sum_{\alpha} |\psi(A_{\alpha}^i)\rangle$. We assume w.l.o.g. that the non-injective MPS A^i cannot be decomposed into smaller blocks that are themselves invariant under the symmetry group G under consideration; the global symmetry then permutes all the blocks into each other. This situation happens precisely when considering the uniform superposition of all ground states of a symmetry broken system. The paradigmatic example of such a system is given by the ferromagnetic

Ising model $H = -\sum_i Z_i Z_{i+1}$ with global symmetry $X^{\otimes N}$, where the symmetric ground state is the superposition of all spins up and all spins down. This state can readily be represented as the following MPS with bond dimension 2: $A^\uparrow = |0\rangle\langle 0|$, $A^\downarrow = |1\rangle\langle 1|$. This so-called GHZ state exhibits long-range order. Because the corresponding MPS is not injective, the tensors A^i exhibit a nontrivial symmetry G on the virtual level represented by the matrices that commute simultaneously with all A^i (σ_z in this GHZ case). MPSs with this property are called G -injective. Note that this symmetry is dual to the physical symmetry that permutes the blocks (represented by σ_x in the case under consideration).

For a given group G , one can construct a particularly simple G -injective MPS that is itself a renormalization group fixed point (all nonzero eigenvalues of the corresponding transfer matrix are equal to 1) and hence provides a natural generalization of the GHZ to arbitrary groups. The physical symmetry action is represented by the regular representation. It is defined as follows by the MPS tensor with physical dimension $|G|^2$ and virtual dimension $|G|$:

$$A^{ij} = \frac{1}{|G|} \sum_{g \in G} \sum_{\alpha, \beta} (L_g)_{\alpha i} (\bar{L}_g)_{\beta j} |\alpha\rangle\langle\beta|, \quad (46)$$

where L_g denotes the left regular representation of the group G (Schuch, Cirac, and Perez-Garcia, 2010). For the case of Z_2 symmetry, this can be written in the GHZ form by going to the dual basis (related by the discrete Fourier transform) on both physical and virtual levels and with a blocking of two sites. Such a construction will be shown to be especially useful to construct topological phases in higher dimensions.

b. SET phases

In many interesting physical applications, only part of the total symmetry of the system is broken, while another part is unbroken. From the point of view of MPSs, the broken symmetry leads to permutations of the different MPS blocks, while the unbroken one exhibits symmetries on the virtual level as encountered in the discussion of injective MPSs. To accommodate both of these symmetries, the corresponding gauge representation X_g acquires the form of an induced representation. Induced representations are a technique in representation theory to lift representations X_h of a subgroup H to representations of the full group G that we assume to be finite. Given a subgroup H , we can consider one representative \tilde{g}_α out of every left coset $\alpha = g \cdot H$; any element of G can then uniquely be written as $\tilde{g}_\alpha \cdot h_\beta$. This defines functions ϕ_1 and ϕ_2 such that $g_\alpha \cdot \tilde{g}_\alpha = \tilde{g}_{\phi_1(a,\alpha)} \cdot h_{\phi_2(a,\alpha)}$. The induced representation is then given by

$$V_\alpha = \sum_{\alpha} |\phi_1(a, \alpha)\rangle\langle\alpha| \otimes X_{h_{\phi_2(a,\alpha)}}.$$

This acts as the regular representation between the blocks, but as an irrep within each individual block. This is indeed precisely the symmetry exhibited by SET phases: the X_h matrices form possibly projective representations of the unbroken symmetry group, while the broken symmetries yield permutations of the different blocks of the noninjective

MPS. Along the lines of the discussion on SPT phases, it can now be established that two systems are in the same phase if and only if the permutation representations $\phi_1(a, \alpha)$ are equal to each other, and furthermore that the X_h must belong to the same equivalence class of $H^2(H, U(1))$ (Schuch, Perez-Garcia, and Cirac, 2011). An alternative approach based on a 1D version of anyon condensation was explained by Garre-Rubio, Iblisdir, and Perez-Garcia (2017).

c. Kramers and Lieb-Schultz-Mattis theorems

One of the most interesting aspects of quantum spin chains is the interplay between symmetry and degeneracy. This has led to a wealth of theorems, of which the Kramers theorem (Kramers, 1930), the Lieb-Schultz-Mattis theorem (Lieb, Schultz, and Mattis (1961), and the Mermin-Wagner theorem (Mermin and Wagner, 1966) are certainly the most familiar and useful ones. We now discuss them in light of MPSs.

Kramers theorem dictates that eigenstates of time-reversal invariant systems must be degenerate if the total spin of the system is half integer. More precisely and in the case of a spin-1/2 system, the theorem is valid whenever time reversal is implemented as an antiunitary transformation in the form $|\psi\rangle \rightarrow (\sigma_y)^{\otimes N} |\bar{\psi}\rangle$, as originally derived by Wigner; see Bargmann (1954). In Sec. III.A.1, it was shown that no normal uniform MPS can exhibit such a symmetry, as there is a topological obstruction involving the global phase making it impossible for a normal uniform MPS to accommodate an on-site symmetry that acts projectively.

To deal with such a situation, we hence have to modify the uniform MPS ansatz. In the case of a spin-1/2 system, this is most easily done by introducing an ansatz with a two-site unit cell as follows:

$$|\psi(A, B)\rangle = \sum \text{Tr}(A^i B^i A^i B^i \dots) |i_1\rangle |i_2\rangle \dots \quad (47)$$

A careful analysis of the possibilities leads to the conclusion that there is always a gauge such that B^i can be chosen as equal to one of the following: \bar{A}^i , $(\sigma_y \otimes 1) \bar{A}^i$, or $(\sigma_y \otimes 1) \bar{A}^i (\sigma_y \otimes 1)$. The other (degenerate) ground state is then obtained either by shifting the MPS over one site or by acting with the time-reversal symmetry on the state. The total time-reversal-invariant uniform MPS can then be written as the superposition of both, yielding a noninjective MPS with tensors

$$\begin{pmatrix} 0 & A^i \\ B^i & 0 \end{pmatrix}. \quad (48)$$

Note that this MPS has no invariant subspaces but exhibits the structure of a limit cycle; see Sec. IV.A. Only by blocking two sites do we get a G -injective structure. Note also that a translational-invariant breaking term in the Hamiltonian can distinguish the two blocks from each another: the blocked MPS $\tilde{A}^{ij} = A^i B^j$ is injective and is hence the unique ground state of a local Hamiltonian. This is precisely the mechanism in the Su-Schrieffer-Heeger model (Su, Schrieffer, and Heeger, 1979), where a staggered field opens a gap and leads to a unique ground state.

Similarly, the Lieb-Schultz-Mattis theorem dictates that the singlet ground state of an $SU(2)$ -invariant quantum spin chain whose unit cell transforms according to a half-integer representation of $SU(2)$ must be gapless or symmetry broken. This theorem has been extended to the case of any half-integer charge, for example, for the case of a $U(1)$ symmetry with one charge per two unit cells (Oshikawa, Yamanaka, and Affleck, 1997). From the point of view of MPSs, this situation is similar to the case of the Kramers theorem. As discussed in Sec. III.A.1, the structure of Clebsch-Gordan coefficients imposes the requirement that a half charge couples to one half-integer and one integer charge. As a consequence, the MPS will be exactly of the form of Eq. (48), with B^i related to A^i by a transpose. As in the case of the Kramers theorem, it follows that any MPS with such a symmetry will be non-injective and will become G -injective after blocking two sites. In the case of a spin-1/2 antiferromagnetic Heisenberg model, the ground state is critical, and hence cannot be represented exactly as a MPS. Nevertheless, DMRG methods are able to reproduce the ground state energy to an astounding precision with a MPS exhibiting $SU(2)$ symmetry. What happens is that the DMRG algorithm artificially introduces a small staggering in the antiferromagnetic strength, a relevant perturbation opening up a gap, breaking the translational invariance. In the uniform case, we get a MPS of the form of Eq. (47), and this representation is of central importance to capturing the topologically nontrivial spinon excitations.

Finally, we say a few words about the Mermin-Wagner theorem, which states that a continuous symmetry in a quantum spin chain cannot be broken with an order parameter (observable) that does not commute with the Hamiltonian. As the unique ground state of a local gapped Hamiltonian can be represented as an injective MPS, the impossibility of defining a MPS with the relevant symmetries of the Hamiltonian (including translational invariance) implies that the ground state of that Hamiltonian has to be critical or has to break translational invariance. If the ground state is critical, any good variational (and hence injective) MPS approximation of that ground state will have to break either the continuous symmetry or the translational invariance; which one leads to a better approximation depends on the respective scaling exponents of the two perturbations.

d. Topological excitations: Domain walls and spinons

A direct implication of symmetry breaking is the emergence of topological excitations. In the case of a G -injective MPS such as the Ising model in the ferromagnetic phase, these are domain wall excitations that tunnel between the different blocks A_a^i of the MPS (Haegeman, Pirvu *et al.*, 2012):

$$|\psi(X)\rangle = \sum \dots A_1^{i_{x-2}} A_1^{i_{x-1}} e^{ikx} X^{i_x} A_2^{i_{x+1}} \dots \otimes |i_y\rangle, \quad (49)$$

where X^{i_x} is a ‘‘tunneling’’ tensor that couples the different blocks A_1^i and A_2^i and the sum runs over all i_y and all positions x of X . Note that such excitations make sense only for an open infinite system, and that the momentum k is defined only up to a constant shift. This ansatz can be readily used to simulate dispersion relations of the elementary excitations of symmetry broken quantum spin chains, where the variational parameters

of these excitations are encoded in X^i , giving rise to an effective Hamiltonian for the quasiparticle excitations. The topological trivial excitations can then be understood as scattering states of such domain walls. This structure also emerges when studying excitations of critical systems using a variational MPS approach: the MPS will slightly break the symmetry, and the elementary excitations will then tunnel from one ground state to the other one. This was observed during a study of the elementary excitations of the Lieb-Liniger model using cMPSs (Draxler *et al.*, 2013).

A similar situation occurs when the translation symmetry is broken instead of the on-site symmetry, as discussed in relation to the Kramers and Lieb-Schultz-Mattis theorems. The MPS description then acquires a $\dots ABAB\dots$, $\dots ABCABC\dots$, or similar structure. The elementary excitations become topological dislocations of the form $\dots ABABXAB\dots$. If we consider the Heisenberg spin-1/2 antiferromagnet and its MPS description with such a two-site unit cell, the emerging topological excitations are spinons: the corresponding tensor X^i transforms according to a half-integer object, as it intertwines between two MPS tensors that have the same half-integer or integer spin index (Zauner-Stauber *et al.*, 2018). This is a topological feature as there is no local operator that can create such an excitation. The MPS picture hence gives a precise meaning to the spin in a spin wave, as originally coined by Faddeev and Takhtajan (1981).

In general, the framework of MPS makes it clear how elementary excitations can acquire fractionalized quantum numbers. This is even more pronounced in the case of two dimensions, where a PEPS provides a natural framework for describing anyons.

4. Fermions and the Majorana chain

The case of virtual symmetries becomes particularly interesting when symmetry breaking is prohibited due to the existence of a superselection rule. This happens in the case of a chain of fermions, where superpositions between states with an even and odd number of fermions are ruled out. In contrast to the situation of symmetry breaking discussed previously, the fermion superselection rule has the power to stabilize a G -injective GHZ state, as all corresponding symmetry broken states $|\psi(A^\alpha)\rangle$ would violate the superselection rule.

This scenario was first discussed by Kitaev (2001), and the corresponding nontrivial Hamiltonian is called the Kitaev or Majorana chain. He demonstrated that there are two distinct phases for interacting fermionic spin chains, and hence that there is no adiabatic gapped path between the trivial phase and the Majorana phase. The ground state of the Kitaev chain is a fermionic MPS with bond dimension 2. As discussed in Sec. II.B.4, the natural language for a fermionic MPS is given in terms of Z_2 graded algebras. As in the case of SPT phases, the Kitaev chain has edge modes that are exponentially localized around the boundary, and this can be understood in terms of the entanglement degrees of freedom that exhibit the virtual symmetry. For a Kitaev chain on a ring with periodic boundary conditions, the following ground state is unique and has odd parity [see Eq. (10)]:

$$|\psi\rangle = \sum_{i_1 \dots i_N} \text{tr}[YA^{i_1}A^{i_2} \dots A^{i_N}]|i_1\rangle \otimes_g |i_2\rangle \otimes_g \dots \quad (50)$$

The tensors $A^0 = \mathbb{1}$ and $A^1 = Y = \sigma_y$ both commute with Y , which forms the representation of the virtual symmetry, and hence the MPS is noninjective and can be written as a sum of two injective MPSs $|\psi_1\rangle + |\psi_2\rangle$. The symmetry broken states $|\psi_i\rangle$, however, contain superpositions of an even and odd number of fermions and hence are unphysical. As demonstrated by [Bultinck, Williamson *et al.* \(2017\)](#), the uniqueness of the ground state is guaranteed by the Z_2 graded version of injectivity. For a system with open boundary conditions, we get a twofold degeneracy, as opposed to the fourfold one found in the case of the AKLT model; the Hilbert space “dimension” of a Majorana fermion is indeed $\sqrt{2}$, as opposed to 2. As a consequence, the Majorana chain has the unique feature that the system with periodic boundary conditions can be represented through a MPS with open boundary conditions and bond dimension 2.

There is also an interesting interplay between time-reversal symmetry and the Z_2 superselection rule. As first demonstrated by [Fidkowski and Kitaev \(2011\)](#), eight different SPT phases emerge. This has to be contrasted with the spin case, where time reversal gives rise to only two cases. These eight phases can be distinguished by studying how the entanglement degrees of freedom transform under the time-reversal symmetry, and this gives rise to three different indices ([Bultinck, Williamson *et al.*, 2017](#)). The first index distinguishes the Majorana case (with a virtual Z_2 symmetry) from the trivial non-Majorana case (without such a symmetry). A new Z_2 index κ emerges according to the transformation rules under conjugation of the tensors $\bar{A}^i = e^{i\kappa} X A^i X^{-1}$; as in the case of spins, the index κ is witnessed as $\bar{X} \cdot X = (-1)^\kappa \mathbb{1}$. A third Z_2 index μ characterizes how the matrix Y , which represents the center of the MPS algebra, transforms under the gauge X : $X \cdot Y = (-1)^\mu Y \cdot X$. Those three Z_2 indices give rise to the Z_8 classification of interacting fermionic spin chains, and a representative of each of the eight classes can be constructed by taking tensor products of Kitaev chains.

A wide variety of such fermionic SPT phases can be constructed by repeating this construction for other groups and symmetries. In analogy with the discussion on SET phases, this can be achieved by making use of induced representations, where the physical and purely virtual symmetries are combined in a natural way.

5. Gauge symmetries

The idea of lifting global symmetries to local ones by introducing new gauge degrees of freedom has proven to be of fundamental importance in the field of particle physics. It turns out that a procedure similar to the minimal coupling prescription can be implemented on the level of wave functions whenever these are expressed in terms of MPSs ([Buyens *et al.*, 2014](#); [Kull *et al.*, 2017](#)): starting with a MPS describing matter fields with a global symmetry U_g implemented (projectively) on the virtual degrees of freedom as X_g , it is straightforward to introduce new (gauge) degrees of freedom and tensors on the edges that will lift the global symmetries to local ones. To achieve this, we now consider a

tensor with physical degrees of freedom corresponding to the group elements and define it as

$$A^{a^{-1} \cdot b} = \sum_{ab} |a\rangle |a^{-1} \cdot b\rangle \langle b|. \quad (51)$$

Acting with the left regular representation L_g on the physical level is equivalent to acting with the right regular representation R_g on $|a\rangle \rightarrow |ag\rangle$, and acting with the right regular representation R_g on the physical level amounts to acting with $R_{g^{-1}}$: $|b\rangle \rightarrow |bg^{-1}\rangle$. Note that this tensor provides the natural generalization of the GHZ state in the dual basis for any group.

6. Critical spin systems: MPO symmetries

In [Sec. III.A.3](#), we discussed the difficulty of representing ground states of critical quantum spin systems using injective MPSs and hinted at the fact that there are topological obstructions to doing so. Whenever the continuous symmetries of a translationally invariant quantum spin Hamiltonian cannot be represented using a uniform injective MPS, the ground state of that Hamiltonian has to either be critical and exhibit power law decay of its correlations, or exhibit symmetry breaking. An important consideration is the characterization of the nonlocal symmetries emerging for such critical systems that precludes an exact description of their ground states with finite bond dimension MPSs. The formalism of MPOs provides exactly that. Additionally, the MPO formalism provides a constructive way of writing Hamiltonians with such a symmetry. It turns out that the same symmetries are the ones responsible for the existence of nonchiral topological order in $2 + 1$ dimensions. This is not surprising, as there is an intimate connection between topological quantum field theory in $2 + 1$ and conformal field theory in $2 + 0$ or $1 + 1$ dimensions ([Elitzur *et al.*, 1989](#); [Moore and Seiberg, 1989](#); [Witten, 1989](#); [Fuchs, Runkel, and Schweigert, 2002](#)). This section therefore also provides the mathematical background for studying topological gapped systems in two dimensions.

The symmetries under consideration have been studied at great length in the fields of quantum groups, integrability, and conformal field theory. The picture that has emerged is that critical spin systems exhibit “topological symmetries” or anomalies that can be seen as lattice remnants of the full conformal group ([Aasen, Mong, and Fendley, 2016](#); [Vanhove *et al.*, 2018](#)). In the example of the critical quantum transverse Ising model, this “symmetry” corresponds to the Kramers-Wannier duality, and the scale-invariant symmetry operations form a closed algebra as opposed to a group. Matrix product operators are precisely the right framework to provide representations of these algebras ([Bultinck, Mariën *et al.*, 2017](#); [Williamson, Bultinck, and Verstraete, 2017](#); [Lootens *et al.*, 2021](#); [Molnar *et al.*, 2021](#); [Şahinoğlu *et al.*, 2021](#)).

a. MPO algebras

Given a tensor



in canonical form (in each direction) we can define the algebras

$$\mathcal{A}^{(N)} = \left\{ \left(\bigotimes_{i=1}^N \square_i \right) : X \right\}$$

with N the system size. We can identify all $\mathcal{A}^{(N)}$ if the product is independent of N . In such a case we say that the algebra

$$\mathcal{A} = \left\{ \left(\bigotimes_{i=1}^{\infty} \square_i \right) : X \right\},$$

is a *MPO algebra* (Bultinck, Mariën *et al.*, 2017; Molnar *et al.*, 2021).

A series of nontrivial consequences can be derived as follows from this definition; for the precise mathematical statements, see Lootens *et al.* (2021):

- (1) Any MPO algebra can be decomposed into a finite set of injective MPOs represented as O_a , with a taken from a set of labels $a \in \mathcal{C}$; these O_a form a ring with non-negative integer fusion coefficients N_{ab}^c : $O_a O_b = \sum_c N_{ab}^c O_c$. We use the notation 2F_a to describe the MPO tensors.
- (2) The fundamental theorem of MPSs implies the existence of a *fusion tensor* 1F which satisfies the following *zipper equation*:

$${}^2F^1F = {}^1F^2F^2F$$

If the labels $a \in \mathcal{C}$ correspond to the irreps of a group, then the 1F can be identified with the Clebsch-Gordan coefficients.

- (3) The associativity of the zipper equation requires the existence of a *recoupling tensor* 0F , which solely depends on the set of labels $a \in \mathcal{C}$ satisfying the following equation:

$${}^1F^1F = {}^0F^1F^1F$$

If the labels $a \in \mathcal{C}$ correspond to the irreps of a group and the MPO tensors encode these irreps, then the 0F are equal to the Racah or Wigner $6j$ symbols.

- (4) Any recoupling tensor 0F has to satisfy the ubiquitous algebraic pentagon equation. For given MPO fusion rules N_{ab}^c , there are only a finite number of possible inequivalent solutions to the pentagon equation. This puts a significant restriction on the possible MPO algebras, and puts its study squarely in the realm of fusion categories.
- (5) The scale invariance of the MPO algebra implies the existence of a different set of fusion tensors 3F acting on the physical degrees of freedom satisfying the following *pulling through* equation:

$${}^2F^3F = {}^3F^2F^2F$$

It follows that there is also a dual algebra obtained by switching the roles of physical and virtual indices of the MPO tensor 2F ; note that this is the same duality as the one in Sec. II.E.2 describing renormalization group fixed points. This vertical MPO algebra can now again be decomposed into its injective blocks, thereby giving rise to a new set of discrete labels $\alpha \in \mathcal{D}$ and fusion coefficients $\tilde{N}_{\alpha\beta}^{\gamma}$. This \mathcal{D} will also form a fusion category. As we make clear in Sec. III.B, we also call 3F the PEPS tensor.

- (6) Recoupling of the fusion tensors 3F implies the existence of a set of fusion tensors 4F satisfying

$${}^3F^3F = {}^4F^3F^3F$$

- (7) The tensor 4F satisfies the pentagon equation, with its solutions completely determined by \tilde{N}_{ij}^k .

The five objects iF and accompanying six consistency equations appear in the field of tensor categories and form the defining equations of a bimodule category. Such categories have been studied extensively in the context of describing boundaries between systems exhibiting topological quantum order (Kitaev and Kong, 2012) but have a completely different meaning here.

A $(\mathcal{C}, \mathcal{D})$ bimodule category \mathcal{M} has a new set of labels $A, B, \dots \in \mathcal{M}$, which represents the *entanglement degrees of freedom*. Therefore, the choice of this bimodule category determines the explicit representation of the MPO, fusion, or PEPS tensor. We can then identify the fusion, MPO, and PEPS tensors as follows (note that all tensor legs are labeled as triple indices belonging to one of the following \mathcal{C} , \mathcal{M} , or \mathcal{D} , some of which might be trivial):

$$\left({}^1F_A^{abC} \right)_{c,mn}^{B,kj} = \begin{array}{c} A \xrightarrow{a} j \\ \swarrow \quad \searrow \\ n \xrightarrow{c} m \xrightarrow{b} k \\ \swarrow \quad \searrow \\ C \end{array},$$

$$\left({}^2F_B^{aC\alpha} \right)_{A,jm}^{D,nk} = \begin{array}{c} A \xrightarrow{a} m \xrightarrow{b} k \\ \swarrow \quad \searrow \\ j \xrightarrow{c} n \xrightarrow{d} k \\ \swarrow \quad \searrow \\ C \quad D \end{array},$$

$$\left({}^3F_B^{A\alpha\beta} \right)_{C,jn}^{\gamma,km} = \begin{array}{c} C \xrightarrow{\alpha} k \xrightarrow{\beta} n \\ \swarrow \quad \searrow \\ j \xrightarrow{\gamma} m \xrightarrow{\delta} k \\ \swarrow \quad \searrow \\ A \quad B \end{array}.$$

For bimodule categories that are invertible, the categories \mathcal{C} and \mathcal{D} are Morita equivalent; this requires their Drinfeld doubles or Drinfeld centers to be equivalent. As described in Sec. III.B.3, this Drinfeld center has a tangible physical meaning, as it represents the output fusion category of the

anyon excitations in topological phases of matter described by string nets defined by the input category \mathcal{D} ; equivalently, it describes the primary fields for lattice realizations of CFTs. A particularly simple choice of an invertible bimodule category is obtained by choosing $\mathcal{C} = \mathcal{D} = \mathcal{M}$; in that case, all iF symbols are equal and the six pentagon equations are equivalent (Bultinck, Mariën *et al.*, 2017).

As an alternative to the categorical description that arises naturally from the fundamental theorem of MPSs, an equivalent formulation of MPO algebras in terms of weak Hopf algebras was given by Molnar *et al.* (2021), where the size independence of the MPO algebra was formalized in the form of the following comultiplication

$$\Delta \left(\begin{array}{c} \text{---} \circlearrowleft \text{---} \\ \text{---} \square \text{---} \end{array} \right) = \begin{array}{c} \text{---} \circlearrowleft \text{---} \square \text{---} \\ \text{---} \square \square \text{---} \end{array} .$$

This equivalence makes the seminal result of Hayashi (1999) connecting fusion categories with weak Hopf algebras explicit. The additional known connection with subfactor theory was also made explicit for MPO algebras by Kawahigashi (2020).

The central pulling through equation can be rephrased as follows completely in terms of the full MPO algebra (Molnar *et al.*, 2021; Şahinoğlu *et al.*, 2021):

$$\begin{array}{c} \text{---} \square \text{---} \square \text{---} \square \text{---} \\ \text{---} \square \text{---} \square \text{---} \square \text{---} \end{array} \begin{array}{c} \text{---} \circlearrowleft \text{---} \\ \text{---} \square \text{---} \end{array} = \begin{array}{c} \text{---} \circlearrowleft \text{---} \square \text{---} \square \text{---} \\ \text{---} \square \text{---} \square \text{---} \square \text{---} \end{array} . \quad (52)$$

Here λ is an extra block-diagonal tensor that is a direct sum of identities acting on the invariant subspaces of the MPO tensors, and weighted with the quantum dimensions of categorical objects corresponding to related MPO-injective blocks. Moreover, reversing the arrows as in the right and bottom tensors means taking the *inverse representation* (Bultinck, Mariën *et al.*, 2017).

We now illustrate this with an example in which \mathcal{C} represents the labels of a group $g \in G$ and $\alpha \in \mathcal{D}$ stands for the labels of its irreps D^α , with each α appearing as many times as its dimension. \mathcal{M} can then be chosen to be trivial, and the injective MPOs O_g are represented by the MPO tensors

$$A_g = \sum_{\alpha ij} D^\alpha(g)_{ij} |g\rangle\langle g| \otimes |i, \alpha\rangle\langle j, \alpha|,$$

where we continue using the notation established in Sec. II.B.1: curved kets and bras $[|\cdot\rangle]$ correspond to the virtual level, and standard ones $(|\cdot\rangle)$ correspond to the physical one.

Up to a unitary transformation on the physical indices, this is equal to $A_g = |g\rangle\langle g| \otimes L_g$, with L_g the regular representation, and leads to the representation for quantum doubles used by Schuch, Cirac, and Perez-Garcia (2010). The G -injective MPO is then defined as [compare this to Eq. (46)]

$$\frac{1}{|G|} \sum_{g \in G} L_g^{\otimes N}. \quad (53)$$

The corresponding pulling through equation (52) then becomes equal to

$$\begin{aligned} L_h^{\otimes 2} \otimes (\mathbb{1}^{\otimes 2}) \sum_g L_g^{\otimes 2} \otimes L_{g^{-1}}^{\otimes 2} \\ = \left(\sum_g L_g^{\otimes 2} \otimes L_{g^{-1}}^{\otimes 2} \right) (\mathbb{1}^{\otimes 2}) \otimes L_h^{\otimes 2}, \end{aligned}$$

which is trivially true.

When we step up one level of sophistication, MPO algebras can accommodate 3-cocycles corresponding to nontrivial solutions to the pentagon equations and requiring nontrivial entanglement degrees of freedom $\in \mathcal{M}$ (Buerschaper, 2014; Williamson *et al.*, 2016). The most general MPO algebras form representations of all bimodule categories with a spherical structure (Lootens *et al.*, 2021).

b. MPO symmetries

The pulling through equation for the 2F tensors can be used as follows to define operators that commute with the full MPO algebra:

$$\begin{array}{c} \text{---} \square \text{---} \square \text{---} \square \text{---} \square \text{---} \square \text{---} \\ \text{---} \square \text{---} \square \text{---} \square \text{---} \square \text{---} \square \text{---} \end{array} \begin{array}{c} \text{---} \text{---} \\ \text{---} \square \text{---} \end{array} = \begin{array}{c} \text{---} \square \text{---} \square \text{---} \square \text{---} \square \text{---} \square \text{---} \\ \text{---} \square \text{---} \square \text{---} \square \text{---} \square \text{---} \square \text{---} \end{array} \begin{array}{c} \text{---} \text{---} \\ \text{---} \square \text{---} \end{array} .$$

If these tensors can be made Hermitian, they define a Hamiltonian on a one-dimensional lattice by taking the sum of their translations; the corresponding full Hamiltonian commutes with the complete MPO algebra. All so-called anyonic spin chains (Gils *et al.*, 2009) can be constructed in this way, and the MPO symmetries hence realize the corresponding topological symmetries.

We now illustrate this with two simple examples. If one considers the two unitary solutions of the pentagon equations for the fusion rules corresponding to the group Z_2 , one of them corresponds to a nontrivial 3-cocycle. The local Hamiltonian commuting with the corresponding MPO is precisely the cluster state Hamiltonian at the critical value of the magnetic field (Bridgeman and Williamson, 2017), which is equivalent to the XY model (Lahtinen and Ardonne, 2015). Similarly, if one starts with the Ising fusion rules, one obtains the critical Ising model in a transverse magnetic field, and for the Fibonacci fusion rules, the critical ‘‘golden chain’’ Hamiltonian emerges (Vanhove *et al.*, 2018; Lootens, Vanhove, and Verstraete, 2019).

In a similar vein, it is possible to construct classical statistical mechanical lattice models using this construction; the construction gives rise to the restricted solid-on-solid models of Andrews, Baxter, and Forrester (Andrews, Baxter, and Forrester, 1984; Aasen, Mong, and Fendley, 2016), which are known to yield lattice critical systems corresponding to all CFTs in the minimal series.

This suggests that the MPO symmetry is the one that is responsible for criticality: it emerges at the critical point and

provides a topological obstruction for a normal or injective MPS to have such a symmetry. Strictly speaking, it is not a symmetry, as the MPOs do not have to be invertible; e.g., in the case of the Ising model, the MPO implementing the Kramers-Wannier duality is not invertible, and this is a consequence of the fact that the critical theory must be symmetric with respect to both the local Z_2 symmetry and the dual disorder symmetry (Kadanoff and Ceva, 1971), which anticommute. Furthermore, it can be shown that a perturbation that commutes with the full MPO algebra and keeps translational invariance is generically prohibited from opening a gap (Buican and Gromov, 2017). However, MPO symmetries are not enough to guarantee criticality, as MPOs encode the topological features of critical systems only; extra constraints related to the geometry, the so-called discrete holomorphicity, have to be imposed and lead to a lattice version of the conformal symmetry (Fendley, 2021).

For this discussion, we now demonstrate that a uniform normal MPS cannot exhibit a MPO symmetry obtained from a nontrivial solution of the pentagon equations. For the group case of 3-cocycles, this was originally proven by Chen *et al.* (2013) [see also Williamson *et al.* (2016) and Molnar, Ge *et al.* (2018)], and their proof can be readily extended to the general case of MPO algebras. This is proven by contradiction and is based on the fundamental theorem. We now sketch the proof.

If we first act with a MPO O_α on an injective MPS $|\psi(A)\rangle$ and it is proportional to $|\psi(A)\rangle$, the fundamental theorem implies the existence of an intertwiner V_α that reduces the local tensors of the MPS $O_\alpha|\psi(A)\rangle$ back those of the original one:

The diagram shows a vertical line representing an MPS tensor with a box labeled α on its left side. A horizontal line representing a MPO O_α passes through the box. This is equated to a vertical line with a box labeled V_α on its left side, and a horizontal line representing the MPO O_α passing through it.

If we act with two MPOs, then there are two inequivalent ways of reducing to the original one: either we first reduce the MPS and O_α via V_α , followed by V_β , or we first reduce the two MPOs with the intertwiner F :

The diagram shows a vertical line with two boxes labeled α and β on its left side. A horizontal line representing a fusion channel $F_{\alpha\beta}^\gamma$ passes through both boxes. This is equated to a vertical line with a box labeled $F_{\alpha\beta}^\gamma$ on its left side, and a horizontal line representing a MPO O_γ passing through it.

Note that, in the case of multiple fusion channels γ , it is immaterial which fusion channel is taken as long as it does not give zero. It was proven by Molnar, Ge *et al.* (2018) in their Theorem 22 that these two ways of reducing to an injective MPS must be equivalent up to a scalar $\lambda(\alpha, \beta; \gamma)$:

The diagram shows a vertical line with two boxes labeled α and β on its left side. A horizontal line representing a MPO O_α passes through the α box, and another horizontal line representing a MPO O_β passes through the β box. This is equated to a scalar $\lambda(\alpha, \beta; \gamma)$ multiplied by a vertical line with a box labeled $F_{\alpha\beta}^\gamma$ on its left side, and a horizontal line representing a MPO O_γ passing through it.

We now act with three MPOs on the supposed injective MPSs, which are all symmetry operators. As in the defining equation of the pentagon equation, there are two different ways of changing the order of the reductions, and they have to be equivalent. It follows that

$$\frac{\lambda(\alpha, \beta; a) \cdot \lambda(a, \gamma; b)}{\lambda(\beta, \gamma; c) \cdot \lambda(\alpha, c; b)} = F_{bac}^{\alpha\beta\gamma}.$$

There is, however, a topological obstruction to achieve this: a nontrivial solution F of the pentagon equation can never be a simple product of functions that act exactly as gauge transforms on these same F symbols. In the case of groups and 3-cocycles, the left-hand side corresponds exactly to the coboundary and enforces the F symbol to be trivial. This is a contradiction and proves that the MPS cannot be injective. As a consequence, any Hamiltonian with a MPO symmetry will either be critical or have a symmetry broken ground state space.

This theorem is powerful and is a clear demonstration of the fact that MPO symmetries yield a Lieb-Schultz-Mattis-like proof for topological symmetries, as opposed to continuous ones. Note that the proof assumed no fusion multiplicities: it is all $N_{ab}^c \leq 1$, and counterexamples can be constructed if this is not the case. Note also that a nontrivial MPO symmetry does not prevent a tensor network description for density matrices, as the renormalization group fixed points discussed in Sec. II.E are of that exact form. Similarly, it is possible to construct MERAs with nontrivial MPO symmetries, and hence allow for the description of critical phases with exact topological symmetries (Bridgeman and Williamson, 2017). Those two facts turn out to be intimately related to each other, as the entanglement Hamiltonian of a MERA is of the exact MPO form (Van Acoleyen *et al.*, 2020).

The fact that local Hamiltonians that commute with nontrivial MPO symmetries necessarily have to be critical or symmetry broken has a significant influence on the edge modes of systems exhibiting topological quantum order in two dimensions, and this is the origin of the CFT-TQFT correspondence and anomalies on those edges. This is discussed in Sec. III.B. The MPO picture for describing critical quantum spin systems transcends to the statistical mechanical world, in which the MPOs become Wilson-loop-type operators that generalize the disorder operators introduced in the context of the 2D Ising model given by Kadanoff and Ceva (1971). A systematic study of these MPO symmetries allows one to represent all fields, including the chiral ones, in terms of the so-called tube algebra, which is a MPO algebra representing the Drinfeld center of the input category. Many of the interesting properties of conformal field theories can, as such, be transmuted to the lattice, including notions like orbifolding and the coset construction (Lootens, Vanhove, and Verstraete, 2019).

B. Symmetries in two dimensions: PEPSs

The full power of symmetries in tensor networks is revealed in the description of quantum many-body systems in two dimensions by PEPSs, in which different phases of matter can be distinguished by the different representations of these symmetries acting on the local PEPS tensors. As such, tensor networks provide local order parameters for topological phases of matter as a direct manifestation of the entanglement properties of such systems. The most general language for describing these symmetries is in terms of matrix product operators, which play the role of Wilson loops on the virtual level. These MPOs provide a unifying framework both for

describing the entanglement structure of the ground state manifold and for characterizing the elementary excitations in these systems.

1. Symmetric PEPSs

The arena of topological quantum phases in two dimensions is much richer than the one for quantum spin chains. From the tensor network point of view, this can be understood from the fact that tensors have a much richer but also more complicated structure than matrices. The most general form of the fundamental theorem of MPSs, upon which much of Sec. III.A was built, does not have an easy generalization to two dimensions, and we therefore concentrate here on the cases for which the symmetries on the virtual level can be described in terms of tensor products of local operators or of matrix product operators.

We distinguish among five different situations: (a) the case of injective PEPSs describing gapped systems with a unique ground state, (b) noninjective PEPSs as unique ground states of gapped SPT phases, (c) noninjective PEPSs as ground states of systems exhibiting genuine topological order, (d) PEPS descriptions of SET phases, and (e) chiral phases.

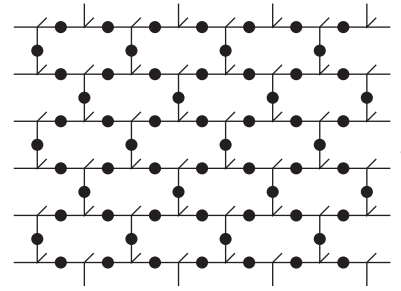
a. Injective PEPSs

Global symmetries of injective PEPSs behave essentially equivalently to global symmetries in the MPS case: the fundamental theorem of injective PEPSs (Sec. IV.B) dictates that two uniform PEPSs are equal if and only if they are related by a gauge transform on the virtual level:

$$\sum_j U_{ij}(g) A_{\alpha\beta\gamma\delta}^j = e^{i\phi} \sum_{\alpha'\beta'\gamma'\delta'} X(g)_{\alpha\alpha'} X(g)_{\beta\beta'}^{-1} Y(g)_{\gamma\gamma'} Y(g)_{\delta\delta'}^{-1} A_{\alpha'\beta'\gamma'\delta'}^i. \quad (54)$$

As in the 1D case, $X(g)$ and $Y(g)$ form possibly projective representations of the group G characterizing the global symmetries of the system. The fact that a PEPS tensor exhibiting this feature has a global symmetry follows immediately from the fact that all these gauge transformations cancel each other pairwise. The surprising content of the fundamental theorem is that it is also a necessary condition. This again implies that the PEPS tensor can be decomposed as a product of Clebsch-Gordan coefficients; this has already been used extensively in numerical PEPS algorithms. Note that different projective representations do not necessarily lead to different phases if one does not impose translational invariance, as blocking several sites together allows one to relate different projective representations to each other.

The canonical example for an injective PEPS with global symmetries is the cluster state (Raussendorf and Briegel, 2001) on the honeycomb lattice, which is the unique ground state of the commuting parent Hamiltonian $\sum_{ijkl} X_i Z_j Z_k Z_l$ of qubits where $j, k,$ and l are the nearest neighbors of site i . This state has the following simple PEPS representation (Verstraete and Cirac, 2004b):



with

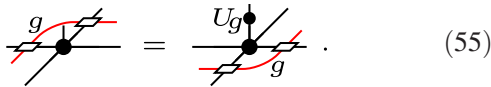
$$\text{---} \begin{array}{c} \diagup \\ | \\ \diagdown \end{array} \text{---} = |0000\rangle + |1111\rangle, \quad \bullet = \frac{1}{\sqrt{2}} \begin{pmatrix} 1 & 1 \\ 1 & -1 \end{pmatrix}.$$

This exhibits the global symmetry $Y^{\otimes N}$, as it is simply the product of all commuting terms of the Hamiltonian. To use the fundamental theorem of PEPSs, we first block two sites of this PEPS so as to make it uniform, and it can then be readily checked to see that the local physical symmetry is equivalent to acting on all virtual legs with the same Y on all four legs. This cluster state is interesting from the point of view of quantum information theory, as it allows one to perform a universal quantum computation by implementing local measurements on its qubits (Raussendorf and Briegel, 2001). The underlying mechanism that allows for this noteworthy feature is the fact that local measurements on the physical qubits effectively teleport the virtual degrees of freedom, and in the process implement quantum gates (Verstraete and Cirac, 2004b). A related mechanism underlies the concept of topological quantum computation by braiding anyons, which can be understood in terms of quantum circuits on the entanglement degrees of freedom of the PEPS describing the topological phase.

Note that we had to block sites of the cluster state to get a uniform PEPS description. From the point of view of space group symmetries, this is not wholly satisfactory, as it leads to a loss of symmetry in the system. It turns out that the full space group symmetry can be done justice for general PEPSs by including matrices that act only on the virtual edges connecting the vertices of the PEPS. By imposing translational symmetry, it will then follow that this decorated PEPS will be uniform and exhibit all lattice symmetries (Jiang and Ran, 2017).

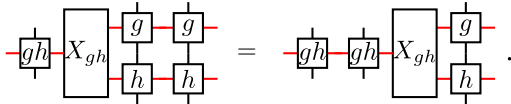
b. Noninjective PEPSs: SPT phases

Injective PEPSs on a square lattice are rare, as the injectivity condition is typically violated at the corners of the region of interest. Unlike in the MPS case, however, noninjective PEPSs can still be unique ground states of local gapped Hamiltonians. The 2D AKLT model on the square lattice is such an example. The noninjectivity gives rise to the following much more interesting algebraic structure in the form of a family of matrix product operator symmetries O_g labeled by the group elements of the global symmetry (Williamson *et al.*, 2016; Molnar, Ge *et al.*, 2018):



This local condition is sufficient for the complete PEPS to be invariant under the global symmetry $U^{\otimes N}(g)$ in the thermodynamic limit.

To be consistent, the MPOs O_g should form a representation of the group G : $O_g \cdot O_h = O_{gh}$. The fundamental theorem of MPSs allows one to translate this condition into a local condition for the tensors defining these MPOs, as two MPOs are equal to each other if and only if there is an intertwiner (or fusion tensor) connecting them to each other:



The associativity condition for these fusion tensors then leads to the condition that the elements both of these MPOs and of the intertwiners can be identified with the elements of a 3-cocycle determined by the third cohomology group $H^3(G, U(1))$. This situation is equivalent to the one discussed in Sec. III.A.6, but for the special case of the fusion algebra being a group. The third cohomology group is well known to classify symmetry-protected topological phases in two dimensions (Chen, Liu, and Wen, 2011), and PEPSs hence provide a natural realization of such phases.

As in the case of 2-cocycles, there is a systematic way of writing PEPS tensors that exhibit such MPO symmetries (Williamson *et al.*, 2016). Indeed, the pulling through equation (55) can, componentwise, be identified with the 3-cocycle condition.

The canonical example of a nontrivial SPT PEPS was derived by Chen, Liu, and Wen (2011) as the CZX state (see Appendix 4.a) with global Z_2 symmetry, for which the virtual MPO symmetry is represented by the following two matrix product unitaries acting on qubits: $O_1 = 1$, $O_Z = \otimes_i CZ_{i,i+1} \otimes \otimes_i X_i$. Here the commuting matrices $CZ_{i,i+1} = \sum_{ij} (-1)^{ij} |ij\rangle\langle ij|$ represent diagonal controlled-Z gates. O_Z has bond dimension 2, but the square of it is not in canonical form and has a one-dimensional invariant subspace equal to $O_1 = 1$.

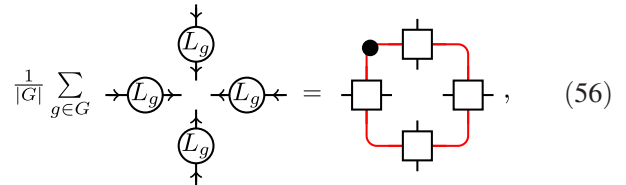
These ideas were worked out by Buerschaper (2014), Williamson *et al.* (2016), and Molnar, Ge *et al.* (2018). It was demonstrated that this notion of MPO-injectivity (also called semi-injective) is sufficient for guaranteeing the uniqueness of the ground state of the corresponding parent Hamiltonian, and that the corresponding PEPSs fully characterize short-range entangled SPT phases.

c. Virtual symmetries

One of the most striking features of two-dimensional quantum spin systems is the fact that there are topological phases of matter that are stable under any perturbations (Bravyi, Hastings, and Michalakis, 2010; Klich, 2010). This robustness is a consequence of its nontrivial entanglement structure, which is reflected in the behavior of the topological entanglement entropy and its edge modes, and in the anyonic statistics of its

elementary excitations. Tensor networks provide a natural language for describing all those features in terms of the local symmetries of the tensors involved.

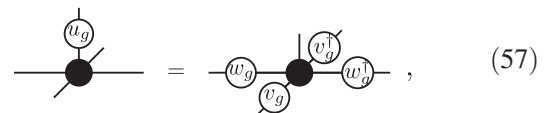
The fact that there is a connection between topological phases of matter and symmetries in the tensors has its roots in the pioneering work of Gu, Levin, and Wen (2008) and was described by Schuch, Cirac, and Perez-Garcia (2010). There it was shown that the symmetries in the virtual indices of a PEPS characterize its topological order. Specifically, a PEPS is constructed for each finite group G , where the local tensor is given as follows by the G -injective MPO (53):



where input indices correspond to the virtual degrees of freedom and output indices to the physical Hilbert space. Strictly speaking, the arrows on the right and bottom tensors must be reversed to make the arrows match in the PEPS construction. In this case, reversing the arrows simply amounts to taking the inverse representation. The PEPS constructed in this way is called G -injective.

The symmetries of the tensor [Eq. (52)] allow one to easily recover all topological invariants (topological entanglement entropy, ground state degeneracy, anyonic statistics, etc.) and correspond to the phase of the quantum double models of Kitaev (2003). It is important to notice that, by acting with an invertible operator on the physical index, one can perturb the tensor and induce finite correlation lengths and, for large perturbations, topological phase transitions. In this sense, G -injective PEPSs allow one to recover not only the quantum double model but also all the associated phases (see Sec. II.C.2) and the phase transitions between them. They also allow one to study particularly relevant models that are not renormalization fixed points such as the nearest-neighbor RVB state (Anderson, 1973), which is an $SU(2)$ invariant spin liquid when defined on a frustrated 2D lattice. As explained by Verstraete *et al.* (2006), this RVB has a simple description in terms of a PEPS with bond dimension 3. As shown by Schuch *et al.* (2012), it exhibits a nontrivial purely virtual Z_2 symmetry, and it can be adiabatically continued to the toric code phase without crossing a phase transition. Indeed, thanks to the PEPS approach, a parent Hamiltonian was derived for it (Schuch *et al.*, 2012; Zhou, Wildeboer, and Seidel, 2014).

The RVB state is an example where the symmetries in the virtual indices arise naturally from physical symmetry constraints. For example, if a global $SU(2)$ spin-1/2 symmetry is encoded locally in the tensor



then the virtual symmetries must necessarily be reducible and contain both integer and half-integer representations, such as

$1/2 \oplus 0$, and the tensor must be supported on the sector containing an odd number of half-integer ones. This enforces a \mathbb{Z}_2 virtual symmetry in the tensor. This effect is simply a version in the context of PEPSs of Hastings’s 2D version of the Lieb-Schultz-Mattis theorem (Hastings, 2004a).

The G -injective construction was generalized by Buerschaper (2014) to twisted quantum double models (twisted G -injective PEPSs) and to the case of an arbitrary fusion category by Şahinoğlu *et al.* (2021), under the name MPO-injective PEPSs. Those MPO constructions were unified by invoking the structure of a bimodule category by Lootens *et al.* (2021).

For the case of topological phases, the pulling through equation (52) becomes similar to the case of SPT phases but without a physical action:

$$\text{Diagram 1} = \text{Diagram 2} \quad (58)$$

As discussed in Sec. III.A.6, the bimodule categories define MPO algebras and PEPS tensors satisfying the pulling through equations through a set of six coupled pentagon equations. This construction starts with two Morita-equivalent fusion categories \mathcal{C} and \mathcal{D} labeling the different MPO tensors and the degrees of freedom of the physical Hilbert space, respectively. The $(\mathcal{C}, \mathcal{D})$ -bimodule category \mathcal{M} then represents the entanglement degrees of freedom of the PEPS tensor depending on \mathcal{D} and \mathcal{M} . The PEPS tensor is represented by 3F of Sec. III.A.6, while the MPO tensor corresponds to 2F . For the case of quantum doubles, \mathcal{D} is given by the group \mathcal{G} and \mathcal{C} can be chosen to be equal either to the irreps of that group, for which \mathcal{M} is trivial, or to \mathcal{G} , in which case $\mathcal{C} = \mathcal{D} = \mathcal{M}$ and nontrivial 3-cocycles become possible.

The same bimodule categorical objects can also be used to define intertwiners between different PEPS realizations of the same state $|\psi\rangle$ (Lootens *et al.*, 2021); the fact that such realizations exist is a consequence of the fact that the category \mathcal{D} corresponding to the physical degrees of freedom can have several Morita-equivalent categories \mathcal{C}_i , each with a compatible \mathcal{M}_i ; different \mathcal{M} lead to completely different but locally equivalent PEPS descriptions such as $\text{PEPS}_{\mathcal{D}, \mathcal{M}_1}$ and $\text{PEPS}_{\mathcal{D}, \mathcal{M}_2}$. Translating the seminal work of Kitaev and Kong (2012) into tensor network language, these intertwiners can again be described in terms of MPOs. It is then possible to construct intertwiners relating different physical and/or virtual tensor network representations of quantum doubles and string nets to each other. In particular, the mapping of quantum double models to string-net tensor network descriptions can be readily completed using such MPOs; see also Buerschaper and Aguado (2009) and Kádár, Marzuoli, and Rasetti (2010).

d. SET phases

As in the one-dimensional case, virtual and physical symmetries can be combined in a nontrivial way. The corresponding phases are called SET phases. Such systems have been studied at length by Barkeshli *et al.* (2019), and the mathematical framework to describe the possible phases is given by graded unitary fusion category theory. Such graded

fusion categories can again be realized within the context of matrix product operators, and the nonchiral case gives rise to a PEPS description where the MPO symmetry reflects this grading (Williamson, Bultinck, and Verstraete, 2017). Analogously to SPT phases, string order parameters can be defined to detect the symmetry fractionalization pattern of SET phases that also involve swaps between distant regions; see Garre-Rubio and Iblisdir (2019) for details.

Graded fusion categories also allow one to characterize topological phases for fermionic systems in terms of super-pivotal categories (Aasen, Lake, and Walker, 2019). By adopting the language of graded tensor networks, it is possible to realize these phases in terms of fermionic PEPS (Bultinck, Williamson *et al.*, 2018), for which the Majorana defects can be explicitly constructed. In addition, the generalization of the toric code to the fermionic case (Gu, Wang, and Wen, 2014) can be readily understood in terms of these graded tensor networks.

e. Chiral phases

Phases with chiral order (Bernevig and Hughes, 2013) exhibit a number of phenomena that distinguish them from the previously discussed nonchiral topologically ordered states. In particular, they exhibit protected gapless edge modes characterized by a chiral CFT, whose spectrum is matched by the entanglement spectrum (Li and Haldane, 2008). These phases can be protected either by the fermionic parity superselection rule or by an additional symmetry, such as time reversal, and can show up in both free fermion and interacting models, most notably Kitaev’s honeycomb model (Kitaev, 2006). However, some of the properties of chiral systems [such as the gapless nature of the entanglement spectrum, which is suggestive of some kind of “nonrenormalizability,” or the fact that their Wannier functions cannot be locally supported (Kohn, 1973)] suggest that it might not be possible to describe them as PEPSs.

As it turns out, PEPS can describe noninteracting fermionic systems with chiral order exactly (Wahl *et al.*, 2013; Dubail and Read, 2015); an example is given in the Appendix. The resulting free fermion PEPSs are ground states of a flatband Hamiltonian with algebraically decaying interactions whose bands have nonzero Chern number; i.e., they exhibit nontrivial chiral order. The simplest of these examples is a topological superconductor (protected by fermionic parity); more complex examples such as topological insulators can be constructed from two or more copies thereof. The flatband Hamiltonian exhibits gapless chiral edge modes and a matching chiral entanglement spectrum, and it exhibits correlations (and thus interactions) that decay as $1/r^3$ (Wahl *et al.*, 2014). The PEPS tensor exhibits a virtual symmetry characterized by an unoccupied mode. As shown by Wahl *et al.* (2014), this unoccupied mode is stable under blocking, and thus gives rise to an empty mode formed jointly by one Majorana mode on both the left and right boundaries at a given momentum k , in analogy with the two Majorana edge modes in the Kitaev chain. These edge modes exactly match the point where the edge mode is absorbed into the bulk. Systems with a higher Chern number (and a higher number of gapless edge modes) correspondingly exhibit a larger number of such symmetries.

Moreover, the same symmetry is needed to construct the ground states on the torus. As in the case of the Majorana chain [Eq. (50)], antiperiodic boundary conditions are required to describe the chiral PEPS wave function.

Numerical findings suggest that PEPSs can also describe interacting chiral phases. One possibility for constructing such interacting models is by Gutzwiller projecting several copies of a noninteracting topological superconductor or insulator, a construction for which field theory predicts an interacting topological model; numerical study of two copies indeed reveals entanglement spectra consistent with a chiral Kalmeyer-Laughlin state but, at the same time, is suggestive of critical correlations (Yang *et al.*, 2015). An alternative approach put forth by Poilblanc, Cirac, and Schuch (2015) and Poilblanc, Schuch, and Affleck (2016) is to construct a PEPS from tensors A , which themselves possess a “chiral symmetry” (that is, they are invariant under combined reflection and conjugation). It is found that the resulting PEPSs exhibit entanglement spectra consistent with chiral theories [depending on the additional symmetry, such as $SU(2)$ and $SU(3)$, encoded in the tensor], as well as algebraic correlations (Poilblanc, Cirac, and Schuch, 2015; Poilblanc, Schuch, and Affleck, 2016; Haegeman and Verstraete, 2017; Chen *et al.*, 2018; Hackenbroich, Sterdyniak, and Schuch, 2018; Chen *et al.*, 2020). In all these cases, a limitation to their analytical study is in the fact that both entanglement spectra and correlations can be determined only numerically, leaving an uncertainty in distinguishing a truly chiral entanglement spectrum from a nonchiral one with a small gap in the entanglement spectrum (and significantly different velocities of the counterpropagating chiral theories), as well as critical correlations from a large but finite correlation length (Hackenbroich, Sterdyniak, and Schuch, 2018).

While PEPSs can represent states with chiral order, there are limitations to their ability to exactly capture chiral systems. As shown by Dubail and Read (2015) and Read (2017), PEPSs cannot capture noninteracting (either intrinsic or symmetry-protected) chiral states with exponentially decaying correlations exactly, and Lemm and Mozgunov (2019) showed that the existence of a gapped parent Hamiltonian with periodic boundaries implies an open boundary spectrum inconsistent with chiral edge modes with linear dispersion (see Sec. IV.C.2 for a precise statement), providing a partial no-go result also for interacting chiral phases.

Despite these no-go theorems, the approximation results for the faithful approximations of low-energy states of gapped Hamiltonians (with a suitable density of states) still apply (Hastings, 2006; Molnar *et al.*, 2015), and it has been found numerically that PEPSs are well suited to approximate ground and thermal states of both noninteracting and interacting Hamiltonians and allow one to simultaneously approximate chiral entanglement spectra and exponentially decaying correlations on the relevant scales (Wahl *et al.*, 2013; Poilblanc, 2017; Chen *et al.*, 2018, 2020).

2. Entanglement spectrum and edge Modes

a. Entanglement Hamiltonians

One of the defining properties of PEPSs is the fact that the tensors describe how entanglement is routed throughout the

system. In practice, tensor networks implement an effective holographic dimensional reduction of the physical degrees of freedom to a one-dimensional system of entanglement degrees of freedom: all correlations in the PEPS are determined by the fixed points or entanglement Hamiltonians of the 1D transfer matrices of the PEPS. The local MPO symmetries of the tensors immediately translate to MPO symmetries of these transfer matrices. As we have discussed, the symmetries on the virtual level can be much richer than the ones on the physical level, and for topological ordered systems amount to nontrivial MPOs. The results reported in Sec. III.A.6 then immediately imply that the corresponding entanglement Hamiltonians ought to be critical, hence realizing an explicit tensor network analog of the fingerprints of conformal field theory in the entanglement spectrum (Dubail, Read, and Rezayi, 2012; Qi, Katsura, and Ludwig, 2012).

The situation is slightly different for SPT phases than for topological phases. In the former case, the transfer matrix has the symmetry $[O_g \otimes \bar{O}_g, T] = 0$ and has a unique fixed point $|\rho\rangle$ that hence inherits this symmetry $O_g \rho O_g^\dagger = \rho$. As first observed by Chen, Liu, and Wen (2011), whenever the symmetry on the entanglement degrees of freedom is realized through a nontrivial cocycle, the corresponding entanglement Hamiltonian $\rho = \exp(-\beta H_E)$ is critical or symmetry broken. Note that whenever the SPT ground state is a renormalization group fixed point with zero correlation length, the corresponding temperature is $\beta = 0$ and hence one has to perturb the system to witness H_E (Bultinck, Vanhove *et al.*, 2018).

For the case of a genuine topological phase, the MPO symmetries do not have to come in pairs, and any off-diagonal combination is also allowed: $[O_a \otimes \bar{O}_b, T] = 0$. This has interesting consequences for the fixed-point structure of the corresponding transfer matrix T : whenever ρ is a fixed point, $O_a \rho O_b^\dagger$ is also a fixed point for any choices of a and b . This degeneracy of the fixed points follows from the noninjectivity of the PEPS and is a clear signature of topological order (Schuch *et al.*, 2013). Given N independent MPO symmetries O_a , one would naively think that there will be N^2 distinct fixed points. This is not the case, however, as there are exactly N fixed points, implying that the entanglement structure exhibits a subtle type of symmetry breaking. Following Haegeman *et al.* (2015) and Duivenvoorden *et al.* (2017), we can understand this from the necessity of having anyons in the system. If the degeneracy is N^2 , then the anyons are confined, and if the degeneracy is 1 all anyons are condensed. Only the case of N different fixed points provides the perfect balance and leads to genuine topological order. A quantum phase transition occurs whenever this fixed-point structure changes.

This result is in complete accordance with the principal formula for topological entanglement entropy (Kitaev and Preskill, 2006; Levin and Wen, 2006), which states that the entanglement entropy of a certain region in the bulk has a $\log(D_q)$ correction, with D_q the total quantum dimension of the underlying fusion algebra. This is a direct consequence of the fact that the edges of the block under consideration do not live in the full Hilbert space but are instead constrained to the MPO-invariant subspace, whose dimension is a constant factor D_q lower than the full one.

b. Edge modes

A notable feature of PEPSs is the fact that it provides a Hilbert space with a tensor product structure on the edge of a PEPS with open boundary conditions: these are precisely the bonds or entanglement degrees of freedom that are unconnected, and hence span a Hilbert space D^L with D the bond dimension and L the number of uncoupled bonds (Yang *et al.*, 2014); see Sec. II.D.3. Note that these degrees of freedom cannot be directly accessed, as they are virtual, and also that Hamiltonian terms acting on the physical boundary of the system will induce an effective Hamiltonian on that Hilbert space. Assuming that the bulk is gapped, low-energy modes can emerge on that virtual Hilbert space, and an important task is to study the spectrum and features of these edge excitations. If the system exhibits nontrivial symmetries, as in the case of topological order or SPT phases, then an interesting situation occurs: when the effective Hilbert space of the spin chain is projected onto the symmetric or invariant subspace of the MPO symmetries, nonlocal features emerge that are impossible for normal spin chains. In the language of quantum field theory, the MPOs induce anomalies in the boundary.

We first discuss the case of SPT phases. Acting with the physical symmetry $U_g^{\otimes N}$ on the wave function induces a nontrivial MPO-symmetry action on the boundary. The effective Hamiltonian of the edge modes is hence MPO symmetric, and, as discussed in Sec. III.A.6, must therefore be either symmetry breaking or critical. Even in the symmetry-breaking case, there will be a ground state with all symmetries, but it will be realized as a highly entangled GHZ or cat state. This is equivalent to the situation in the 1D AKLT model, where the only SO(3)-invariant state is one in which the dangling spins at the ends form a singlet. The ground state of any SPT state with open boundary conditions can therefore not be unique and, from the physics point of view, symmetry breaking will occur.

The situation is different for the topological case, where the bulk symmetry is purely virtual. This implies that the Hilbert space of the edge modes has to be projected on the MPO-symmetric subspace. If P_s is the projector on the O_g -invariant subspace, then the Hamiltonian $P_s H_{\text{edge}} P_s$ can be gapped and has a unique ground state (Yang *et al.*, 2014). If the MPO symmetry is nontrivial, that ground state must be MPO symmetric and hence has to be a GHZ state. The various components in this GHZ are related to each other through their interactions with O_g . This is an interesting phenomenon: the physics on the edge induces stable highly entangled states that would be impossible to create in a genuine one-dimensional system. For the case of quantum doubles, twisted quantum doubles, and string nets, the boundaries can always be gapped, a fact that is known to follow from the feature that the bulk theory of these systems always yields a Lagrangian subgroup of the anyons (Kitaev and Kong, 2012; Levin, 2013): the set of anyons in the bulk can be divided into two sets, one in which every anyon has trivial statistics with respect to each other one, and a second subset for which every one exhibits nontrivial statistics with at least one of the first set. As we show in Sec. III.B.3, anyons are described by idempotents of an extended MPO algebra and always satisfy this criterion. The corresponding ground state will be of GHZ type or not

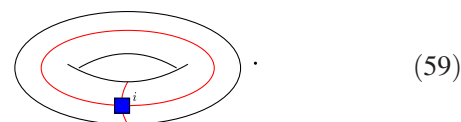
depending on whether the underlying MPO algebra is trivial (as in the case of quantum doubles) or not (as in the cases of twisted quantum doubles and string nets).

3. Topological sectors and anyons

Two defining features of topological phases are the facts that the ground state degeneracy depends on the genus of the manifold on which the spins are defined, and that the elementary excitations are anyons with nontrivial statistics. The fact that both of these features are intimately connected with each other is made explicit when one studies them from the point of view of PEPSs: both are defined by the same tensors (Schuch, Cirac, and Perez-Garcia, 2010; Bultinck, Mariën *et al.*, 2017).

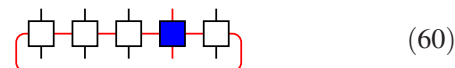
a. Topological sectors

We first discuss the different ground states for a topological spin system on a torus. Consider, on the one hand, a uniform PEPS and, on the other hand, the same uniform PEPS but with a virtual nontrivial MPO winding in one of the directions of the torus. As the PEPS exhibits the MPO symmetry, the location of the MPO is immaterial and this second state turns out to be orthogonal to the first one. Note that winding two MPOs O_a and O_b in the same direction is equivalent to the sum of $\sum_c N_{ab}^c O_c$, as we can always pull them through the lattice until they touch each other. We could also wind a MPO in the other direction and get a different state. A problem arises, however, when we try to wind two MPOs in two different directions. This inevitably leads to a crossing of the two MPOs, and we have to introduce the following new tensor object [blue square in Eq. (59)] in order to define this crossing:



By varying this tensor and requiring that it can be pulled through the PEPS tensors, we are able to completely characterize all ground states of the topological theory. Physically, the pulling through property implies that the topological sector is invisible by local measurements on the physical Hilbert space.

It is possible to put more MPOs in the PEPS, and doing so induces more and more crossings. However, it should not lead to new ground states, and hence the enlarged MPOs



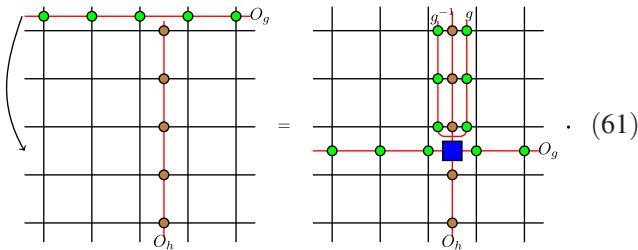
themselves should form an algebra. It was proven that they form a C^* algebra, which means that they form a closed algebra when multiplied by each other and under conjugation (Bultinck, Mariën *et al.*, 2017).

Such a C^* algebra has a natural decomposition into minimal central idempotents $P_i, P_i P_j = \delta_{ij} P_i$, and these blocks provide the full set of orthogonal ground states or topological sectors on the torus. From the categorical point of view, this construction is called the Drinfeld center (Drinfel'd, 1987;

Müger, 2003b), and the C^* algebra is called the Ocneanu tube algebra (Evans and Kawahigashi, 1995). The states corresponding to the idempotents are the ground states with minimal entanglement (Zhang *et al.*, 2012), which indeed provide a natural partitioning of the ground state sector. From a practical point of view, these idempotents can be calculated from the structure factors of this enlarged MPO algebra. This program can be realized in a straightforward way for all PEPSs described in the language of bimodule categories. Similarly, it can be worked out in terms of weak Hopf algebras: using the condition that physical and virtual indices in the associated MPOs correspond, respectively, to the algebras \mathcal{A} and \mathcal{A}^* , the enlarged MPO gives a representation, as vector space, of $\mathcal{A} \otimes \mathcal{A}^*$. Apart from the previously discussed algebra structure, there is a natural coproduct, given by $\Delta_{\mathcal{A}} \otimes \Delta_{\mathcal{A}^*}$, that makes it a weak Hopf algebra. This is called the Drinfeld double, and it is precisely the weak Hopf algebra associated with the Drinfeld center category; see Sec. III.A.6.

We now illustrate in the particular case of the G -injective PEPS defined by tensor (56) the process just described that obtains the Drinfeld double of a finite group G by simply imposing a pulling through condition on the enlarged MPOs of the associated G -injective PEPS (Schuch, Cirac, and Perez-Garcia, 2010).

For that purpose, we start by analyzing the conditions of the crossing tensor needed to pull it through the lattice. When we move a horizontal virtual MPO $O_g = L_g^{\otimes N}$ one row down, if there is also a vertical virtual MPO $O_h = L_h^{\otimes M}$, the group element of the vertical MPO associated with the position between the two rows is conjugated by g :



Therefore, the crossing tensor needed for that action is precisely a linear combination of tensors of the form

$$|g\rangle\langle g| \otimes |ghg^{-1}\rangle\langle h|. \quad (62)$$

The enlarged MPO associated with the crossing tensor (62) is precisely $L_g^{\otimes N} \otimes |ghg^{-1}\rangle\langle h|$, which corresponds to the element $g \otimes \delta_h \in \mathbb{C}(G) \otimes \mathbb{C}^G$, where \mathbb{C}^G denotes the set of functions $G \rightarrow \mathbb{C}$ and δ_h is the function defined by $\delta_h(k) = 1$ for $k = h$ [and $\delta_h(k) = 0$ otherwise].

Given two pairs (g, δ_h) and $(g', \delta_{h'})$ in $\mathbb{C}(G) \otimes \mathbb{C}^G$, the multiplication induced by their associated enlarged MPOs is given by

$$(g, \delta_h) \cdot (g', \delta_{h'}) = (gg', \delta_h(g'h'g^{-1})\delta_{h'})$$

since, trivially,

$$\begin{aligned} & (L_g^{\otimes N} \otimes |ghg^{-1}\rangle\langle h|) \cdot (L_{g'}^{\otimes N} \otimes |g'h'g'^{-1}\rangle\langle h'|) \\ &= L_{gg'}^{\otimes N} \otimes \delta_h(g'h'g'^{-1})|ghg^{-1}\rangle\langle h'| \\ &= L_{gg'}^{\otimes N} \otimes \delta_h(g'h'g'^{-1})|(gg')h'(gg')^{-1}\rangle\langle h'|. \end{aligned}$$

The algebra $\mathbb{C}(G) \otimes \mathbb{C}^G$ equipped with this multiplication is precisely the definition of the Drinfeld double of the group G .

Gould (1993) showed that the generating idempotents in this case are given by fixing a conjugacy class, a representative $h \in G$ for it, and an irrep α of the centralizer of h , $Z(h) = \{g \in G : gh = hg\}$. The associated central idempotent is the one given by a crossing tensor proportional to

$$T_{h,\alpha} = \sum_{k \in G} \sum_{g \in Z(h)} \chi_\alpha(g^{-1})|k^{-1}gk\rangle\langle k^{-1}gk| \otimes |k^{-1}hk\rangle\langle k^{-1}hk|,$$

which gives an enlarged MPO proportional to

$$P_{h,\alpha} = \sum_{k \in G} \sum_{g \in Z(h)} \chi_\alpha(g^{-1})L_{k^{-1}gk}^{\otimes N} \otimes |k^{-1}hk\rangle\langle k^{-1}hk|,$$

where χ_α is the character of α .

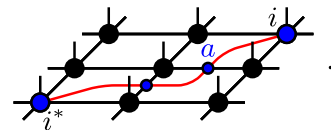
Note that the conjugation by k can be absorbed in the PEPS due to the virtual symmetry, which finally gives the following simpler crossing tensor and enlarged MPO:

$$\sum_{g \in Z(h)} \chi_\alpha(g^{-1})|g\rangle\langle g| \otimes |h\rangle\langle h| P_{h,\alpha} = \sum_{g \in Z(h)} \chi_\alpha(g^{-1})L_g^{\otimes N} \otimes |h\rangle\langle h|.$$

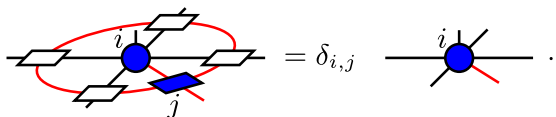
The topological sectors are then indexed using a conjugacy class and an irrep of its centralizer, as expected (Kitaev, 2003). For the particular case of the toric code, we obtain the projectors $(\mathbb{1}^{\otimes N} \pm X^{\otimes N}) \otimes |h\rangle\langle h|$, with $h \in \{0, 1\}$. For the general case of bimodule categories, the idempotents can readily be found by diagonalizing linear combinations of the adjoint representation of the C^* algebra (Lootens *et al.*, 2021).

b. Anyons

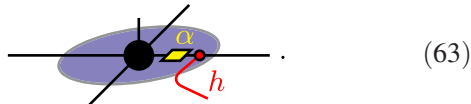
In a notable twist, it turns out that the idempotents defining the ground state manifold on the torus also define the elementary bulk excitations. The orthogonality of the idempotents provides a natural decomposition of the Hilbert space into topological sectors, and some of them have a nontrivial MPO string attached to them. The corresponding anyons have nontrivial self-statistics and nontrivial braiding. All of these features can be succinctly understood from the fact that virtual MPO strings are attached to them, which is immaterial as they can be moved at will through the lattice (Schuch, Cirac, and Perez-Garcia, 2010; Bultinck, Mariën *et al.*, 2017). A pair of anyons in the PEPS picture hence has the following form:



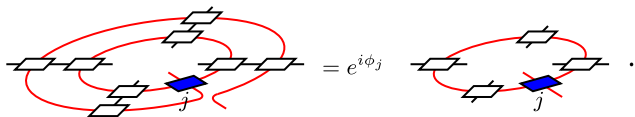
Here the tensor labeled i (blue) projects onto one of the previously defined idempotents as follows:



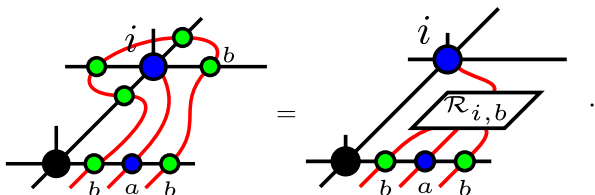
In the particular case of G -injective PEPSs, that tensor takes the following form:



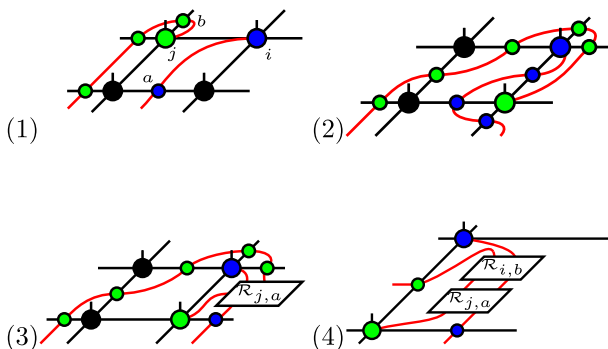
The topological spin of an anyon characterizes the phase that the wave function acquires when rotating the anyon over 2π as follows:



For the case of the toric code, one sees that the anyon characterized by the idempotent $(I - Z^{\otimes N})/2$ with a string attached to it has topological spin $1/2$ and is hence called a fermion. Anyons have new fusion rules generating the output category. Those are precisely the ones associated with the Drinfeld center. Anyons also exhibit braiding properties, encoded in a tensor \mathcal{R} , that give the following generalized pulling through equation:



With this one can compute the braiding of one anyon around another by performing the following four steps:



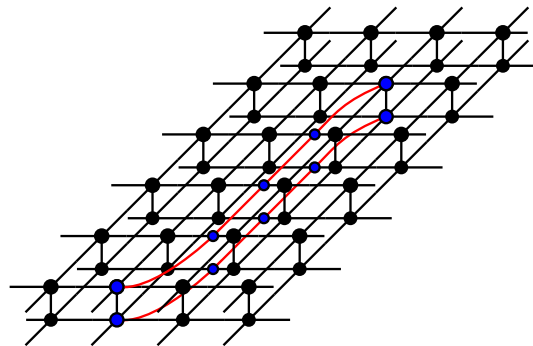
This idea can readily be exploited to show that the concept of topological quantum computation (Freedman *et al.*, 2003; Kitaev, 2003), in which anyons are braided, can be described in terms of the usual quantum circuit model for quantum computation applied to the entanglement degrees of freedom; see (Bultinck, Mariën *et al.* (2017) for details.

Braiding takes a simpler and more explicit form in the group case. For instance, in case of a trivial irrep α , braiding corresponds to conjugation (adjoint action), as illustrated in Eq. (61).

Note that distinct input categories can lead to equivalent Drinfeld doubles; this, e.g., happens in the case of a twisted $Z_2 \times Z_2$ and a Z_4 quantum double. Two categories with this feature are called Morita equivalent (Müger, 2003a; Kitaev and Kong, 2012) and, as discussed in Sec. III.B.1.c, it is then possible to construct an intertwiner (in the form of a MPO) between the two corresponding PEPSs that preserves all topological features and effectively implements an automorphism of the corresponding topological sectors. This idea has been extended to a systematic study of boundaries between different theories (such as boundaries between a topological phase and a trivial phase with open boundary conditions) and allows one to construct all possible boundary conditions that are compatible with the anyonic bulk physics. In the case of the toric code, this leads to the concept of rough and smooth edges: absorbing electric versus magnetic excitations on the boundary (Bravyi and Kitaev, 1998; Lootens *et al.*, 2021).

c. Anyon condensation

Although the topological phases described using quantum doubles and string nets are stable with respect to any perturbation (Bravyi, Hastings, and Michalakis, 2010; Klich, 2010), a topological phase transition will occur whenever the perturbation becomes large. From the point of view of PEPSs, such a transition is characterized by a change in the MPO-symmetry-breaking pattern of the eigenvectors of the transfer matrix (Schuch *et al.*, 2013). In the topological phase described by an input category with N labels (and hence N corresponding MPOs), there are N linearly independent eigenvectors σ_i of the transfer matrix with eigenvalues of modulus 1, obtained by acting with the MPOs on a fiducial one ρ : $\sigma_i = O_i \rho$. Note that for the toric code $\rho = \mathbb{1}$. An important property is that the MPOs $O_i \rho O_i^\dagger$ do not yield new fixed points, and furthermore $O_i \rho O_i^\dagger$ is not linearly independent of ρ . As demonstrated by Haegeman *et al.* (2015) and Duivenvoorden *et al.* (2017), this can easily be considered a necessary condition for the possibility of having anyons, as otherwise the expectation value of a PEPS with a pair of anyons connected with a MPO string would be zero, as illustrated in the following graphic:



If the fixed point $O_i \rho O_i^\dagger$ were orthogonal to ρ , the norm of the state with two anyons connected by a string would decay

exponentially in the distance between the anyons, as it would be obtained by raising a mixed transfer matrix with spectral radius strictly smaller than 1 to the distance between the anyons. This explains why the eigenvectors of the transfer matrix must strike a delicate balance of the symmetry-breaking pattern.

This immediately clarifies the fact that a large perturbation increasing the number of fixed points of the transfer matrix will lead to confinement of the anyons, and hence to a topological phase transition. Conversely, the situation in which the number of distinct fixed points decreases makes the existence of strings irrelevant; this corresponds to the condensation of anyons. As shown by [Duivenvoorden *et al.* \(2017\)](#), the PEPS description is fully compatible with the standard rules of anyon condensation ([Bais, Schroers, and Slingerland, 2002](#)): (1) Only particles with trivial self-statistics can condense, (2) anyons become condensed if and only if they have mutual nonbosonic statistics with a condensed anyon, (3) noncondensed anyons that differ by a condensed anyon become indistinguishable, and (4) anyons that can fuse to two different condensed anyons split into two distinguishable anyons. Similar rules apply in the context of orbifolding in conformal field theory. This connection can indeed be fully established by making use of the formalism of strange correlators ([Vanhove *et al.*, 2018](#)) and of noninvertible bimodule categories ([Lootens *et al.*, 2021](#)), thereby helping us to realize all possible ways in which anyons can condense.

When restricting to the group case, this leads to a natural connection between anyon condensation and SET phases ([Garre-Rubio, Iblisdir, and Perez-Garcia, 2017](#)). Given a group G and a normal subgroup H , there is a natural way of condensing anyons that restricts the G -injective tensor to the subgroup H . The strings of the anyons then fulfill the pulling through equation (55) if they come from H . If they do not, they get confined and the pulling through equation degrades to one of the form of Eq. (58), where a unitary must be applied in the physical level. These unitaries precisely form a representation of the quotient group $Q = G/H$. That is, condensing anyons make a global symmetry emerge under which the new condensed model is in a SET phase. One can show that all SET phases appear in this way. This bimodule MPO point of view of anyon condensation is a generalization of this idea.

IV. FORMAL RESULTS: FUNDAMENTAL THEOREMS AND HAMILTONIANS

In this section, we provide formal statements for two types of mathematical problems linked to tensor networks. In Secs. IV.A and IV.B, we enunciate the fundamental theorems for matrix product vectors and PEPSs, respectively. These fundamental theorems relate different MPS representations of the same MPS, MPO, or PEPS and are essential in the classification of phases under symmetries, renormalization fixed points, and MPO algebras describing topological order. In Sec. IV.C, we discuss the relation of MPSs or PEPSs and Hamiltonians. In particular, we explain how MPSs and PEPSs appear as ground states of parent Hamiltonians and review the known theorems about their ground space structure, their gap, and their robustness against perturbations.

A. The fundamental theorem of matrix product vectors

1. Overview

Thus far, we have encountered different kinds of tensor networks: MPS, MPOs, MPDOs, and MPUs. All these live on a sequence of spaces $\mathcal{H}_d^{\otimes N}$, $N \in \mathbb{N}$, where \mathcal{H}_d is the corresponding d -dimensional local Hilbert space of states or operators. Therefore, all these cases can be seen as special cases of matrix product vectors (MPVs),

$$|V^{(N)}(A)\rangle = \sum_{i_1, \dots, i_N=1}^d \text{tr}(A^{i_1} \cdots A^{i_N}) |i_1 \cdots i_N\rangle \in \mathcal{H}_d^{\otimes N}, \quad (64)$$

where the A^i are $D \times D$ matrices. We denote the family of MPVs generated by A by $\mathcal{V}(A) := \{|V^{(N)}(A)\rangle, N \in \mathbb{N}\}$.

The map $A \mapsto \mathcal{V}(A)$ is not one to one; that is, different tensors B and C can generate the same family of vectors, $|\mathcal{V}^{(N)}(A)\rangle = |\mathcal{V}^{(N)}(B)\rangle \forall N$. This is, for instance, the case if A and B are related by a similarity transformation (or *gauge transformation*), $B^i = YA^iY^{-1} \forall i$, as Y cancels out in Eq. (64). The goal of the fundamental theorem of MPVs is to characterize the most general way in which two MPV representations A and B of the same family $\mathcal{V}(A) = \mathcal{V}(B)$ are related.

The relevance of the fundamental theorem is manifold. It is the basic tool in the classification of phases in 1D systems under symmetries, $U^{\otimes N} |V^{(N)}(A)\rangle = |V^{(N)}(A)\rangle$, where $B^i = \sum u_{ij} A^j$ and A^i describe the same MPV (Sec. III.A.2). Its application to MPO algebras is relevant in the study of topological order in MPO-injective PEPSs (Sec. III.B.1), as well as the characterization of SPT phases in two dimensions (Sec. III.B.1). It is also being applied in the characterization of RG fixed points through bulk-boundary correspondence (Sec. II.E.2), and in the classification of MPUs and quantum cellular automata (Sec. II.B.2).

The derivation of the fundamental theorem consists of two steps. First, we show that any MPV tensor D can be brought into a canonical form A such that they describe the same MPV family, $|\mathcal{V}^{(N)}(A)\rangle = |\mathcal{V}^{(N)}(D)\rangle$. Second, we present the fundamental theorem, which in essence states that, given any two tensors A and B in canonical form with $|\mathcal{V}^{(N)}(A)\rangle = |\mathcal{V}^{(N)}(B)\rangle$, they are related by the following gauge transformation:

$$B^i = YA^iY^{-1} \quad \text{for all } i. \quad (65)$$

The ensuing discussion closely follows [Cirac *et al.* \(2017a\)](#), who provided further details.

2. Canonical form and normal tensors

In the following, we introduce the canonical form of MPVs and show how to get a tensor into its canonical form. The reason we require a canonical form is that the similarity transform (65) is not the only way in which two tensors can generate the same MPV. Consider a case in which B^i are upper triangular, such as

$$B^i = \begin{pmatrix} B_1^i & B_o^i \\ 0 & B_2^i \end{pmatrix}, \quad (66)$$

where B_k^i are $D_k \times D_k$ matrices and B_o^i is a $D_1 \times D_2$ matrix. As the off-diagonal block drops out in the trace, the MPV generated by B is the same for any choice of B_o^i . The goal of the canonical form is to get rid of those unphysical off-diagonal blocks.

The upper triangular form of B^i can be abstractly characterized by the presence of a subspace \mathcal{S}_1 of dimension D_1 that is left invariant under the action of all B^i . That is, $B^i \mathcal{S}_1 \subset \mathcal{S}_1$ or, equivalently, denoting by P_1 ($Q_1 = \mathbb{1} - P_1$) the orthogonal projector onto \mathcal{S}_1 (\mathcal{S}_1^\perp),

$$B^i P_1 = P_1 B^i P_1, \quad Q_1 B^i = Q_1 B^i Q_1. \quad (67)$$

Note that this shows that there is a nontrivial left-invariant subspace if and only if there is a nontrivial right-invariant one.

Arguably the easiest way to lift the redundancy in Eq. (66) is to fix $B_o^i = 0$. This corresponds to changing B^i to $P_1 B^i P_1 + Q_1 B^i Q_1$, which yields the same family of MPVs. Moreover, there is no loss of generality in assuming that \mathcal{S}_1 does not contain any smaller invariant subspace (if it would, we could choose \mathcal{S}_1 to be that smaller invariant subspace instead). We thus replace

$$B^i \rightarrow P_1 B^i P_1 + Q_1 B^i Q_1$$

and repeat the argument with the block $Q_1 B^i Q_1$ (yielding projections P_2), etc. After a finite number of steps, there will no longer be a nontrivial invariant subspace. The matrices $\{A^i\}$, defined as

$$A^i = \sum_{k=1}^r P_k B^i P_k = \bigoplus_{k=1}^r \mu_k A_k^i, \quad (68)$$

generate the same family $\mathcal{V}(A) = \mathcal{V}(B)$ of MPVs as the initial B^i . Note that in a suitable basis, the A^i are all block diagonal with r blocks. The positive numbers μ_k are scaled such that the CP map \mathcal{E}_k , defined as

$$\mathcal{E}_k(X) = \sum_{i=1}^d A_k^i X A_k^{i\dagger}, \quad (69)$$

has a spectral radius equal to 1. Note that \mathcal{E}_k is simply the transfer operator of the tensor A_k associated with the k th block.

As shown by Fannes, Nachtergaele, and Werner (1992b) and Perez-Garcia *et al.* (2007) [see also Wolf (2012)], each CP map \mathcal{E}_k has a unique eigenvalue $\lambda = 1$ and the corresponding left and right eigenvectors are positive and full rank. A CP map with these properties is called irreducible (Wolf, 2012).

However, irreducible CP maps can have other eigenvalues of magnitude 1, always of the form $e^{i2\pi q/p}$, where p and q are integers, $\gcd(q, p) = 1$, and p is a divisor of D . To remove them, we block p spins. This blocking procedure results in a new tensor $C^{i_1 \dots i_p} = A^{i_1} \dots A^{i_p}$. As shown by Cadarso *et al.* (2013), the blocked matrices are still block diagonal, such that

the corresponding transfer operators have a unique eigenvalue of magnitude (and value) equal to 1, and the corresponding left and right eigenvectors are positive and full rank (as there are no invariant subspaces). A CP map with these properties is called primitive (Wolf, 2012).

One can now state the main definition of the section.

Definition IV.1.—A tensor A_k is called normal if its transfer operator \mathcal{E}_k , Eq. (69), is a primitive channel. The corresponding MPV $|V^N(A_k)\rangle$ is called a normal MPV. We say that a tensor A is in canonical form if

$$A^i = \bigoplus_{k=1}^r \mu_k A_k^i \quad (70)$$

and the tensors A_k are normal tensors.

Definition IV.1 provides an algorithm for transforming any tensor B after blocking into another tensor A that is in canonical form such that they both generate the same family of MPVs, $\mathcal{V}(A) = \mathcal{V}(B)$.

3. Basis of normal tensors

While the canonical form no longer suffers from ambiguities due to off-diagonal blocks, there is still a source of ambiguity: Among the blocks there could be some that generate the same (or linearly dependent) vectors. To properly treat this case one needs to introduce the concept of a basis of normal tensors.

Definition IV.2.—A basis of normal tensors for A is a set of normal tensors A_j ($j = 1, \dots, g$) such that (i) for each N , $|V^N(A)\rangle$ can be written as a linear combination of $V^N(A_j)$, and (ii) there is some N_0 such that, for all $N > N_0$, $|V^N(A_j)\rangle$ are linearly independent.

The following result from Cirac *et al.* (2017a) characterizes bases of normal tensors and, in particular, shows that such a basis always exists.

Proposition IV.3.—The tensors A_j ($j = 1, \dots, g$) form basis normal tensors for A if and only if (i) for all normal tensors \tilde{A}_k appearing in the canonical form (70) of A , there is a j , a nonsingular matrix X_k , and a phase ϕ_k such that

$$\tilde{A}_k = e^{i\phi_k} X_k A_j X_k^{-1} \quad (71)$$

holds, and (ii) the set is minimal, in the sense that for any element A_j there is no other j' for which Eq. (71) is possible.

Note that given a set of normal tensors, a basis of normal tensors can be constructed (and efficiently obtained numerically) by computing the largest eigenvalue λ_{jk} of the mixed transfer operator $\mathcal{F}_{jk}(X) = \sum_i A_j^i X (A_k^i)^\dagger$ and choosing a maximal subset for which $|\lambda_{jk}| < 1$ for all pairs j and k . The X relating A_j and $A_k = e^{i\phi} X A_j X^\dagger$ with $|\lambda_{jk}| = 1$ is then obtained by comparing the largest eigenvector ρ of \mathcal{F}_{kk} to the eigenvector $X\rho_k$ of \mathcal{F}_{jk} . The phase can then be inferred immediately.

One can then write the matrices of any tensor A in canonical form in terms of a basis of normal tensors A_j as

$$A^i = \bigoplus_{j=1}^g \bigoplus_{q=1}^{r_j} \mu_{j,q} X_{j,q} A_j^i X_{j,q}^{-1} \quad (72a)$$

$$= X \left[\bigoplus_{j=1}^g (M_j \otimes A_j^i) \right] X^{-1}, \quad (72b)$$

where M_j is a diagonal matrix with entries $\mu_{j,q}$ and

$$X = \bigoplus_{j=1}^g \bigoplus_{q=1}^{r_j} X_{j,q}, \quad (73)$$

such that

$$|V^N(A)\rangle = \sum_{j=1}^g \left(\sum_{q=1}^{r_j} \mu_{j,q}^N \right) |V^N(A_j)\rangle. \quad (74)$$

4. Fundamental theorem of MPVs

We are now ready to state the *fundamental theorem of matrix product vectors* (Cirac *et al.*, 2017a). It clarifies which degree of freedom is left for two tensors A and B in canonical form that generate families of MPVs proportional to (or equal to) one another.

Theorem IV.4 (fundamental theorem for proportional MPVs).—Let A and B be two tensors in canonical form with bases of normal tensors $A_{k_a}^i$ and $B_{k_b}^i$ ($k_{a,b} = 1, \dots, g_{a,b}$), respectively. If, for all N , A and B generate MPVs that are proportional to one another, then (i) $g_a = g_b =: g$, and (ii) for all k there are a j_k , phases ϕ_k , and nonsingular matrices X_k such that $B_k^i = e^{i\phi_k} X_k A_{j_k}^i X_k^{-1}$.

Corollary IV.5 (fundamental theorem for equal MPVs).—If two tensors A and B in canonical form generate the same MPV for all N , then (i) the dimensions of the matrices A^i and B^i coincide, and (ii) there is an invertible matrix X such that $A^i = X B^i X^{-1}$. X_k and ϕ_k can again be obtained constructively and numerically efficiently following the procedure described after Proposition IV.3.

Note that one can select a gauge such that the CP maps \mathcal{E}_k associated with the normal tensors are unital, i.e., $\mathcal{E}_k(\mathbb{1}) = \mathbb{1}$ (by replacing A_k with $\rho^{-1/2} A_k \rho^{1/2}$, with ρ the fixed point of \mathcal{E}_k). In that case both Theorem IV.4 and Corollary IV.5 hold, with the extra condition that X and X_k be unitary matrices.

The fundamental theorem of MPVs can be generalized to hold without the need of blocking to remove p -periodic components (De las Cuevas *et al.*, 2017), which allows one to apply the fundamental theorem to analyze symmetries with regard to the original unit cell. We state only the analog of Corollary IV.5; see De las Cuevas *et al.* (2017) for the analog of Theorem IV.4. De las Cuevas *et al.* (2018) applied this result to the analysis of the existence of a continuum limit in the context of MPSs.

Theorem IV.6.—Let A and B be tensors in block-diagonal form as in Eq. (68); that is, the CP map of each block is irreducible. If $|V^N(A)\rangle = |V^N(B)\rangle$ for all N , then there is a diagonal matrix Z and an invertible matrix Y such that

- (i) $[Z, A^i] = 0$ for all i ,
- (ii) $ZA^i = YB^iY^{-1}$ for all i , and

(iii) $|V^N(A)\rangle = |V^N(ZA)\rangle$ for all N .

The idea behind the appearance of the diagonal matrix Z is that the MPV associated with a block A_k whose CP map has eigenvalues $e^{i2\pi q/p}$ satisfies the property that $|V^N(A_k)\rangle = 0$ unless N is a multiple of p . Hence, we can multiply this block by any complex p th root of unity and the entire MPV $|V^N(A)\rangle$ will not be affected, giving an extra degree of freedom. What is proven in Theorem IV.6 is that this is essentially the only extra freedom one gets in the general case without blocking.

B. Fundamental theorems for PEPSs

Fundamental theorems for PEPSs exist only for a number of special cases. We first discuss the case of normal PEPSs.

Definition IV.7.—A PEPS tensor A is called injective if it is injective as a linear map $A: (\mathbb{C}^D)^{\otimes r} \rightarrow \mathbb{C}^d$ from the virtual to the physical system (with r the coordination number), that is, if there is a left-inverse A^{-1} ,

$$A^{-1}A = \mathbb{1}_{(\mathbb{C}^D)^{\otimes r}}.$$

Definition IV.8.—A tensor A generating a 2D PEPS is called normal if it becomes injective after blocking a sufficiently large rectangular region $H \times V$.

Tensors that are injective on two regions are also injective on their union, and thus if a normal tensor A becomes injective in a region of size $H \times V$, it is also injective for any region $\tilde{H} \times \tilde{V}$ with $\tilde{H} \geq H$ and $\tilde{V} \geq V$ (Perez-Garcia, Verstraete *et al.*, 2008; Molnar, Garre-Rubio *et al.*, 2018). It has been shown that if A is normal, the required H and V are upper bounded by a constant that depends only on the bond dimension D and the graph, not the specific A (Michalek, Seynnaeve, and Verstraete, 2019).

For MPSSs, the earlier defined notion of normality is equivalent to the previously introduced notion (Definition IV.1) of a normal tensor (Sanz *et al.*, 2010). Injectivity implies that the tensor A must be normal and, conversely, the quantum version of Wieland's theorem states that, after blocking at most $2D^2(6 + \log_2 D)$ sites, every normal tensor becomes injective; see Michalek and Shitov (2018), as well as Perez-Garcia *et al.* (2010) and Rahaman (2018).

This yields the following version of the fundamental theorem for normal PEPSs given by Molnar, Garre-Rubio *et al.* (2018) [an earlier version of which was proven by Perez-Garcia *et al.* (2010)].

Theorem IV.9 (fundamental theorem for normal PEPSs).—Let A and B be two normal tensors such that every $H \times L$ region is injective, and let A and B generate the same PEPS for some system size $n \times m \geq (2H + 1) \times (2L + 1)$. Then, there exist invertible matrices X , Y , and $\lambda \in \mathbb{C}$ such that $A = \lambda B(X^{-1} \otimes Y^{-1} \otimes X \otimes Y)$ and $\lambda^{nm} = 1$.

Based on this we have the desired 2D analog of Corollary IV.5 for normal 2D PEPSs.

Corollary IV.10.—Let A and B be two normal tensors generating 2D PEPSs. They define the same state for all sizes if and only if there are invertible matrices X and Y such that $A^i = B^i(X^{-1} \otimes Y^{-1} \otimes X \otimes Y)$ for all i . Moreover, X and Y are unique up to proportionality.

As is the case in one dimension, this theorem, in particular, provides a local characterization of all normal PEPSs having a global on-site symmetry or a spatial symmetry; see [Perez-Garcia *et al.* \(2010\)](#) for details.

Beyond the normal case, a fundamental theorem for PEPS has also been proven for so-called semi-injective PEPSs (see [Sec. III.B.1](#)), which, in particular, encompass 2D SPT phases such as the CZX model of [Chen, Liu, and Wen \(2011\)](#) and its generalizations ([Chen *et al.*, 2013](#); [Williamson *et al.*, 2016](#)). There, the relation between two PEPS tensors A and B generating the same state is given by matrix product operators instead ([Molnar, Ge *et al.*, 2018](#)). Using the theory of bimodule categories, it is also possible to construct such MPO intertwiners between equivalent PEPSs with different bond dimensions ([Lootens *et al.*, 2021](#)). We note that one cannot hope for a fundamental theory for PEPSs in the same generality as in one dimension, since the corresponding problem in its full generality is undecidable ([Scarpa *et al.*, 2020](#)).

C. Hamiltonians

In this section, we discuss the relation of MPSs and PEPSs with Hamiltonians. In particular, we provide the construction of the parent Hamiltonian, detail the precise conditions under which it has a unique ground state or a ground space with a controlled degeneracy, and discuss the conditions under which these Hamiltonians can be proven to be gapped. We also discuss constructions that provide alternative Hamiltonians associated to a MPS. These results extend the seminal results of [Affleck *et al.* \(1987, 1988\)](#) and [Fannes, Nachtergaele, and Werner \(1992b\)](#) on exact parent Hamiltonians for the AKLT states and for finitely correlated states.

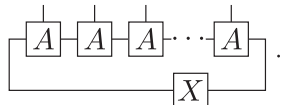
1. Parent Hamiltonians and ground space

a. Construction of the parent Hamiltonian

We start with the 1D case. Given a MPS, consider the space

$$\mathcal{G}_L = \left\{ \sum_{i_1, \dots, i_L} \text{tr}(A^{i_1} \dots A^{i_L} X) |i_1 \dots i_L\rangle : X \in \mathcal{M}_D \right\} \quad (75)$$

of all states spanned by L consecutive sites of the MPS, given arbitrary boundary conditions X . Graphically, this corresponds to the states



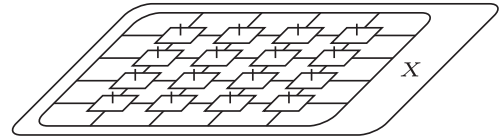
(76)

In some cases, we also write $\mathcal{G}_{i, \dots, j}$ to denote \mathcal{G}_{i-j+1} on sites i, \dots, j .

Definition IV.11 (parent Hamiltonian).—A parent interaction is any Hermitian positive semidefinite operator $h \geq 0$ acting on L sites whose kernel equals \mathcal{G}_L [Eq. (75)]. The corresponding parent Hamiltonian of the MPS with tensor A on N sites is then given by $H_N = \sum_{i=1}^N h_i$, where h_i denotes h acting on sites $i, \dots, i + L - 1 \bmod (N) \times$.

Since the dimension of \mathcal{G}_L is at most D^2 , the parent Hamiltonian will necessarily be nontrivial as soon as $d^L > D^2$ (as \mathcal{G}_L cannot be the full space).

Similarly, we can define parent Hamiltonians in two dimensions (or on other graphs) by considering a sufficiently large region R , where \mathcal{G}_R is the space spanned by the states



(77)

with arbitrary boundary conditions X , and the terms in the Hamiltonian are again positive semidefinite operators with kernel \mathcal{G}_R . Note that in two dimensions the resulting parent Hamiltonian can have different types of terms if one considers more than one type of region (e.g., two rectangular regions of size 2×1 and 1×2). Note that the same construction can be carried out without translational invariance and for general graphs.

The parent Hamiltonian has the MPS or PEPS $|\psi\rangle$ as a ground state, as $H_N = \sum h_i \geq 0$ and $H_N|\psi\rangle = \sum h_i|\psi\rangle = 0$. Hamiltonians with the property that the ground states minimize the local terms are called frustration free. In the following, we discuss the conditions under which H_N has a unique ground state or, more generally, a ground space with a controlled structure.

b. Normality, injectivity, and unique ground states

We first recall the notion of injectivity from [Definition IV.7](#) in [Sec. IV.B](#): An MPS or PEPS tensor is injective if it has a left-inverse A^{-1} when considered as a map from a virtual to a physical system, $A^{-1}A = \mathbb{1}$. For MPSs, this is equivalent to the property that the matrices A^i span the entire set of $\mathcal{M}_{D \times D}$ matrices. We also recall that any injective MPS tensor is normal, and any normal MPS tensor becomes injective after blocking at most $L_0 \leq 2D^2(6 + \log_2 D)$ sites.

For a MPS or PEPS with injective tensors, it can easily be proven that the parent Hamiltonian defined on nearest neighbors has a unique ground state. To this end, it is convenient to construct the PEPS as in [Sec. II.B.1](#), by applying local linear maps to maximally entangled pairs. That is, given a regular graph G of degree r with vertex set V and edge set E , one can consider the so-called isometric PEPS of bond dimension D ,

$$|\Omega^G\rangle := \bigotimes_{e \in E} |\omega\rangle_e,$$

where $|\omega\rangle$ is the maximally entangled state of dimension D . A general MPS or PEPS $|\Psi^G(A)\rangle$ is then given by a linear map (the tensor) $A: (\mathbb{C}^D)^{\otimes r} \rightarrow \mathbb{C}^d$

$$|\Psi^G(A)\rangle := \left(\bigotimes_{v \in V} A \right) \bigotimes_{e \in E} |\omega\rangle_e = \left(\bigotimes_{v \in V} A \right) |\Omega^G\rangle, \quad (78)$$

see [Fig. 1](#). We omit the superscript G whenever the graph is unambiguous.

For the isometric PEPS $|\Omega\rangle$, a possible parent Hamiltonian is given by $h = 1 - |\omega\rangle\langle\omega|$, and it is immediate to see that $H_N = \sum h_i$ has $|\psi\rangle$ as its unique ground state. We can now construct a parent Hamiltonian for $|\Psi(A)\rangle$ as

$$h' = (A^{-1} \otimes A^{-1})^\dagger h (A^{-1} \otimes A^{-1}). \quad (79)$$

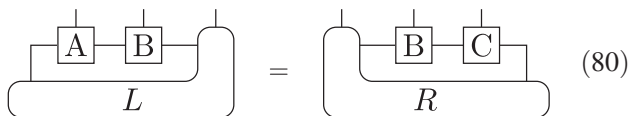
The kernel of h' is \mathcal{G}_L , and thus $|\Psi(A)\rangle$ is a ground state of $H'_N = \sum h'_i$. Now assume that H'_N had another ground state $|\Phi\rangle$, i.e., $h'_i|\Phi\rangle = 0$. In that case, $h_i(A^{-1})^{\otimes N}|\Phi\rangle = Xh'_i|\Phi\rangle = 0$ [here X acts as A^\dagger on sites $i, i + 1$, and (A^{-1}) on all others]; i.e., $(A^{-1})^{\otimes N}$ would be another ground state of H_N whose ground state, however, is unique. Thus, the ground state of H'_N must be unique as well. This technique can more generally be seen as establishing a one-to-one correspondence between ground states of the parent Hamiltonians of two PEPSs $|\psi\rangle$ and $|\psi'\rangle = R^{\otimes N}|A\rangle$ that are related by an invertible map R (not necessarily the PEPS map A) and thus can also be applied to the cases with the topological or otherwise degenerate ground space structure described in Sec. IV.C.1.c.

This leads to the following result (Perez-Garcia, Verstraete *et al.*, 2008).

Theorem IV.12.—Consider a PEPS where the tensors have been blocked such that all tensors are injective. Then, the two-body parent Hamiltonian constructed from all nearest-neighbor sites has a unique ground state. This result holds regardless of the graph and translational invariance.

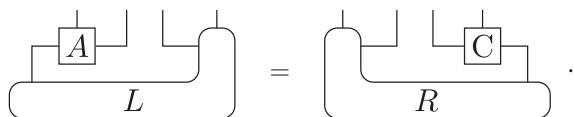
In particular, given a square lattice, if injectivity is reached by blocking $H \times V$ sites, then the parent Hamiltonian containing all terms derived for patches of size $H \times (2V)$ and $(2H) \times V$ has a unique ground state. In one dimension, the result correspondingly applies for parent Hamiltonians acting on $2L_0$ sites, with L_0 the injectivity length (Perez-Garcia *et al.*, 2007).

The injectivity length of a normal MPS is the smallest number of sites that have to be blocked such that its tensors become injective. This result can be considerably strengthened (yielding more local Hamiltonians) by avoiding to block until injectivity is reached. For a normal MPS, consider two Hamiltonian terms h and h' acting on sites $1, \dots, L_0 + 1$ and $2, \dots, L_0 + 2$, where L_0 is the injectivity length, and denote by A, B , and C the tensors on site 1, the blocked tensor of site $2, \dots, L_0 + 1$, and the tensor at site $L_0 + 2$, respectively; note that B is injective. The joint ground space of h and h' is the intersection $\mathcal{I} = \mathcal{G}_{1, \dots, L_0+1} \cap \mathcal{G}_{2, \dots, L_0+2}$, i.e., all states of the form



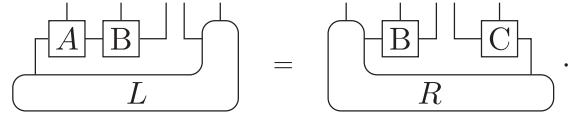
$$\text{Diagram with } A, B \text{ and boundary } L = \text{Diagram with } B, C \text{ and boundary } R \quad (80)$$

for arbitrary boundary conditions L and R . We can invert A , which yields



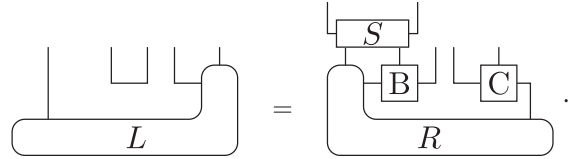
$$\text{Diagram with } A \text{ and boundary } L = \text{Diagram with } C \text{ and boundary } R$$

We can now reattach (“grow back”) B to A as follows:



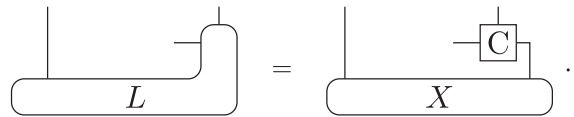
$$\text{Diagram with } A, B \text{ and boundary } L = \text{Diagram with } B, C \text{ and boundary } R$$

Since B is injective, so are A and B together, and we can invert them as follows (calling the inverse S):



$$\text{Diagram with } A, B \text{ and boundary } L = \text{Diagram with } S \text{ and boundary } R$$

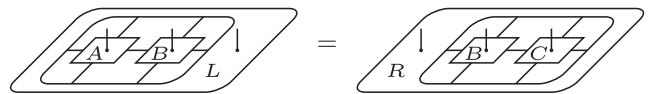
We thus find that



$$\text{Diagram with boundary } L = \text{Diagram with } X \text{ and boundary } R$$

That is, any state in the intersection \mathcal{I} is also contained in $\mathcal{G}_{1, \dots, L_0+2}$, and the converse is trivially true. We can now iterate this argument to show that the ground space of a Hamiltonian with terms acting on $L_0 + 1$ sites is the same as for a Hamiltonian with terms acting on $L_0 + k$, $k > 1$, sites. Once we have reached $k = L_0$, we can resort to the Theorem IV.12 or, alternatively, can apply a similar argument when closing the boundaries. [These two properties are called the intersection property and closure property, respectively (Fannes, Nachtergaele, and Werner, 1992b; Perez-Garcia *et al.*, 2007; Schuch, Cirac, and Perez-Garcia, 2010).]

The same technique (inverting and growing back) also works in two dimensions; on the square lattice we would start with the equality



$$\text{Patch with } A, B \text{ and boundary } L = \text{Patch with } B, C \text{ and boundary } R$$

and apply the previous arguments. This yields the following strengthened result (Fannes, Nachtergaele, and Werner, 1992b; Perez-Garcia *et al.*, 2007; Schuch *et al.*, 2012).

Theorem IV.13 (uniqueness of ground state).—Consider a normal MPS that becomes injective upon blocking L_0 sites. Then, the parent Hamiltonian defined on $L_0 + 1$ sites has a unique ground state.

Consider a normal PEPS on the square lattice that becomes injective upon blocking $H_0 \times V_0$ sites. Then, the parent Hamiltonian defined on $(H_0 + 1) \times V_0$ and $H_0 \times (V_0 + 1)$ sites has a unique ground state. Both results hold regardless of translational invariance.

Note that the locality bound need not be tight. For example, the AKLT model has $L_0 = 2$, yet the two-site parent Hamiltonian is sufficient to obtain a unique ground state. This can be seen by checking by hand that $\mathcal{G}_{1,2} \cap \mathcal{G}_{2,3} = \mathcal{G}_{1,2,3}$.

For MPS, this provides a full characterization of all MPSs that appear as unique ground states of local Hamiltonians: Non-normal MPSs, which have more than one block in their canonical form, exhibit long-range order, and we see in Sec. IV.C.1.c that their parent Hamiltonian exhibits a degenerate ground state subspace.

For PEPS, there are classes of states that, despite not being injective, are unique ground states of a parent Hamiltonian. This holds for all states constructed analogously to Eq. (78) by replacing $|\Omega\rangle$ with any other state that is a unique ground state of a frustration-free local Hamiltonian. For instance, this is the case for semi-injective PEPSs [see Molnar, Ge *et al.* (2018); cf. Secs. III.B.1 and IV.B], where $|\Omega\rangle$ is a product of entangled states across plaquettes that is a unique ground state of a four-body Hamiltonian (acting on each plaquette). Another class of PEPSs with unique ground states are given by the family of MPO-injective PEPSs that fulfill the requirement that the MPO has a single block in the canonical form (Sec. IV.A).

c. Block injectivity, entanglement symmetries, and degenerate ground spaces

The proof for the uniqueness of the ground state of parent Hamiltonians breaks down once the correspondence between the physical and virtual systems captured by the concept of injectivity is lost, that is, if there are degrees of freedom in the virtual space that have no physical correspondence. For instance, this happens for MPSs which have more than one block ($r > 1$) in their canonical form [Eq. (70)]: In that case, one can easily see that any state corresponding to a single block A_k^i is a ground state, as they are all supported on \mathcal{G}_L [Eq. (75)]. In this scenario, we can define a generalization of injective tensors where the physical-virtual correspondence holds blockwise [that is, for block-diagonal boundary conditions X in Eq. (75)].

Definition IV.14.—A tensor A is in block-injective canonical form if it is in canonical form, and for each element $X \in \bigoplus_{j=1}^g \mathcal{M}_{D_j \times D_j}$ there is a vector $c(X)$ such that $X = \sum_i c_i(X) \tilde{A}^i$, where $\tilde{A}^i := \bigoplus_{j=1}^g A_j^i$ and A_j are a basis of normal tensors (cf. Definition IV.2) of A .

Using the quantum version of Wielandt’s theorem (Sanz *et al.*, 2010), it was shown by Perez-Garcia *et al.* (2007) and Cirac *et al.* (2017a) that, after blocking at most $L_0 \leq 3D^5$ spins, any tensor A in canonical form acquires block-injective canonical form. One can then prove the following generalization of Theorem IV.12.

Theorem IV.15 (Fannes, Nachtergaele, and Werner, 1992b; Perez-Garcia *et al.*, 2007).—For any $N \geq 2L_0$, the ground space of any parent Hamiltonian is exactly the vector space generated by a basis of normal tensors of the initial tensor A .

Following the same steps as in Eq. (80) (inverting and regrowing tensors, where the inverse projects on the space of block-diagonal matrices, and restricting to boundary conditions L and R , which are themselves block diagonal), we can strengthen this result in analogy with Theorem IV.13.

Theorem IV.16.—For any $N \geq L_0 + 1$, the ground space of any parent Hamiltonian is exactly the vector space generated by a basis of normal tensors of the initial tensor A .

The reason for the degenerate ground space can be understood from the fact that such MPSs have decoupled blocks in

the virtual space. Alternatively, this can be explained using a symmetry $[A^i, U_g] = 0$ of the MPS tensor A^i , with U_g a unitary representation of an Abelian group (where the blocks are supported on the different irreducible representations). In that case, $[A^i, U_g] = 0$ implies that projectors $P_\alpha = \sum_k \overline{\chi_k(g)} U_g$ onto irreps (blocks) k commute with A , and thus cannot be detected by the parent Hamiltonian; placing them on a link thus selects different ground states. These two perspectives suggest two different generalizations to two dimensions: We can first choose a 2D PEPS tensor with a “direct sum” block structure over all virtual indices as in Eq. (70), as in the PEPS for the GHZ state (Appendix 2.a). Such a PEPS will have a GHZ-type structure; in particular, if under blocking injectivity of all blocks is reached, the parent Hamiltonian with terms acting on two blocks will have a ground space spanned by the individual blocks.

The second generalization to PEPS is based on generalizing the commutation relation $U_g A^i U_g^\dagger = A^i$ to tensors that are invariant under the action of some symmetry on all the indices simultaneously. This, in particular, encompasses the G -injective PEPS and the MPO-injective PEPS introduced in Sec. III.B. In this case, the pulling through condition is exactly what allows one to create projections onto different sectors that can be commuted (i.e., moved) through the tensor network and are thus invisible to the Hamiltonian. In the case of G -injective PEPSs, the condition for a controlled ground space is precisely that the blocked PEPS tensor is injective on the subspace that is invariant under the symmetry action (G -injective). See Schuch, Cirac, and Perez-Garcia (2010) for the formal result, Buerschaper (2014) for the generalization to twisted G -injective PEPSs, and Bultinck, Mariën *et al.* (2017) and Şahinoğlu *et al.* (2021) for the generalization to MPO-injective PEPSs. Note also that tricks similar to the “regrowing” used in one dimension to construct parent Hamiltonians on $L_0 + 1$ sites can also be used in the case of topologically ordered PEPSs in two dimensions to obtain smaller Hamiltonians. This was carried out by Schuch *et al.* (2012) in their Appendix D for the kagome RVB model to obtain a two-star Hamiltonian [which can be broken down to a one-star Hamiltonian by direct inspection (Zhou, Wildeboer, and Seidel, 2014), similar to the two-body Hamiltonian in the AKLT model].

d. Converse: MPS ground states for frustration-free Hamiltonians

As we have seen, every MPS is the ground state of a frustration-free Hamiltonian. Under certain conditions the converse holds as well: Every frustration-free Hamiltonian has a MPS ground state.

The following result is due to Matsui (1998) [generalizations of this connection were given recently by Ogata (2016a, 2016b, 2017)].

Theorem IV.17.—Let $h \geq 0$ be a Hamiltonian acting on $r + 1$ sites, and let $H_{[M,N]} = \sum_{i=M}^{N-r} h_i$, where h_i is h acting on sites $i, \dots, i + r$ (i.e., the translational-invariant open boundary condition Hamiltonian with interaction h).

If there is a $C > 0$ such that the dimension of the kernel of $H_{[M,N]}$ is $\leq C$ for all M, N , then any translational-invariant frustration-free ground state $|\phi\rangle$ in the thermodynamic limit

can be described by a MPS with a normal tensor. See the original works for the precise mathematical formulation of the result in the thermodynamic limit.

2. Gaps

Having defined parent Hamiltonians and given conditions that control their ground space structure, we now turn toward the question as to when these Hamiltonians are gapped. As we have seen, parent Hamiltonians of MPSs are frustration free; i.e., the ground state minimizes each interaction term individually. There are two techniques for making statements about gaps of frustration-free Hamiltonians: the martingale method and Knabe-type bounds. Both techniques relate the gap in the thermodynamic limit to the gap of a finite-size problem, which can subsequently be solved numerically or analytically. It turns out that the martingale method allows one to prove the existence of a gap, and to provide explicit lower bounds on it, for all MPS parent Hamiltonians.

Recently these methods were used to prove the gap of a class of decorated AKLT models (Abdul-Rahman *et al.*, 2019), as well as to numerically show the gap of a range of models (among others, the honeycomb AKLT model) by numerically checking the corresponding finite-size problems (Lemm, Sandvik, and Wang, 2019; Pomata and Wei, 2019).

a. The martingale method

The martingale method (Fannes, Nachtergaele, and Werner, 1992b; Nachtergaele, 1996; Kastoryano and Lucia, 2018) relates the minimum nonzero angle between the ground spaces of overlapping regions to the gap. The system is gapped in the thermodynamic limit if and only if, by blocking, the overlaps of vectors in overlapping ground spaces become sufficiently large (which intuitively allows one to detect excitations locally).

More precisely, consider a frustration-free Hamiltonian $H = \sum h_i$ with w.l.o.g. projectors h_i . (If the h_i are not projectors, they are still lower bounded and upper bounded by projectors up to a constant.) Having a gap γ is equivalent to $H^2 \geq \gamma H$, which (using $h_i^2 = h_i$) is equivalent to

$$\sum h_i + \sum' h_i h_j + \sum'' h_i h_j \geq \gamma \sum h_i, \quad (81)$$

where \sum' and \sum'' denote sums over overlapping and non-overlapping h_i , respectively. $\sum'' h_i h_j \geq 0$, and thus Eq. (81) is satisfied as long as

$$h_i h_j + h_j h_i \geq -c_{ij}(1 - \gamma)(h_i + h_j) \quad (82)$$

for all overlapping pairs (i, j) , where c_{ij} has to be chosen to add up to 1 (e.g., if each h_i overlaps with three others, $c_{ij} = 1/3$). Thus, finding a blocking for which Eq. (82) is thus sufficient to prove a gap. Note that Eq. (82) effectively poses a lower bound on the smallest nonzero angle between the ground spaces of h_i and h_j .

The martingale condition (82) is also sufficient. As shown by Kastoryano and Lucia (2018), whenever a frustration-free Hamiltonian is gapped, $\delta(\ell) := \|h_i h_j - P\|$ (with P the

projector onto the kernel of $h_i + h_j$) goes to zero exponentially with universal constants in the size ℓ of the overlap region, which, in particular, implies the validity of Eq. (82) (as both quantities depend only on the principal angles between $\ker h_i$ and $\ker h_j$).

Using the martingale method, one can prove that all MPS parent Hamiltonians (for both normal and block-injective MPSs) have a gap (Fannes, Nachtergaele, and Werner, 1992b; Nachtergaele, 1996):

Theorem IV.18.—All MPS parent Hamiltonians are gapped; that is, there is a $\gamma > 0$ such that for the parent Hamiltonian H_N on N sites, the smallest nonzero eigenvalue $\lambda(H_N) \geq \gamma$ uniformly in N .

For the dependence of γ on the MPS tensor, see Fannes, Nachtergaele, and Werner (1992b) and Nachtergaele (1996).

For systems in two or more dimensions, no comparably strong result is known. In particular, injectivity does not imply a gap, since examples of injective PEPSs are known that exhibit power law correlations (such as the “Ising PEPS” [see Verstraete *et al.* (2006), Appendix A] on the honeycomb lattice at the critical point), and thus cannot be ground states of gapped Hamiltonians (Hastings and Koma, 2006; Nachtergaele and Sims, 2006).

One can, however, derive a lower bound on the gap of the parent Hamiltonian for a PEPS whose tensor A is sufficiently close to a PEPS B with parent Hamiltonian h that satisfies the martingale condition (82) (such as a commuting Hamiltonian), in the sense that $A^i = \sum \Lambda_{ij} B^j$, with $\Lambda - \mathbb{1}$ small. This is based on the fact that, following the logic of Sec. IV.C.1.b given near Eq. (79), $h' = (\Lambda^{-1\dagger})^{\otimes k} h (\Lambda^{-1})^{\otimes k}$ is a parent Hamiltonian for A (with k the locality of the Hamiltonian), and the bound γ on the gap in the martingale condition changes smoothly with Λ . Alternatively, this can be determined from the fact that Eq. (82) lower bounds the angle between the ground spaces $\mathcal{G}_{i,j}$ of h_i and h_j , which changes smoothly under deformations $\Lambda^{\otimes k} \mathcal{G}_{i,j}$. This was carried out explicitly in their Appendix E by Schuch, Perez-Garcia, and Cirac (2011) for a commuting Hamiltonian h acting on 2×2 blocks, and it was found that the gap is stable as long as the ratio of the smallest and largest singular value of Λ is above ≈ 0.967 .

b. The Knabe bound

The Knabe bound relates the existence of a gap of a translational-invariant and frustration-free Hamiltonian in the thermodynamic limit with the scaling of the gap of the same Hamiltonian on a finite chain. In particular, Knabe (1988) showed that if the gap of an open boundary 1D chain with a nearest-neighbor projector Hamiltonian is larger than $1/(n-1)$ for some $n > 2$, then the system with periodic boundaries is gapped in the thermodynamic limit. This result was later improved to $6/n(n+1)$ by Gosset and Mozgunov (2016) and generalized to two dimensions. The method was also extended to frustration-free Hamiltonians with open boundary conditions (stating that for gapless systems the gap must close at least as $n^{-3/2}$, showing the impossibility of chiral edge modes with frustration-free Hamiltonians whose gap should scale as $1/n$) by Lemm and Mozgunov (2019).

3. Stability

A key consideration in the definition of quantum phases is their stability against arbitrary small perturbations (or, when one is considering SPT phases, against arbitrary symmetry-preserving perturbations). Here stability can refer to different properties, such as a smooth dependence of various physical properties on the perturbation. The most commonly considered property is the stability of the spectral gap, as it implies the stability of local properties through quasiadiabatic continuation (Hastings and Wen, 2005). Parent Hamiltonians of MPSs and PEPSs do not necessarily have such a stability property: For instance, the parent Hamiltonian of a GHZ state (which is a PEPS) is a ferromagnetic Ising Hamiltonian whose twofold degenerate ground space is susceptible to small perturbations.

In the following, we discuss conditions under which the ground space of a MPS or PEPS parent Hamiltonian can be shown to be stable under perturbations.

a. The LTQO condition

For frustration-free Hamiltonians, stability of the spectral gap is implied by the local topological quantum order (LTQO) condition (Bravyi, Hastings, and Michalakis, 2010; Bravyi and Hastings, 2011; Michalakis and Pytel, 2013). Roughly speaking, it states that the effect of boundary conditions is exponentially suppressed in the bulk (as a function of the distance of the boundary).

Definition IV.19.—Consider a translational-invariant frustration-free Hamiltonian on a 2D square lattice. We say that a region A satisfies LTQO if there is a superpolynomially decaying function $f_A(m)$ [i.e., $\lim_{m \rightarrow \infty} m^k f_A(m) = 0$ for all $k > 0$] such that for any observable O_a supported on A and all bounded regions B containing A , it holds that for any pair of normalized ground states $|\Psi\rangle, |\Psi'\rangle$ of the Hamiltonian restricted to region B ,

$$|\langle \Psi | O_a | \Psi \rangle - \langle \Psi' | O_a | \Psi' \rangle| \leq \|O_a\| f_A(m), \quad (83)$$

where m is the distance between A and ∂B (the boundary of B).

We say that a particular observable O_a satisfies LTQO if it verifies Eq. (83). We finally say that a system satisfies LTQO if all its regions A satisfy it and the function f in Eq. (83) is independent of A .

LTQO implies stability of the gap under local perturbations under some additional local gap conditions.

Theorem IV.20 (Michalakis and Pytel, 2013).—Let $H_N = \sum h_i$ be a local Hamiltonian that satisfies LTQO, and let $V = \sum_k v_k$, with v_k a bounded local term centered at site k . Moreover, assume that there is a $\gamma > 0$ such that H_N has a gap $\Delta_N \geq \gamma$ with periodic boundaries, and let the spectral gap of H_N restricted to open boundaries decay at most polynomially with the system size. Then, there exist N_0 and $\epsilon_0 > 0$ such that $H_N + \epsilon V$ has a gap at least $\gamma/2$ for any $N \geq N_0$ and $\epsilon \leq \epsilon_0$.

For a more precise formulation of the theorem, including several generalizations, see Michalakis and Pytel (2013) and Nachtergaele, Sims, and Young (2020).

In the context of PEPSs, the LTQO condition has two additional advantages: First, it can be checked numerically for

specific regions (and possibly observables), by relating it to an eigenvalue problem. Second, it allows for direct conclusions about the stability of physical observables under the class of natural PEPS perturbations $A^i \rightarrow \sum \Lambda(\epsilon)_{ij} A^j$, where $\Lambda(\epsilon) \rightarrow 1$ smoothly (as $\epsilon \rightarrow 0$). In that case, the derivative of any observable $O_a(\epsilon)$ changes smoothly at around $\epsilon = 0$ as well (Cirac *et al.*, 2013).

b. Stability in one dimension

One can prove for one-dimensional MPSs with normal tensors that the LTQO condition always holds (Cirac *et al.*, 2013). This implies the following theorem.

Theorem IV.21.—For MPS with normal tensors, the gap of the parent Hamiltonians is stable under perturbations $V_N = \sum_k v_k$, with v_k a bounded local perturbation centered around k . That is, there is an $\epsilon_0 > 0$ and $\gamma > 0$ such that $H_N + \epsilon V_N$ has a unique ground state with a gap $\Delta_N > \gamma$ for all $\epsilon < \epsilon_0$ and all N .

An alternative proof of this stability that does not build on the LTQO condition was given by Szechr and Wolf (2015).

c. Stability in two dimensions

In two dimensions, the LTQO condition is generally hard to prove. Specific cases in which it holds are PEPSs with commuting parent Hamiltonians, such as isometric PEPSs, G -isometric PEPSs (Schuch, Cirac, and Perez-Garcia, 2010), and MPO-isometric PEPSs (Şahinoğlu *et al.*, 2021), which are therefore robust against local perturbations.

d. Perturbations of the tensor

An alternative way to perturb MPSs and PEPSs is to perturb the tensor, rather than the Hamiltonian. There are two types of these perturbations.

- (i) *Physical perturbations* are perturbations that can be understood as acting only on the physical index, $A^i \rightarrow \sum \Lambda_{ij} A^j$. As discussed, these correspond to perturbations of the parent Hamiltonian of the form $h \rightarrow (\Lambda^{-1\dagger})^{\otimes k} h (\Lambda^{-1})^{\otimes k}$. They are thus physical in the sense that they correspond to a physical perturbation of the Hamiltonian. As discussed in Secs. IV.C.3.a–IV.C.3.c, this immediately implies that for normal MPSs in 1D, and in the presence of LTQO in 2D, these perturbations only give rise to smooth changes in the properties of the system and do not close the gap; alternatively, this also follows from the stability of the martingale condition. Note that for normal MPSs and PEPSs, any perturbation of the tensor is a physical perturbation on injective blocks. For example, one can first invert the injective tensor by acting on the physical block, then use the perturbed tensor instead.

- (ii) An *unphysical perturbation* is a perturbation of the tensor that cannot be understood as a physical perturbation, i.e., as one that acts only on the physical index. Such perturbations exist only for non-normal tensors. It has been shown that, unlike physical perturbations, unphysical perturbations of

the tensor can have a drastic effect. Perturbing a G -injective PEPS immediately breaks topological order (Chen *et al.*, 2010) by condensing the anyons (cf. Sec. III), and the same is true for a MPO-injective PEPS (Shukla *et al.*, 2018), although MPO-injective PEPSs are stable against certain unphysical perturbations. This immediately implies that unphysical perturbations cannot be related to physical perturbations of the parent Hamiltonian, since the toric code is stable against any perturbation of the Hamiltonian. Within the framework of parent Hamiltonians, these perturbations are thus generally unphysical and not of direct interest. It is possible, however, to introduce other types of Hamiltonians, such as the uncle Hamiltonians discussed later, which are stable under general perturbations. At the same time, understanding which perturbations are unphysical is relevant for the numerical simulation of topological phases since one needs to protect against breaking of these symmetries (i.e., enforce G symmetry or MPO symmetry) in order to obtain systems that exhibit topological order.

4. Alternative Hamiltonians

There are ways to obtain Hamiltonians with different properties than parent Hamiltonians. This can be achieved in one of at least two ways: by considering tensors that are not in canonical form or by considering an alternative construction for the Hamiltonian.

a. Product vacua with boundary states (PVBS)

PVBS (Bachmann and Nachtergaele, 2012, 2014) are models that are constructed from MPSs that are not in their canonical form, such as

$$A^0 = (1 + \lambda)|0\rangle\langle 0| + |1\rangle\langle 1|, A^1 = |0\rangle\langle 1|,$$

where $\lambda \in [-1, 1]$. The parent Hamiltonian of this MPS will have the MPS on an open boundary condition chain as its ground space. This model will support two ground states, namely, the all-0 state and a state with a single 1 state that “binds” to the left ($\lambda < 0$) or right ($\lambda > 1$) edge: the edge states. On the other hand, the periodic boundary condition ground space supports only the all-0 state: the product vacuum. PVBS models demonstrate that the classification of phases is different on a system with boundaries or, alternatively, that one has to consider whether a closing gap affects the bulk behavior (which in the previous model is smooth even when λ changes sign). Note that these models have been generalized to higher dimensions outside the framework of tensor networks (Bachmann *et al.*, 2015).

b. Uncle Hamiltonians

Uncle Hamiltonians (Fernández-González *et al.*, 2012, 2015) are defined to overcome the noncontinuity of the parent Hamiltonian under physical perturbations. They are defined by first applying a potentially unphysical perturbation to the tensor, constructing the parent Hamiltonian, and subsequently

taking the limit of the perturbation to zero. The obtained Hamiltonians are termed *uncle Hamiltonians* and are by construction continuous under the perturbation considered. On the other hand, depending on the bond dimension of the MPS or PEPS, they might not be unique but might depend on the path of perturbations considered. Uncle Hamiltonians have significantly different properties: in particular, they are generally gapless for noninjective MPSs and PEPSs, such as for the 1D Ising or the 2D toric code model (where momentum eigenstates of domain walls or anyons, respectively, through which the perturbation destroys the conventional or topological order, have low energy).

V. CONCLUSIONS

In this review we have covered some of the basic concepts in the field of tensor networks and many-body quantum systems, paying special attention to MPSs and PEPSs on regular lattices. While we have revised in certain depth many results that were not obtained until recently, we have left out entire areas of research on tensor networks that are rapidly developing and that could themselves be the subject of one or several reviews. In this outlook we list some of those areas, as well as some open research directions.

We start with the numerical algorithms built on tensor networks to describe different aspects of many-body quantum systems. While this review deals exclusively with analytical results, the fact that tensor network states efficiently approximate many-body systems immediately provides a powerful playground for addressing complex problems with that technique. In one spatial dimension, the success of the DMRG (White, 1992) method in addressing the physical properties of one-dimensional spin chains at zero temperature can be traced back to the fact that it can be viewed as a variational method over the manifold of MPSs. One can naturally extend this algorithm to higher spatial dimensions through PEPSs, although the scaling of the computational complexity with the bond dimension is not as friendly as in one dimension, and one has to use approximate techniques in order to compute expectation values of physical observables (Verstraete and Cirac, 2004a). Thus, arguably the most important subject of research in tensor networks is the development of powerful algorithms in more than one spatial dimension. One can also extend these methods to finite temperatures by using MPDOs or PEPOs (Czarnik and Dziarmaga, 2015), and to time-dependent problems (Czarnik, Dziarmaga, and Corboz, 2019). The latter can be carried out by using either a variational method or a Trotterization of the evolution operator followed by truncations of the time evolved states after each time step. Tensor networks have also been employed to express many-body operators, like Hamiltonians, to compute elementary excitations, spectral functions, densities of states, etc. (McCulloch, 2007; Pirvu *et al.*, 2010). The extension of those methods to higher dimensions remains one of our main challenges. Other tensor network states, like TTNs and MERAs, have also played an important role in certain many-body problems and are particularly appropriate for describing critical systems (Silvi *et al.*, 2010; Evenbly and Vidal, 2014). Methods based on MPSs and PEPSs have also been developed recently that

allow one to compute physical properties of critical systems based on the scaling as a function of the bond dimension (Tagliacozzo *et al.*, 2008; Pirvu, Haegeman, and Verstraete, 2012; Stojevic *et al.*, 2015; Corboz *et al.*, 2018; Rader and Läuchli, 2018; Vanhecke, Haegeman *et al.*, 2019). In a parallel effort, mathematicians have investigated different concepts to apply tensor trains (which are analogous to MPSs) to diverse problems (Grasedyck, 2010; Oseledets, 2011; Hackbusch, 2012). Here the idea is also to compress high-rank tensors in terms of smaller ones, thus saving time and memory in computations.

Another active area of research is continuous tensor networks. We have reviewed here the theory underlying the one-dimensional version, cMPS. Constructing algorithms that integrate the related quantum-Gross-Pitaevskii equation (Haegeman *et al.*, 2017) is challenging, although considerable progress in this direction was recently made by Tuybens *et al.* (2020). Much effort is also currently being devoted to constructing the higher-dimensional versions (Tilloy and Cirac, 2019) or the continuous MERAs (Haegeman, Osborne *et al.*, 2013; Cotler *et al.*, 2019; Fernandez-Melgarejo, Molina-Vilaplana, and Torrente-Lujan, 2019; Zou, Ganahl, and Vidal, 2019; Fernandez-Melgarejo and Molina-Vilaplana, 2020) for computations in quantum field theories. Here the main challenge is to make practical algorithms to deal with quantum field theories. Another relatively unexplored direction is the use of tensor networks with infinite bond dimension, like infinite matrix product states, in order to describe critical or chiral topological systems (Cirac and Sierra, 2010; Nielsen, Cirac, and Sierra, 2012; Nielsen, Sierra, and Cirac, 2013; Tu *et al.*, 2014).

As for applications of the computational techniques, tensor networks have been used to address atomic, condensed matter, and, more recently, high-energy physics problems. In particular, the fact that symmetries (both global and local) can be easily incorporated into the tensors appears to be an attractive feature aiding in the numerical investigation of symmetry-protected phases, topological models, and lattice gauge theories. The main challenge here is to extend current methods to higher spatial dimensions. MPSs and TTNs have also been applied to problems in quantum chemistry, yielding promising results, although there are still open questions about the suitability of different tensor networks for various chemical structures (White and Martin, 1999; Chan and Sharma, 2011; Szalay *et al.*, 2015). More recently tensor networks have been used to construct toy models of holographic principles in hyperbolic geometries (Swingle, 2012; Pastawski *et al.*, 2015; Hayden *et al.*, 2016). This was triggered by the observation that MERA explicitly leads to the Ryu-Takayanagi formula for the entanglement entropy of critical states in $1+1$ dimensions, where the renormalization direction can be interpreted as the radial coordinate in an AdS bulk. The language of tensor networks seems to be appropriate to construct and analyze simple models displaying some of the expected features of the AdS/CFT correspondence. Furthermore, it has also been used to describe some of the physics expected in black holes and wormholes.

Tensor networks are also being widely used in machine learning (Stoudenmire and Schwab, 2016; Glasser, Pancotti, and Cirac, 2018; Carleo *et al.*, 2019; Glasser *et al.*, 2019;

Huggins *et al.*, 2019). In fact, some of the most traditional methods in that field are closely related to those networks. There is also an intimate connection between tensor networks and so-called neural network states (as well as string-bond states, entangled plaquette states, etc.), which in their simplest incarnation are simply MPSs. However, those states can be extended to other sets of states that have the property that physical observables can be computed using Monte Carlo methods, and thus they can be employed to study the ground states of many-body systems with variational Monte Carlo techniques. All those states are intimately related to graph models in the field of machine learning. This connection is being successfully exploited in both directions. On the one hand, the techniques of deep neural networks can be applied to construct powerful computational methods for many-body quantum systems. On the other hand, the theory of tensor networks and its connection with entanglement can help to devise better methods in machine learning.

Tensor network techniques have also been proposed and used in quantum optics experiments. For instance, quantum tomography can become much more efficient if the states one deals with can be approximated by MPSs or MPDOs, as with fewer measurements one can fully characterize the many-body state (Cramer *et al.*, 2010). Furthermore, in many physical systems MPSs appear in a natural way, for instance, in sequential generation, where a physical system produces or interacts with other subsystems sequentially (Schön *et al.*, 2005; Osborne, Eisert, and Verstraete, 2010). This can occur when atoms cross a cavity where they interact with one or a few optical modes or when an emitter generates photons one after another.

Tensor networks appear naturally in the field of quantum computing in different incarnations. Measurement-based quantum computing can be easily explained in terms of a simple PEPS, the cluster state, and teleportation-based gates acting on the auxiliary indices of the tensor whenever one performs a measurement (Verstraete and Cirac, 2004b). Quantum circuits have a natural expression in terms of tensor networks, so the analysis of different quantum algorithms, and even the effects of the errors, can sometimes be easily traced (Nielsen and Chuang, 2000). Additionally, quantum error correcting codes typically have simple characterizations as tensor networks (Terhal, 2015). This is the case of surface codes, which are the basis of physical implementations where gates occur locally. Tensor network techniques also seem to be essential to analyzing more sophisticated quantum error correcting codes based on string nets.

Finally, there are interesting connections between tensor networks and some areas in mathematics. For instance, MPOs can be used to construct representations of fusion categories, weak Hopf algebras, and subfactors (Kawahigashi, 2020; Lootens *et al.*, 2021; Molnar *et al.*, 2021), which in turn are related to topological field theories, conformal field theories, and integrability through the Yang-Baxter equation.

ACKNOWLEDGMENTS

This review would not have been possible without the numerous colleagues (too many to list) with whom we have both collaborated on and extensively discussed the various

aspects of tensor networks, ranging from their mathematical structure to their physical use and numerical utility. We are deeply grateful to each and every one of them. We also thank all of the people who kept encouraging us to both start and finish this review. Finally, we are grateful to José Garre Rubio for creating most of the figures in the review. This work has received support from the European Research Council (ERC) under the European Union's Horizon 2020 program [Grant Agreements No. 636201 (WASCOSYS), No. 647905 (QUTE), No. 648913 (GAPS), No. 742102 (QENOCOBA), and No. 863476 (SEQUAM)], from the DFG (German Research Foundation) under Germany's Excellence Strategy (Grant No. EXC2111-390814868), and through Severo Ochoa Grant No. CEX2019-000904-S funded by MCIN/AEI.

APPENDIX: EXAMPLES

This appendix collects the MPS and PEPS descriptions for a variety of widely used tensor network states.

1. One dimension: MPSs

We start by giving a range of examples of one-dimensional MPSs.

a. Product states

Any product state $|\psi\rangle = |\phi^1\rangle \otimes |\phi^2\rangle \otimes \cdots \otimes |\phi^N\rangle$ is a trivial MPS with $D = 1$. With the convention that $|\phi^s\rangle = \sum_i a^{i,[s]}|i\rangle$, we have

$$|\psi\rangle = \sum_{i_1, \dots, i_N} a^{i_1, [1]} \cdots a^{i_N, [N]} |i_1, \dots, i_N\rangle. \quad (\text{A1})$$

b. The GHZ state

The GHZ state on a d -level system,

$$|\text{GHZ}\rangle = \sum_{i=0}^{d-1} |i, i, \dots, i\rangle,$$

is a MPS with $A_{\alpha\beta}^i = \delta_{i=\alpha=\beta}$.

c. The W state

The W state

$$|W\rangle = |100\dots\rangle + |010\dots\rangle + \cdots + |0\dots001\rangle$$

is a MPS with open boundary conditions and $D = 2$, with

$$A^0 = \begin{pmatrix} 1 & 0 \\ 0 & 1 \end{pmatrix}, \quad A^1 = \begin{pmatrix} 0 & 1 \\ 0 & 0 \end{pmatrix}, \quad (\text{A2})$$

and left and right boundary conditions ($|l\rangle = |0\rangle$ and $|r\rangle = |1\rangle$), respectively, i.e.,

$$|W\rangle = \sum (l|A^1 A^2 \cdots A^N|r)|i_1, \dots, i_N\rangle. \quad (\text{A3})$$

Note that this is not a translationally invariant representation of the MPS due to the nonperiodic boundary condition. This begs the question of which bond dimension is optimal for representing the W state as a translationally invariant MPS. In this case the bond dimension D must scale polynomially with the system size N . In particular, combining the results of [Perez-Garcia *et al.* \(2007\)](#) and [Michalek and Shitov \(2018\)](#), one determines that D must fulfill a bound of the form $D^3 \log D = \Omega(N)$, which implies, in particular, that, for each $\delta > 0$, $D = \Omega(N^{1/(3+\delta)})$.

d. The cluster state

The 1D cluster state ([Raussendorf and Briegel, 2001](#)) is a MPS with

$$A^0 = |0\rangle(+), \quad A^1 = |1\rangle(-)$$

([Verstraete and Cirac, 2004b](#)). This can be derived by using the fact that the cluster state can be constructed by acting with a controlled-Z gate between nearest neighbors, starting with a $|+\rangle^{\otimes N}$ state.

e. The AKLT state

The 1D AKLT state ([Affleck *et al.*, 1987](#)) is constructed by taking spin-1/2 singlets as bonds and projecting the two spin-1/2 at each site on the joint spin-1 subspace. The resulting tensor is (labeling the physical states as $S_z = 0, \pm 1$)

$$A^{+1} = \begin{pmatrix} 1 & 0 \\ 0 & 0 \end{pmatrix} Y, \quad A^0 = \frac{1}{\sqrt{2}} \begin{pmatrix} 0 & 1 \\ 1 & 0 \end{pmatrix} Y, \quad A^{-1} = \begin{pmatrix} 0 & 0 \\ 0 & 1 \end{pmatrix} Y,$$

where

$$Y = \begin{pmatrix} 0 & -1 \\ 1 & 0 \end{pmatrix} \quad (\text{A4})$$

encodes the singlet. When expressed in the basis $|+\rangle = i(|-1\rangle + |+1\rangle)/\sqrt{2}$, $|-\rangle = (|-1\rangle - |+1\rangle)/\sqrt{2}$, and $|0\rangle$, these tensors become

$$A^- = \frac{1}{\sqrt{2}} \sigma_x, \quad A^+ = \frac{1}{\sqrt{2}} \sigma_y, \quad A^0 = \frac{1}{\sqrt{2}} \sigma_z.$$

f. The Majumdar-Ghosh model

The Majumdar-Ghosh model is the 1D version of the RVB state and appears as the ground state of the spin-1/2 Hamiltonian $H = \sum S_i \cdot S_{i+1} + (1/2) \sum S_i \cdot S_{i+2}$ ([Majumdar and Ghosh, 1969](#)). Its ground state is a superposition of singlet pairs (1, 2), (3, 4), ... and (2, 3), (4, 5), ..., (N, 1) and can be written as a MPS with

$$A = [|0\rangle[|02\rangle + |20\rangle] + |1\rangle[|12\rangle + |21\rangle]] \otimes Y$$

([Verstraete *et al.*, 2006](#)), with Y as in Eq. (A4).

2. Two dimensions: PEPSs

Next we give a range of examples for two-dimensional PEPSs, where we follow the convention to order the virtual indices top, right, down, left, as introduced in Sec. II.B.1.

a. The GHZ state

As in one dimension, the 2D GHZ state

$$|\text{GHZ}\rangle = \sum_{i=0}^{d-1} |i, i, \dots, i\rangle$$

can be written as a PEPS with $D = d$ and $A_{\alpha\beta\gamma\delta}^i = \delta_{i=\alpha=\beta=\gamma=\delta}$.

b. The cluster state

The 2D cluster state (Raussendorf and Briegel, 2001) on the square lattice can be written as a PEPS with

$$A = |0\rangle(00++ + |1\rangle(11--|,$$

where $(\pm| = [(|0\rangle \pm |1\rangle)/\sqrt{2}]$. This can again be understood by rewriting the circuit preparing the cluster state (controlled-Z gates between nearest neighbors acting on the $|+\rangle^{\otimes N}$ state) as a tensor network (Verstraete and Cirac, 2004b). Indeed, this tensor network description straightforwardly generalized to arbitrary graphs.

c. The AKLT model

The 2D AKLT model (Affleck *et al.*, 1988) is obtained by placing singlets on the links of the lattice (commonly honeycomb or square) and projecting onto the symmetric subspace. This can be directly translated into a PEPS by absorbing the singlets

$$Y = \begin{pmatrix} 0 & -1 \\ 1 & 0 \end{pmatrix}$$

into the projectors Π_{sym} onto the symmetric space. For the square lattice, this yields tensors

$$A = \Pi_{\text{sym}}(\mathbb{1} \otimes \mathbb{1} \otimes Y \otimes Y).$$

d. The RVB state

The nearest-neighbor RVB state on a 2D lattice is the superposition of all ways of covering the lattice with nearest-neighbor singlets. The corresponding $D = 3$ PEPS tensor (Verstraete *et al.*, 2006) is given by combining the projector

$$P = |0\rangle[(0222| + (2022| + \dots) + |1\rangle[(1222| + (2122| + \dots|$$

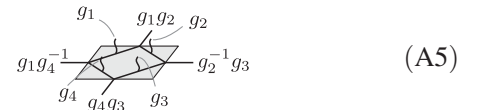
(illustrated here for coordination number 4) with $\pm Y$ tensors for each link (with the sign corresponding to the orientation of

the singlet). For the square lattice with a translational invariant orientation of singlets, the tensor would be

$$A = P(\mathbb{1} \otimes \mathbb{1} \otimes Y \otimes Y).$$

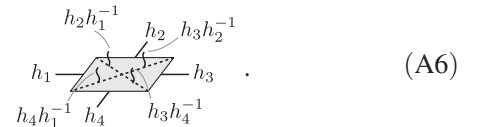
e. The toric code and quantum double models

The quantum double model for a finite group G (Kitaev, 2003) on an oriented square lattice has spins with basis $\{|g\rangle\}_{g \in G}$ assigned to every edge and is the equal weight superposition of all basis configurations that satisfy Gauss's law across a vertex, $g_1 g_2 g_3^{-1} g_4^{-1} = 0$, where the inverses relate to the orientation of the edges. A PEPS representation can be obtained by blocking every other plaquette (containing four edges) into a tensor (aligned diagonally with respect to the lattice) and using the virtual indices (which sit at the vertices of the original lattice) to enforce the Gauss law; i.e., the nonzero configurations are



(where the lines inside the tensor indicate the original lattice).

Alternatively, a dual PEPS representation can be obtained by assigning dual "color" variables $g \in G$ to the plaquettes and defining the physical spins as the difference of adjacent plaquette colors (Schuch, Cirac, and Perez-Garcia, 2010). The equal weight superposition of all plaquette colors then corresponds to the equal weight superposition of all Gauss law configurations. The corresponding tensor is thus



Note that this representation is G -injective (in fact, G -isometric) with respect to the regular representation, as shifting all plaquette colors does not affect the physical state. On the other hand, in the representation (A5), the four virtual indices in the group basis fuse to the identity and thus possess a symmetry under the action of any irreducible representation.

From the point of view of bimodule categories (Lootens *et al.*, 2021), the case (A5) corresponds to $\mathcal{D} = G$, $\mathcal{M} = \text{Vec}$, $\mathcal{C} = \text{Rep}_G$. Hence, the MPO symmetries are labeled as the irreps. The case (A6) corresponds to $\mathcal{C} = \mathcal{M} = \mathcal{D} = G$ up to a blocking, and the MPOs are hence labeled as the group elements.

f. String-net models

The string-net picture provides the most natural description of topological phases of matter in terms of MPO-symmetric tensors. As discussed in Secs. III.A.6 and III.B, the PEPS description involves a $(\mathcal{C}, \mathcal{D})$ -bimodule category \mathcal{M} with labels $\{a, b, c, \dots\} \in I_{\mathcal{C}}$, $\{A, B, C, \dots\} \in I_{\mathcal{M}}$, and

$\{\alpha, \beta, \gamma, \dots\} \in I_{\mathcal{D}}$. As a special case, the categories might all be chosen as equal to one another. For the case of a bipartite hexagonal lattice and a gauge in which all F symbols are unitary, one can choose the A -type PEPS tensors of the bipartite lattice as

$$\left(\frac{d_\alpha d_\beta}{d_\gamma d_C^2}\right)^{1/4} \left({}_3F_B^{A\alpha\beta}\right)_{C,jn}^{\gamma,km} = \begin{array}{c} \text{---} j \text{---} \\ \text{---} \alpha \text{---} \\ \text{---} k \text{---} \\ \text{---} \beta \text{---} n \text{---} \\ \text{---} C \text{---} \\ \text{---} m \text{---} \\ \text{---} B \text{---} \\ \text{---} A \text{---} \end{array},$$

and the PEPS tensors on the B -type sublattice obtained by reflecting the previously mentioned tensor around the x axis and reversing all arrows as the complex conjugate. The d_i are the quantum dimensions of the different categorical objects. Additionally, an extra factor d_A has to be introduced for every closed loop of virtual labels \mathcal{M} .

The quantum double description for a group G as discussed in Appendix 2.e is a special case of these string-net representations. The two previously discussed options correspond to $\mathcal{D} = \mathcal{M} = \text{Vec}_G$ and $\mathcal{D} = \text{Vec}_G, \mathcal{M} = \text{Vec}, \mathcal{C} = \text{Rep}(G)$. Additionally, one can define two more Morita-equivalent PEPS with physical labels in $\text{Rep}(G)$ as $\mathcal{D} = \mathcal{M} = \mathcal{C} = \text{Rep}(G)$ or $\mathcal{D} = \text{Rep}(G), \mathcal{M} = \text{Vec}, \mathcal{C} = \text{Vec}_G$. Here Vec_G is the category with the group elements as labels, and Vec is the trivial category consisting of only one element.

g. PEPSs from classical models

With each classical model H and a finite inverse temperature β there is associated a PEPS that reproduces the expectation value of any diagonal observable (in particular, the classical correlation functions) present in the Gibbs state $e^{-\beta H}/Z$. For simplicity, we restrict to the case of nearest-neighbor interactions on a square lattice $H(\sigma_1, \dots, \sigma_N) = \sum_{(i,j)} h_{i,j}$. Define the matrix $M = \sum_{i,j} e^{-(\beta/2)h(i,j)} |i\rangle\langle j|$. The corresponding PEPS is then given by the tensor (Verstraete *et al.*, 2006)

$$A = \left[\sum_i |i\rangle\langle iii| \right] (\mathbb{1} \otimes \mathbb{1} \otimes M \otimes M).$$

This shows that expectation values of the classical Gibbs state correspond to expectation values of the associated PEPS for diagonal observables. In particular, for the critical temperature β_c the associated PEPS has power law decaying correlations, and hence its parent Hamiltonian must be gapless (Hastings and Koma, 2006; Nachtergaele and Sims, 2006).

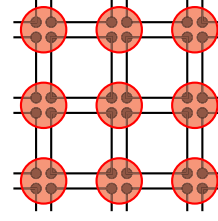
h. The CZX model

The CZX model (Chen, Liu, and Wen, 2011) is a product state of GHZ states of qubits ($d = 2$) across plaquettes of a square lattice placed on a torus of the size $2N \times 2M$,

$$\bigotimes_{i,j=1}^{N,M} |GHZ_{ij}\rangle,$$

with $|GHZ_{ij}\rangle$ the GHZ state on sites $(2i, 2j), (2i + 1, 2j), (2i + 1, 2j + 1), (2i, 2j + 1)$. The CZX model

is simply the state resulting from considering blocked sites formed by $(2i - 1, 2j - 1), (2i, 2j - 1), (2i, 2j), (2i - 1, 2j)$,



Using the previous description of the GHZ, the PEPS tensor with bond dimension $D = d^2 = 4$ is then given by

$$\sum_{i,j,k,l=0}^1 |ijkl\rangle((i, j), (j, k), (k, l), (l, i)).$$

As explained in Sec. III.B.1, the CZX model belongs to the nontrivial SPT sector of a global on-site \mathbb{Z}_2 symmetry.

3. Fermionic MPSs and PEPSs

a. The Kitaev chain

The Kitaev chain, or the Majorana chain (Kitaev, 2001), consists of a chain of spinless fermions. Each fermion consists of two Majorana fermions, which can be paired up either within a site or across adjacent sites, which can be changed by tuning the Hamiltonian. Here we are interested in the limit where the Majorana modes pair up solely across sites, as this corresponds to a nontrivial topological phase.

To describe the corresponding ground state as a fermionic MPS, we start with $2N$ Majorana modes $c_j, \{c_j, c_k\} = 2\delta_{ij}$. Denote by $|\Omega\rangle$ the vacuum, defined via $c_{2n}c_{2n+1}|\Omega\rangle = 0, n = 1, \dots, N$. The nontrivial fixed point of the Kitaev chain is the state of the N complex Dirac fermions $a_n = (c_{2n-1} + ic_{2n})/2$ in the state $|\psi\rangle = |\Omega\rangle$. The corresponding description in terms of graded tensor networks is given in Eq. (10) and has tensors (Bultinck, Williamson *et al.*, 2017)

$$A^0 = \begin{pmatrix} 1 & 0 \\ 0 & 1 \end{pmatrix}$$

and

$$A^1 = \begin{pmatrix} 0 & 1 \\ -1 & 0 \end{pmatrix},$$

with a twist $Y = A^1$ at the boundary.

b. Free fermionic and chiral PEPSs

Free (or noninteracting) fermions are fermionic systems governed by a Hamiltonian that is quadratic in the fermionic creation and annihilation operators a_x^\dagger and a_x , where x denotes the lattice position (and possibly other degrees of freedom such as spin). Ground and thermal states ρ of such Hamiltonians (“Gaussian states”) are fully characterized by their second moments $\gamma_{xy} = (i/2)\text{tr}(\rho[c_x, c_y])$ due to Wick’s

theorem, where we use a Majorana representation $c_{2x-1} = a_x + a_x^\dagger$, $c_{2x} = -i(a_x - a_x^\dagger)$. A special case involves PEPSs constructed using Gaussian states as bonds and Gaussian maps as PEPS tensors (that is, maps that map Gaussian states to Gaussian states). Because of their compact representation and the possibility of exactly solving, for instance, for the ground state of translational invariant quadratic Hamiltonians, these Gaussian fermionic PEPSs form an important test bed for the investigation of PEPSs and their ability to describe certain types of systems.

A translational invariant Gaussian fermionic PEPS in D spatial dimensions with n physical Majorana modes per site and m Majorana modes per bond is specified by a $(n + 2Dm) \times (n + 2Dm)$ real antisymmetric matrix with a block structure

$$\Gamma = \begin{pmatrix} X & Y \\ -Y^T & Z \end{pmatrix}$$

(where X is $n \times n$ and Z is $2Dm \times 2Dm$), which satisfies $\Gamma^2 = -\mathbb{1}$ (Kraus *et al.*, 2010). It describes a Gaussian state with correlations

$$\hat{\gamma}(k) = X + Y[Z + \omega(k)]^{-1}Y^T,$$

$$\omega(k) = \bigoplus_{\alpha=1}^D \begin{pmatrix} 0 & e^{ik_\alpha} \mathbb{1}_m \\ e^{-ik_\alpha} \mathbb{1}_m & 0 \end{pmatrix}$$

in momentum space, $\hat{\gamma}(\vec{k}) = (i/2)\text{tr}(\rho[\hat{c}_k, \hat{c}_{-k}])$, $\hat{c}_k = \sum e^{ik \cdot x} c_x / \sqrt{N}$. Since the entries of the inverse of a matrix $M = Z + \omega(k)$ are the quotient of the determinant of minors of M and of $\det(M)$, any Gaussian fermionic PEPS has the special property that $\hat{\gamma}(k)$ is the ratio of polynomials of a degree of at most $2Dm$ in $e^{\pm ik_\alpha}$ (Schuch, Wolf, and Cirac, 2008).

One important example is a Gaussian fermionic PEPS that describes a topological superconductor in $D = 2$ spatial dimensions, that is, a system with chiral order (Wahl *et al.*, 2013, 2014) for which $n = 2$, $m = 1$ (i.e., each bond consists of only a single Majorana mode), and

$$X = \begin{pmatrix} 0 & 1 - 2\lambda \\ -1 + 2\lambda & 0 \end{pmatrix},$$

$$Y = \sqrt{\lambda - \lambda^2} \begin{pmatrix} 1 & -1 & 0 & -\sqrt{2} \\ -1 & -1 & -\sqrt{2} & 0 \end{pmatrix},$$

$$Z = \begin{pmatrix} 0 & 1 - \lambda & -\lambda/\sqrt{2} & -\lambda/\sqrt{2} \\ -1 + \lambda & 0 & \lambda/\sqrt{2} & -\lambda/\sqrt{2} \\ \lambda/\sqrt{2} & -\lambda/\sqrt{2} & 0 & 1 - \lambda \\ \lambda/\sqrt{2} & \lambda/\sqrt{2} & -1 + \lambda & 0 \end{pmatrix},$$

where $0 < \lambda < 1$.

4. MPOs and MPUs

a. The CZX MPU

As explained in Sec. III.B.1, the reason behind the fact that the CZX model is a nontrivial SPT phase is the existence of a nontrivial MPU symmetry in the associated PEPS determined by a nontrivial 3-cocycle. This MPU is given by the tensor

$$|0\rangle\langle 1| \otimes |0\rangle\langle +| + |1\rangle\langle 0| \otimes |1\rangle\langle -|$$

and can be understood as the product of overlapping controlled- Z gates $CZ = \text{diag}(1, 1, 1, -1)$ between all adjacent sites (since they commute, the ordering does not matter), followed by a Pauli X on all sites (thus the name) (Chen, Liu, and Wen, 2011).

This MPO, which we denote as $O(A)$, is injective, as can easily be seen by considering the algebra generated by the matrices

$$A^{01} = \begin{pmatrix} 1 & 1 \\ 0 & 0 \end{pmatrix}, \quad A^{10} = \begin{pmatrix} 0 & 0 \\ 1 & -1 \end{pmatrix}.$$

We now square this MPO, thereby getting a MPO $O(B)$ with bond dimension 4 that is given by the following matrices:

$$B^{00} = \begin{pmatrix} 1 & 1 \\ 0 & 0 \end{pmatrix} \otimes \begin{pmatrix} 0 & 0 \\ 1 & -1 \end{pmatrix} = \begin{pmatrix} 0 & 0 & 0 & 0 \\ 1 & -1 & 1 & -1 \\ 0 & 0 & 0 & 0 \\ 0 & 0 & 0 & 0 \end{pmatrix},$$

$$B^{11} = \begin{pmatrix} 0 & 0 \\ 1 & -1 \end{pmatrix} \otimes \begin{pmatrix} 1 & 1 \\ 0 & 0 \end{pmatrix} = \begin{pmatrix} 0 & 0 & 0 & 0 \\ 0 & 0 & 0 & 0 \\ 1 & 1 & -1 & -1 \\ 0 & 0 & 0 & 0 \end{pmatrix}.$$

This MPO is not injective, and it has an invariant subspace given by the projector

$$P = \begin{pmatrix} 0 & 0 & 0 & 0 \\ 0 & 1 & 0 & 0 \\ 0 & 0 & 1 & 0 \\ 0 & 0 & 0 & 0 \end{pmatrix}.$$

By the canonical form construction (Sec. IV), we can therefore also work with the block

$$B^{00} = \begin{pmatrix} -1 & 1 \\ 0 & 0 \end{pmatrix}, \quad B^{11} = \begin{pmatrix} 0 & 0 \\ 1 & -1 \end{pmatrix}.$$

But this MPO again has an invariant subspace given by the projector

$$Q = 1/2 \begin{pmatrix} 1 & -1 \\ -1 & 1 \end{pmatrix}.$$

Applying once more the canonical form construction, we arrive at the following canonical form for the MPO:

$B^{ij} = (-1)\delta_{ij}$, which globally means that $O(A)^2 = (-1)^N I$. The CZX MPO hence provides a good example showing how the canonical form construction works.

b. The shift MPU

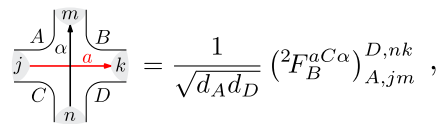
The shift is the paradigmatic example of a MPU that cannot be approximated using a short-range time evolution; see Sec. II.B.2 (Cirac *et al.*, 2017b). Its tensor is given by

$$\sum_{i,j} |i\rangle\langle j| \otimes |i\rangle\langle j|.$$

c. The MPO for the Fibonacci model

String nets in the PEPS picture are described using a $(\mathcal{C}, \mathcal{D})$ -bimodule category \mathcal{M} with labels $\{a, b, c, \dots\} \in I_{\mathcal{C}}$, $\{A, B, C, \dots\} \in I_{\mathcal{M}}$, and $\{\alpha, \beta, \gamma, \dots\} \in I_{\mathcal{D}}$.

The MPOs are given by



$$\begin{array}{c} \begin{array}{c} A \\ \uparrow \\ j \end{array} \begin{array}{c} \alpha \\ \uparrow \\ m \end{array} \begin{array}{c} B \\ \uparrow \\ k \end{array} \\ \begin{array}{c} C \\ \downarrow \\ n \end{array} \end{array} = \frac{1}{\sqrt{d_A d_D}} ({}^2F_B^{aC\alpha})_{A, jm}^{D, nk},$$

with 2F a solution of the six coupled pentagon equations and d_i the quantum dimensions of the categorical objects. For the Fibonacci model, we can take $\mathcal{C} = \mathcal{M} = \mathcal{D}$, and hence ${}^1F = {}^2F = {}^3F = {}^4F = {}^5F = F$. The categorical objects are $I_{\mathcal{C}} = \{1, \tau\}$, with quantum dimensions $d_1 = 1$ and $d_{\tau} = (1 + \sqrt{5})/2$ and the fusion rules given by

$$N_{11}^1 = N_{\tau 1}^{\tau} = N_{1\tau}^{\tau} = N_{\tau\tau}^1 = N_{\tau\tau}^{\tau} = 1.$$

The elements of $(F_d^{abc})_e^f$ are zero unless $N_{ab}^c > 0$, $N_{cd}^e > 0$, $N_{ad}^f > 0$, $N_{bcf} > 0$, and the only allowed elements that cannot be chosen as equal to 1 by an appropriate gauge choice are

$$(F_{\tau}^{\tau\tau\tau})_b^a = \left(\frac{1}{d_{\tau}} \frac{1}{\sqrt{d_{\tau}}} \frac{1}{\sqrt{d_{\tau}}} - \frac{1}{d_{\tau}} \right)_{ab}.$$

REFERENCES

Aasen, D., E. Lake, and K. Walker, 2019, *J. Math. Phys. (N.Y.)* **60**, 121901.
 Aasen, D., R. S. Mong, and P. Fendley, 2016, *J. Phys. A* **49**, 354001.
 Abdul-Rahman, H., M. Lemm, A. Lucia, B. Nachtergaele, and A. Young, 2019, [arXiv:1901.09297](https://arxiv.org/abs/1901.09297).
 Accardi, L., 1981, *Topics in Quantum Probability* (Elsevier Science, New York).
 Affleck, I., T. Kennedy, E. H. Lieb, and H. Tasaki, 1987, *Phys. Rev. Lett.* **59**, 799.
 Affleck, I., T. Kennedy, E. H. Lieb, and H. Tasaki, 1988, *Commun. Math. Phys.* **115**, 477.
 Aguado, M., and G. Vidal, 2008, *Phys. Rev. Lett.* **100**, 070404.

Albeverio, S., and R. Høegh-Krohn, 1978, *Commun. Math. Phys.* **64**, 83.
 Anderson, P. W., 1973, *Mater. Res. Bull.* **8**, 153.
 Anderson, P. W., 2018, *Basic Notions of Condensed Matter Physics* (CRC Press, Boca Raton).
 Andrews, G. E., R. J. Baxter, and P. J. Forrester, 1984, *J. Stat. Phys.* **35**, 193.
 Arad, I., A. Kitaev, Z. Landau, and U. Vazirani, 2013, [arXiv:1301.1162](https://arxiv.org/abs/1301.1162).
 Arad, I., Z. Landau, U. Vazirani, and T. Vidick, 2017, *Commun. Math. Phys.* **356**, 65.
 Avella, A., and F. Mancini, 2011, *Strongly Correlated Systems: Theoretical Methods*, Springer Series in Solid-State Sciences Vol. 171 (Springer, New York).
 Bachmann, S., E. Hamza, B. Nachtergaele, and A. Young, 2015, *J. Stat. Phys.* **160**, 636.
 Bachmann, S., S. Michalakis, B. Nachtergaele, and R. Sims, 2012, *Commun. Math. Phys.* **309**, 835.
 Bachmann, S., and B. Nachtergaele, 2012, *Phys. Rev. B* **86**, 035149.
 Bachmann, S., and B. Nachtergaele, 2014, *Commun. Math. Phys.* **329**, 509.
 Bais, F. A., B. J. Schroers, and J. K. Slingerland, 2002, *Phys. Rev. Lett.* **89**, 181601.
 Bal, M., M. Mariën, J. Haegeman, and F. Verstraete, 2017, *Phys. Rev. Lett.* **118**, 250602.
 Bargmann, V., 1954, *Ann. Math.* **59**, 1.
 Barkeshli, M., P. Bonderson, M. Cheng, and Z. Wang, 2019, *Phys. Rev. B* **100**, 115147.
 Barthel, T., M. Kliesch, and J. Eisert, 2010, *Phys. Rev. Lett.* **105**, 010502.
 Barthel, T., C. Pineda, and J. Eisert, 2009, *Phys. Rev. A* **80**, 042333.
 Bauer, B., and C. Nayak, 2013, *J. Stat. Mech.* P09005.
 Baxter, R., 1968, *J. Math. Phys. (N.Y.)* **9**, 650.
 Baxter, R., 1981, *Physica (Amsterdam)* **106A**, 18.
 Baxter, R., 2007, *Exactly Solved Models in Statistical Mechanics*, Dover Books on Physics (Dover Publications, New York).
 Becca, F., and S. Sorella, 2017, *Quantum Monte Carlo Approaches for Correlated Systems* (Cambridge University Press, Cambridge, England).
 Bekenstein, J. D., 1973, *Phys. Rev. D* **7**, 2333.
 Bennett, C. H., H. J. Bernstein, S. Popescu, and B. Schumacher, 1996, *Phys. Rev. A* **53**, 2046.
 Bernevig, B., and T. Hughes, 2013, *Topological Insulators and Topological Superconductors* (Princeton University Press, Princeton, NJ).
 Beylkin, G., and M. J. Mohlenkamp, 2002, *Proc. Natl. Acad. Sci. U.S.A.* **99**, 10246.
 Biamonte, J., 2019, [arXiv:1912.10049](https://arxiv.org/abs/1912.10049).
 Brandao, F. G., T. S. Cubitt, A. Lucia, S. Michalakis, and D. Perez-Garcia, 2015, *J. Math. Phys. (N.Y.)* **56**, 102202.
 Brandao, F. G., and A. W. Harrow, 2016, *Commun. Math. Phys.* **342**, 47.
 Brandao, F. G., and M. Horodecki, 2013, *Nat. Phys.* **9**, 721.
 Bravyi, S., and M. B. Hastings, 2011, *Commun. Math. Phys.* **307**, 609.
 Bravyi, S., M. B. Hastings, and S. Michalakis, 2010, *J. Math. Phys. (N.Y.)* **51**, 093512.
 Bravyi, S., M. B. Hastings, and F. Verstraete, 2006, *Phys. Rev. Lett.* **97**, 050401.
 Bravyi, S. B., and A. Y. Kitaev, 1998, [arXiv:quant-ph/9811052](https://arxiv.org/abs/quant-ph/9811052).
 Bridgeman, J. C., and C. T. Chubb, 2017, *J. Phys. A* **50**, 223001.
 Bridgeman, J. C., and D. J. Williamson, 2017, *Phys. Rev. B* **96**, 125104.

- Buerschaper, O., 2014, *Ann. Phys. (Amsterdam)* **351**, 447.
- Buerschaper, O., and M. Aguado, 2009, *Phys. Rev. B* **80**, 155136.
- Buerschaper, O., M. Aguado, and G. Vidal, 2009, *Phys. Rev. B* **79**, 085119.
- Buican, M., and A. Gromov, 2017, *Commun. Math. Phys.* **356**, 1017.
- Bultinck, N., M. Mariën, D. J. Williamson, M. B. Şahinoğlu, J. Haegeman, and F. Verstraete, 2017, *Ann. Phys. (Amsterdam)* **378**, 183.
- Bultinck, N., R. Vanhove, J. Haegeman, and F. Verstraete, 2018, *Phys. Rev. Lett.* **120**, 156601.
- Bultinck, N., D. J. Williamson, J. Haegeman, and F. Verstraete, 2017, *Phys. Rev. B* **95**, 075108.
- Bultinck, N., D. J. Williamson, J. Haegeman, and F. Verstraete, 2018, *J. Phys. A* **51**, 025202.
- Buyens, B., J. Haegeman, K. Van Acoleyen, H. Verschelde, and F. Verstraete, 2014, *Phys. Rev. Lett.* **113**, 091601.
- Cadarso, A., M. Sanz, M. M. Wolf, J. I. Cirac, and D. Perez-Garcia, 2013, *Phys. Rev. B* **87**, 035114.
- Calabrese, P., and A. Lefevre, 2008, *Phys. Rev. A* **78**, 032329.
- Carleo, G., I. Cirac, K. Cranmer, L. Daudet, M. Schuld, N. Tishby, L. Vogt-Maranto, and L. Zdeborová, 2019, *Rev. Mod. Phys.* **91**, 045002.
- Chaikin, P. M., T. C. Lubensky, and T. A. Witten, 1995, *Principles of Condensed Matter Physics*, Vol. 10 (Cambridge University Press Cambridge, England).
- Chan, G. K.-L., and S. Sharma, 2011, *Annu. Rev. Phys. Chem.* **62**, 465.
- Chen, C.-F., K. Kato, and F. G. Brandão, 2020, [arXiv:2010.14682](https://arxiv.org/abs/2010.14682).
- Chen, J.-Y., S. Capponi, A. Wietek, M. Mambrini, N. Schuch, and D. Poilblanc, 2020, *Phys. Rev. Lett.* **125**, 017201.
- Chen, J.-Y., L. Vanderstraeten, S. Capponi, and D. Poilblanc, 2018, *Phys. Rev. B* **98**, 184409.
- Chen, X., Z.-C. Gu, Z.-X. Liu, and X.-G. Wen, 2013, *Phys. Rev. B* **87**, 155114.
- Chen, X., Z.-C. Gu, and X.-G. Wen, 2011a, *Phys. Rev. B* **83**, 035107.
- Chen, X., Z.-C. Gu, and X.-G. Wen, 2011b, *Phys. Rev. B* **84**, 235128.
- Chen, X., Z.-X. Liu, and X.-G. Wen, 2011, *Phys. Rev. B* **84**, 235141.
- Chen, X., B. Zeng, Z. Gu, I. L. Chuang, and X. Wen, 2010, *Phys. Rev. B* **82**, 165119.
- Cirac, J., S. Michalakis, D. Perez-Garcia, and N. Schuch, 2013, *Phys. Rev. B* **88**, 115108.
- Cirac, J., D. Perez-Garcia, N. Schuch, and F. Verstraete, 2017a, *Ann. Phys. (Amsterdam)* **378**, 100.
- Cirac, J. I., D. Perez-Garcia, N. Schuch, and F. Verstraete, 2017b, *J. Stat. Mech.* 083105.
- Cirac, J. I., D. Poilblanc, N. Schuch, and F. Verstraete, 2011, *Phys. Rev. B* **83**, 245134.
- Cirac, J. I., and G. Sierra, 2010, *Phys. Rev. B* **81**, 104431.
- Cirac, J. I., and F. Verstraete, 2009, *J. Phys. A* **42**, 504004.
- Coleman, A., 1972, *J. Math. Phys. (N.Y.)* **13**, 214.
- Corboz, P., 2016, *Phys. Rev. B* **94**, 035133.
- Corboz, P., P. Czarnik, G. Kapteijns, and L. Tagliacozzo, 2018, *Phys. Rev. X* **8**, 031031.
- Corboz, P., G. Evenbly, F. Verstraete, and G. Vidal, 2010, *Phys. Rev. A* **81**, 010303(R).
- Coser, A., and D. Perez-Garcia, 2018, [arXiv:1810.05092](https://arxiv.org/abs/1810.05092).
- Cotler, J. S., M. R. M. Mozaffar, A. Mollabashi, and A. Naseh, 2019, *Phys. Rev. D* **99**, 085005.
- Cramer, M., M. B. Plenio, S. T. Flammia, R. Somma, D. Gross, S. D. Bartlett, O. Landon-Cardinal, D. Poulin, and Y.-K. Liu, 2010, *Nat. Commun.* **1**, 149.
- Crosswhite, G. M., and D. Bacon, 2008, *Phys. Rev. A* **78**, 012356.
- Czarnik, P., and J. Dziarmaga, 2015, *Phys. Rev. B* **92**, 035152.
- Czarnik, P., J. Dziarmaga, and P. Corboz, 2019, *Phys. Rev. B* **99**, 035115.
- Czech, B., G. Evenbly, L. Lamprou, S. McCandlish, X.-l. Qi, J. Sully, and G. Vidal, 2016, *Phys. Rev. B* **94**, 085101.
- Daley, A. J., C. Kollath, U. Schollwöck, and G. Vidal, 2004, *J. Stat. Mech.* P04005.
- Dalzell, A. M., and F. G. Brandao, 2019, [arXiv:1903.10241](https://arxiv.org/abs/1903.10241).
- De las Cuevas, G., J. I. Cirac, N. Schuch, and D. Perez-Garcia, 2017, *J. Math. Phys. (N.Y.)* **58**, 121901.
- De las Cuevas, G., T. S. Cubitt, J. I. Cirac, M. M. Wolf, and D. Perez-Garcia, 2016, *J. Math. Phys. (N.Y.)* **57**, 071902.
- De las Cuevas, G., N. Schuch, D. Perez-Garcia, and J. I. Cirac, 2013, *New J. Phys.* **15**, 123021.
- De las Cuevas, G., N. Schuch, D. Perez-Garcia, and J. I. Cirac, 2018, *Phys. Rev. B* **98**, 174303.
- De Lathauwer, L., B. De Moor, and J. Vandewalle, 2000, *SIAM J. Matrix Anal. Appl.* **21**, 1253.
- Denisov, L. V., 1989, *Theory Probab. Appl.* **33**, 392.
- den Nijs, M., and K. Rommelse, 1989, *Phys. Rev. B* **40**, 4709.
- Dennis, E., A. Kitaev, A. Landahl, and J. Preskill, 2002, *J. Math. Phys. (N.Y.)* **43**, 4452.
- Dirac, P. A., 1930, *Math. Proc. Cambridge Philos. Soc.* **26** 376.
- Draxler, D., J. Haegeman, T. J. Osborne, V. Stojevic, L. Vanderstraeten, and F. Verstraete, 2013, *Phys. Rev. Lett.* **111**, 020402.
- Drinfel'd, V., 1987, in *Proceedings of the International Congress of Mathematicians, Berkeley, CA, 1986*, Vols. 1 and 2, edited by A. M. Gleason (American Mathematical Society, Providence), pp.798–820.
- Dubail, J., and N. Read, 2015, *Phys. Rev. B* **92**, 205307.
- Dubail, J., N. Read, and E. Rezayi, 2012, *Phys. Rev. B* **86**, 245310.
- Duivendoorn, K., M. Iqbal, J. Haegeman, F. Verstraete, and N. Schuch, 2017, *Phys. Rev. B* **95**, 235119.
- Dukelsky, J., M. A. Martín-Delgado, T. Nishino, and G. Sierra, 1998, *Europhys. Lett.* **43**, 457.
- Eisert, J., M. Cramer, and M. Plenio, 2010, *Rev. Mod. Phys.* **82**, 277.
- Elitzur, S., G. Moore, A. Schwimmer, and N. Seiberg, 1989, *Nucl. Phys.* **B326**, 108.
- Estienne, B., Z. Papić, N. Regnault, and B. A. Bernevig, 2013, *Phys. Rev. B* **87**, 161112.
- Evans, D., and Y. Kawahigashi, 1995, *Int. J. Math.* **06**, 205.
- Evenbly, G., 2017, *Phys. Rev. B* **95**, 045117.
- Evenbly, G., and G. Vidal, 2009, *Phys. Rev. Lett.* **102**, 180406.
- Evenbly, G., and G. Vidal, 2011, *J. Stat. Phys.* **145**, 891.
- Evenbly, G., and G. Vidal, 2014, *J. Stat. Phys.* **157**, 931.
- Evenbly, G., and G. Vidal, 2015, *Phys. Rev. Lett.* **115**, 180405.
- Evenbly, G., and G. Vidal, 2016, *Phys. Rev. Lett.* **116**, 040401.
- Faddeev, L., and L. Takhtajan, 1981, *Phys. Lett.* **85A**, 375.
- Fannes, M., B. Nachtergaele, and R. F. Werner, 1989, *Europhys. Lett.* **10**, 633.
- Fannes, M., B. Nachtergaele, and R. F. Werner, 1991, *J. Phys. A* **24**, L185.
- Fannes, M., B. Nachtergaele, and R. F. Werner, 1992a, *Lett. Math. Phys.* **25**, 249.
- Fannes, M., B. Nachtergaele, and R. F. Werner, 1992b, *Commun. Math. Phys.* **144**, 443.
- Fannes, M., B. Nachtergaele, and R. F. Werner, 1992c, *J. Stat. Phys.* **66**, 939.
- Fannes, M., B. Nachtergaele, and R. F. Werner, 1994, *J. Funct. Anal.* **120**, 511.
- Fannes, M., B. Nachtergaele, and R. F. Werner, 1996, *Commun. Math. Phys.* **174**, 477.
- Fendley, P., 2021, *J. Stat. Phys.* **182**, 43.

- Fernandez-Gonzalez, C., N. Schuch, M. M. Wolf, J. I. Cirac, and D. Perez-Garcia, 2015, *Commun. Math. Phys.* **333**, 299.
- Fernández-González, C., N. Schuch, M. M. Wolf, J. I. Cirac, and D. Perez-Garcia, 2012, *Phys. Rev. Lett.* **109**, 260401.
- Fernandez-Melgarejo, J. J., and J. Molina-Vilaplana, 2020, *J. High Energy Phys.* **07**, 149.
- Fernandez-Melgarejo, J. J., J. Molina-Vilaplana, and E. Torrente-Lujan, 2019, *Phys. Rev. D* **100**, 065025.
- Feynman, R., 1988, in *Variational Calculations in Quantum Field Theory*, edited by L. Polley and D. Pottinger (World Scientific, Singapore).
- Fidkowski, L., and A. Kitaev, 2011, *Phys. Rev. B* **83**, 075103.
- Fradkin, E., 2013, *Field Theories of Condensed Matter Physics* (Cambridge University Press, Cambridge, England).
- Freedman, M., A. Kitaev, M. Larsen, and Z. Wang, 2003, *Bull. Am. Math. Soc.* **40**, 31.
- Fuchs, J., I. Runkel, and C. Schweigert, 2002, *Nucl. Phys.* **B646**, 353.
- Garre-Rubio, J., and S. Iblisdir, 2019, *New J. Phys.* **21**, 113016.
- Garre-Rubio, J., S. Iblisdir, and D. Perez-Garcia, 2017, *Phys. Rev. B* **96**, 155123.
- Gils, C., E. Ardonne, S. Trebst, A. W. Ludwig, M. Troyer, and Z. Wang, 2009, *Phys. Rev. Lett.* **103**, 070401.
- Gioev, D., and I. Klich, 2006, *Phys. Rev. Lett.* **96**, 100503.
- Giovannetti, V., S. Montangero, and R. Fazio, 2008, *Phys. Rev. Lett.* **101**, 180503.
- Girvin, S. M., and K. Yang, 2019, *Modern Condensed Matter Physics* (Cambridge University Press, Cambridge, England).
- Glasser, I., N. Pancotti, and J. I. Cirac, 2018, [arXiv:1806.05964](https://arxiv.org/abs/1806.05964).
- Glasser, I., R. Sweke, N. Pancotti, J. Eisert, and J. I. Cirac, 2019, [arXiv:1907.03741](https://arxiv.org/abs/1907.03741).
- Gosset, D., and E. Mozgunov, 2016, *J. Math. Phys. (N.Y.)* **57**, 091901.
- Gould, M., 1993, *Bull. Aust. Math. Soc.* **48**, 275.
- Grasedyck, L., 2010, *SIAM J. Matrix Anal. Appl.* **31**, 2029.
- Gross, D., V. Nesme, H. Vogts, and R. F. Werner, 2012, *Commun. Math. Phys.* **310**, 419.
- Gu, Z.-C., M. Levin, and X.-G. Wen, 2008, *Phys. Rev. B* **78**, 205116.
- Gu, Z.-C., Z. Wang, and X.-G. Wen, 2014, *Phys. Rev. B* **90**, 085140.
- Gu, Z.-C., and X.-G. Wen, 2009, *Phys. Rev. B* **80**, 155131.
- Hackbusch, W., 2012, *Tensor Spaces and Numerical Tensor Calculus*, Springer Series in Computational Mathematics Vol. 42 (Springer, New York).
- Hackenbroich, A., A. Sterdyniak, and N. Schuch, 2018, *Phys. Rev. B* **98**, 085151.
- Haegeman, J., J. I. Cirac, T. J. Osborne, I. Pižorn, H. Verschelde, and F. Verstraete, 2011, *Phys. Rev. Lett.* **107**, 070601.
- Haegeman, J., J. I. Cirac, T. J. Osborne, H. Verschelde, and F. Verstraete, 2010, *Phys. Rev. Lett.* **105**, 251601.
- Haegeman, J., J. I. Cirac, T. J. Osborne, and F. Verstraete, 2013, *Phys. Rev. B* **88**, 085118.
- Haegeman, J., D. Draxler, V. Stojevic, J. I. Cirac, T. J. Osborne, and F. Verstraete, 2017, *SciPost Phys.* **3**, 6.
- Haegeman, J., C. Lubich, I. Oseledets, B. Vandereycken, and F. Verstraete, 2016, *Phys. Rev. B* **94**, 165116.
- Haegeman, J., M. Mariën, T. J. Osborne, and F. Verstraete, 2014, *J. Math. Phys. (N.Y.)* **55**, 021902.
- Haegeman, J., S. Michalakis, B. Nachtergaele, T. J. Osborne, N. Schuch, and F. Verstraete, 2013, *Phys. Rev. Lett.* **111**, 080401.
- Haegeman, J., T. J. Osborne, H. Verschelde, and F. Verstraete, 2013, *Phys. Rev. Lett.* **110**, 100402.
- Haegeman, J., D. Perez-Garcia, I. Cirac, and N. Schuch, 2012, *Phys. Rev. Lett.* **109**, 050402.
- Haegeman, J., B. Pirvu, D. J. Weir, J. I. Cirac, T. J. Osborne, H. Verschelde, and F. Verstraete, 2012, *Phys. Rev. B* **85**, 100408.
- Haegeman, J., and F. Verstraete, 2017, *Annu. Rev. Condens. Matter Phys.* **8**, 355.
- Haegeman, J., V. Zauner, N. Schuch, and F. Verstraete, 2015, *Nat. Commun.* **6**, 8284.
- Haferkamp, J., D. Hangleiter, J. Eisert, and M. Gluza, 2020, *Phys. Rev. Research* **2**, 013010.
- Hallberg, K. A., 2006, *Adv. Phys.* **55**, 477.
- Hastings, M. B., 2004a, *Phys. Rev. B* **69**, 104431.
- Hastings, M. B., 2004b, *Phys. Rev. Lett.* **93**, 140402.
- Hastings, M. B., 2006, *Phys. Rev. B* **73**, 085115.
- Hastings, M. B., 2007, *J. Stat. Mech.* P08024.
- Hastings, M. B., and T. Koma, 2006, *Commun. Math. Phys.* **265**, 781.
- Hastings, M. B., and X. Wen, 2005, *Phys. Rev. B* **72**, 045141.
- Hayashi, T., 1999, [arXiv:math.QA/9904073](https://arxiv.org/abs/math/9904073).
- Hayden, P., S. Nezami, X.-L. Qi, N. Thomas, M. Walter, and Z. Yang, 2016, *J. High Energy Phys.* **11**, 009.
- Holzhey, C., F. Larsen, and F. Wilczek, 1994, *Nucl. Phys.* **B424**, 443.
- Horodecki, R., P. Horodecki, M. Horodecki, and K. Horodecki, 2009, *Rev. Mod. Phys.* **81**, 865.
- Huang, Y., 2014, [arXiv:1403.0327](https://arxiv.org/abs/1403.0327).
- Huang, Y., 2019, *Quantum Views* **3**, 26.
- Huang, Y., 2020, [arXiv:2001.10763](https://arxiv.org/abs/2001.10763).
- Huggins, W., P. Patil, B. Mitchell, K. B. Whaley, and E. M. Stoudenmire, 2019, *Quantum Sci. Technol.* **4**, 024001.
- Imbrie, J. Z., 2016, *J. Stat. Phys.* **163**, 998.
- Jarkovsky, J. G., A. Molnar, N. Schuch, and J. I. Cirac, 2020, *PRX Quantum* **1**, 010304.
- Jennings, D., C. Brockett, J. Haegeman, T. J. Osborne, and F. Verstraete, 2015, *New J. Phys.* **17**, 063039.
- Jiang, H.-C., Z.-Y. Weng, and T. Xiang, 2008, *Phys. Rev. Lett.* **101**, 090603.
- Jiang, S., and Y. Ran, 2017, *Phys. Rev. B* **95**, 125107.
- Jordan, J., R. Orus, G. Vidal, F. Verstraete, and J. I. Cirac, 2008, *Phys. Rev. Lett.* **101**, 250602.
- Kadanoff, L. P., and H. Ceva, 1971, *Phys. Rev. B* **3**, 3918.
- Kádár, Z., A. Marzuoli, and M. Rasetti, 2010, *Adv. Theor. Math. Phys.* **2010**, 671039.
- Kastoryano, M. J., and A. Lucia, 2018, *J. Stat. Mech.* 033105.
- Kastoryano, M. J., A. Lucia, and D. Perez-Garcia, 2019, *Commun. Math. Phys.* **366**, 895.
- Kawahigashi, Y., 2020, *Lett. Math. Phys.* **110**, 1113.
- Kennedy, T., and H. Tasaki, 1992, *Phys. Rev. B* **45**, 304.
- Kholevo, A. S., 1987, *Theory Probab. Appl.* **31**, 493.
- Kitaev, A., 2001, *Phys. Usp.* **44**, 131.
- Kitaev, A., 2003, *Ann. Phys. (Amsterdam)* **303**, 2.
- Kitaev, A., 2006, *Ann. Phys. (Amsterdam)* **321**, 2.
- Kitaev, A., and L. Kong, 2012, *Commun. Math. Phys.* **313**, 351.
- Kitaev, A., and J. Preskill, 2006, *Phys. Rev. Lett.* **96**, 110404.
- Klich, I., 2010, *Ann. Phys. (N.Y.)* **325**, 2120.
- Knabe, S., 1988, *J. Stat. Phys.* **52**, 627.
- Kohler, T., and T. Cubitt, 2019, *J. High Energy Phys.* **08**, 017.
- Kohn, W., 1973, *Phys. Rev. B* **7**, 4388.
- Kolda, T. G., and B. W. Bader, 2009, *SIAM Rev.* **51**, 455.
- König, R., B. W. Reichardt, and G. Vidal, 2009, *Phys. Rev. B* **79**, 195123.
- Kramers, H. A., 1930, *Proc. K. Ned. Akad. Wet.* **33**, 959.
- Kramers, H. A., and G. H. Wannier, 1941, *Phys. Rev.* **60**, 263.
- Kraus, C. V., N. Schuch, F. Verstraete, and J. I. Cirac, 2010, *Phys. Rev. A* **81**, 052338.

- Kull, I., A. Molnar, E. Zohar, and J. I. Cirac, 2017, *Ann. Phys. (N.Y.)* **386**, 199.
- Kuwahara, T., Álvaro M. Alhambra, and A. Anshu, 2021, *Phys. Rev. X* **11**, 011047.
- Kuwahara, T., and K. Saito, 2020, *Nat. Commun.* **11**, 4478.
- Lahtinen, V., and E. Ardonne, 2015, *Phys. Rev. Lett.* **115**, 237203.
- Landau, L. D., 1937, *Ukr. Phys. J.* **11**, 19.
- Landau, Z., U. Vazirani, and T. Vidick, 2013, [arXiv:1307.5143](https://arxiv.org/abs/1307.5143).
- Lemm, M., and E. Mozgunov, 2019, *J. Math. Phys. (N.Y.)* **60**, 051901.
- Lemm, M., A. W. Sandvik, and L. Wang, 2019, [arXiv:1910.11810](https://arxiv.org/abs/1910.11810).
- Levin, M., 2013, *Phys. Rev. X* **3**, 021009.
- Levin, M., and C. P. Nave, 2007, *Phys. Rev. Lett.* **99**, 120601.
- Levin, M., and X.-G. Wen, 2006, *Phys. Rev. Lett.* **96**, 110405.
- Levin, M. A., and X.-G. Wen, 2005, *Phys. Rev. B* **71**, 045110.
- Li, H., and F. D. M. Haldane, 2008, *Phys. Rev. Lett.* **101**, 010504.
- Liao, H.-J., J.-G. Liu, L. Wang, and T. Xiang, 2019, [arXiv:1903.09650](https://arxiv.org/abs/1903.09650).
- Lieb, E., T. Schultz, and D. Mattis, 1961, *Ann. Phys. (Amsterdam)* **16**, 407.
- Lieb, E. H., and M. B. Ruskai, 1973, *Les rencontres physiciens-mathématiciens de Strasbourg-RCP25* **19**, 36.
- Liu, Y.-K., M. Christandl, and F. Verstraete, 2007, *Phys. Rev. Lett.* **98**, 110503.
- Lootens, L., J. Fuchs, J. Haegeman, C. Schweigert, and F. Verstraete, 2021, *SciPost Phys.* **10**, 53.
- Lootens, L., R. Vanhove, and F. Verstraete, 2019, [arXiv:1907.02520](https://arxiv.org/abs/1907.02520).
- Lou, J., S. Tanaka, H. Katsura, and N. Kawashima, 2011, *Phys. Rev. B* **84**, 245128.
- Maeshima, N., Y. Hieida, Y. Akutsu, T. Nishino, and K. Okunishi, 2001, *Phys. Rev. E* **64**, 016705.
- Majumdar, C. K., and D. Ghosh, 1969, *J. Math. Phys. (N.Y.)* **10**, 1388.
- Maldacena, J., 1999, *Int. J. Theor. Phys.* **38**, 1113.
- Matsui, T., 1998, *Infin. Dimens. Anal. Quantum Probab. Relat. Top.* **01**, 647.
- McCulloch, I. P., 2007, *J. Stat. Mech.* P10014.
- McCulloch, I. P., and M. Gulácsi, 2002, *Europhys. Lett.* **57**, 852.
- Mermin, N. D., and H. Wagner, 1966, *Phys. Rev. Lett.* **17**, 1133.
- Michalakakis, S., and J. Pytel, 2013, *Commun. Math. Phys.* **322**, 277.
- Michalek, M., T. Seynnaeve, and F. Verstraete, 2019, *SIAM J. Matrix Anal. Appl.* **40**, 1125.
- Michalek, M., and Y. Shitov, 2018, [arXiv:1809.04387](https://arxiv.org/abs/1809.04387).
- Milsted, A., and G. Vidal, 2017, *Phys. Rev. B* **96**, 245105.
- Molnar, A., J. Garre-Rubio, D. Perez-Garcia, N. Schuch, and J. I. Cirac, 2018, *New J. Phys.* **20**, 113017.
- Molnar, A., J. Garre-Rubio, D. Perez-Garcia, N. Schuch, and J. I. Cirac, 2021 (to be published).
- Molnar, A., Y. Ge, N. Schuch, and J. I. Cirac, 2018, *J. Math. Phys. (N.Y.)* **59**, 021902.
- Molnar, A., N. Schuch, F. Verstraete, and J. I. Cirac, 2015, *Phys. Rev. B* **91**, 045138.
- Moore, G., and N. Seiberg, 1989, *Commun. Math. Phys.* **123**, 177.
- Movassagh, R., and P. W. Shor, 2016, *Proc. Natl. Acad. Sci. U.S.A.* **113**, 13278.
- Müger, M., 2003a, *J. Pure Appl. Algebra* **180**, 81.
- Müger, M., 2003b, *J. Pure Appl. Algebra* **180**, 159.
- Murg, V., F. Verstraete, Ö. Legeza, and R. M. Noack, 2010, *Phys. Rev. B* **82**, 205105.
- Nachtergaele, B., 1996, *Commun. Math. Phys.* **175**, 565.
- Nachtergaele, B., and R. Sims, 2006, *Commun. Math. Phys.* **265**, 119.
- Nachtergaele, B., and R. Sims, 2010, in *Entropy and the Quantum*, Contemporary Math Vol. 529, edited by R. Sims and D. Ueltschi (American Mathematical Society, Providence), p. 141.
- Nachtergaele, B., R. Sims, and A. Young, 2020, [arXiv:2010.15337](https://arxiv.org/abs/2010.15337).
- Nandkishore, R., and D. A. Huse, 2015, *Annu. Rev. Condens. Matter Phys.* **6**, 15.
- Nielsen, A. E., J. I. Cirac, and G. Sierra, 2012, *Phys. Rev. Lett.* **108**, 257206.
- Nielsen, A. E. B., G. Sierra, and J. I. Cirac, 2013, *Nat. Commun.* **4**, 2864.
- Nielsen, M. A., and I. A. Chuang, 2000, *Quantum Computation and Quantum Information* (Cambridge University Press, Cambridge, England).
- Niggemann, H., A. Klümper, and J. Zittartz, 1997, *Z. Phys. B* **104**, 103.
- Nishino, T., 2010, <http://quattro.phys.sci.kobe-u.ac.jp/dmrg/condmat91.html>.
- Nishino, T., and K. Okunishi, 1996, *J. Phys. Soc. Jpn.* **65**, 891.
- Nishino, Y., N. Maeshima, A. Gendiar, and T. Nishino, 2004, [arXiv:cond-mat/0401115](https://arxiv.org/abs/cond-mat/0401115).
- Ogata, Y., 2016a, *Commun. Math. Phys.* **348**, 847.
- Ogata, Y., 2016b, *Commun. Math. Phys.* **348**, 897.
- Ogata, Y., 2017, *Commun. Math. Phys.* **352**, 1205.
- Orus, R., 2014, *Ann. Phys. (Amsterdam)* **349**, 117.
- Orus, R., J. I. Latorre, J. Eisert, and M. Cramer, 2006, *Phys. Rev. A* **73**, 060303.
- Osborne, T. J., 2007, *Phys. Rev. A* **75**, 042306.
- Osborne, T. J., J. Eisert, and F. Verstraete, 2010, *Phys. Rev. Lett.* **105**, 260401.
- Oseledets, I. V., 2011, *SIAM J. Sci. Comput.* **33**, 2295.
- Oshikawa, M., M. Yamanaka, and I. Affleck, 1997, *Phys. Rev. Lett.* **78**, 1984.
- Östlund, S., and S. Rommer, 1995, *Phys. Rev. Lett.* **75**, 3537.
- Pastawski, F., B. Yoshida, D. Harlow, and J. Preskill, 2015, *J. High Energy Phys.* **06**, 149.
- Perez-Garcia, D., and A. Pérez-Hernández, 2020, [arXiv:2004.10516](https://arxiv.org/abs/2004.10516).
- Perez-Garcia, D., M. Sanz, C. E. Gonzalez-Guillen, M. M. Wolf, and J. I. Cirac, 2010, *New J. Phys.* **12**, 025010.
- Perez-Garcia, D., F. Verstraete, J. I. Cirac, and M. M. Wolf, 2008, *Quantum Inf. Comput.* **8**, 0650.
- Perez-Garcia, D., F. Verstraete, M. M. Wolf, and J. I. Cirac, 2007, *Quantum Inf. Comput.* **7**, 401.
- Perez-Garcia, D., M. Wolf, M. Sanz, F. Verstraete, and J. Cirac, 2008, *Phys. Rev. Lett.* **100**, 167202.
- Peschel, I., M. Kaulke, and Ö. Legeza, 1999, *Ann. Phys. (Berlin)* **8**, 153.
- Pfeifer, R. N., G. Evenbly, and G. Vidal, 2009, *Phys. Rev. A* **79**, 040301.
- Piroli, L., A. Turzillo, S. Shukla, and J. I. Cirac, 2020, [arXiv:2007.11905](https://arxiv.org/abs/2007.11905).
- Pirvu, B., J. Haegeman, and F. Verstraete, 2012, *Phys. Rev. B* **85**, 035130.
- Pirvu, B., V. Murg, J. I. Cirac, and F. Verstraete, 2010, *New J. Phys.* **12**, 025012.
- Plenio, M. B., J. Eisert, J. Dreissig, and M. Cramer, 2005, *Phys. Rev. Lett.* **94**, 060503.
- Poiblanc, D., 2017, *Phys. Rev. B* **96**, 121118.
- Poiblanc, D., J. I. Cirac, and N. Schuch, 2015, *Phys. Rev. B* **91**, 224431.
- Poiblanc, D., N. Schuch, and I. Affleck, 2016, *Phys. Rev. B* **93**, 174414.
- Pollmann, F., E. Berg, A. M. Turner, and M. Oshikawa, 2012, *Phys. Rev. B* **85**, 075125.

- Pollmann, F., and A. M. Turner, 2012, *Phys. Rev. B* **86**, 125441.
- Pollmann, F., A. M. Turner, E. Berg, and M. Oshikawa, 2010, *Phys. Rev. B* **81**, 064439.
- Pomata, N., and T.-C. Wei, 2019, [arXiv:1911.01410](https://arxiv.org/abs/1911.01410).
- Porras, D., F. Verstraete, and J. I. Cirac, 2006, *Phys. Rev. B* **73**, 014410.
- Qi, X.-L., H. Katsura, and A. W. W. Ludwig, 2012, *Phys. Rev. Lett.* **108**, 196402.
- Qi, X.-L., and Z. Yang, 2018, [arXiv:1801.05289](https://arxiv.org/abs/1801.05289).
- Qi, X.-L., Z. Yang, and Y.-Z. You, 2017, *J. High Energy Phys.* **08**, 060.
- Rader, M., and A. M. Läuchli, 2018, *Phys. Rev. X* **8**, 031030.
- Raggio, G., and R. Werner, 1989, *Helv. Phys. Acta* **62**, 980.
- Rahaman, M., 2018, [arXiv:1807.06872](https://arxiv.org/abs/1807.06872).
- Rams, M. M., V. Zauner, M. Bal, J. Haegeman, and F. Verstraete, 2015, *Phys. Rev. B* **92**, 235150.
- Raussendorf, R., and H. J. Briegel, 2001, *Phys. Rev. Lett.* **86**, 5188.
- Read, N., 2017, *Phys. Rev. B* **95**, 115309.
- Richter, S., 1994, Ph.D. thesis (Universität Osnabrück).
- Rispler, M., K. Duivenvoorden, and N. Schuch, 2015, *Phys. Rev. B* **92**, 155133.
- Rispler, M., K. Duivenvoorden, and N. Schuch, 2017, *J. Phys. A* **50**, 365001.
- Rommer, S., and S. Östlund, 1997, *Phys. Rev. B* **55**, 2164.
- Şahinoğlu, M. B., S. K. Shukla, F. Bi, and X. Chen, 2018, *Phys. Rev. B* **98**, 245122.
- Şahinoğlu, M. B., D. Williamson, N. Bultinck, M. Marien, J. Haegeman, N. Schuch, and F. Verstraete, 2021, *Ann. Inst. Henri Poincaré* **22**, 563.
- Sanz, M., D. Perez-Garcia, M. M. Wolf, and J. I. Cirac, 2010, *IEEE Trans. Inf. Theory* **56**, 4668.
- Sanz, M., M. M. Wolf, D. Perez-Garcia, and J. I. Cirac, 2009, *Phys. Rev. A* **79**, 042308.
- Scarpa, G., A. Molnar, Y. Ge, J. J. Garcia-Ripoll, N. Schuch, D. Perez-Garcia, and S. Iblisdir, 2020, *Phys. Rev. Lett.* **125**, 210504.
- Schollwöck, U., 2005, *Rev. Mod. Phys.* **77**, 259.
- Schollwöck, U., 2011, *Ann. Phys. (Amsterdam)* **326**, 96.
- Schön, C., E. Solano, F. Verstraete, J. I. Cirac, and M. M. Wolf, 2005, *Phys. Rev. Lett.* **95**, 110503.
- Schuch, N., I. Cirac, and D. Perez-Garcia, 2010, *Ann. Phys. (Amsterdam)* **325**, 2153.
- Schuch, N., I. Cirac, and F. Verstraete, 2008, *Phys. Rev. Lett.* **100**, 250501.
- Schuch, N., D. Perez-Garcia, and I. Cirac, 2011, *Phys. Rev. B* **84**, 165139.
- Schuch, N., D. Poilblanc, J. I. Cirac, and D. Perez-Garcia, 2012, *Phys. Rev. B* **86**, 115108.
- Schuch, N., D. Poilblanc, J. I. Cirac, and D. Perez-Garcia, 2013, *Phys. Rev. Lett.* **111**, 090501.
- Schuch, N., and F. Verstraete, 2017, [arXiv:1711.06559](https://arxiv.org/abs/1711.06559).
- Schuch, N., M. M. Wolf, and J. I. Cirac, 2008, in *Quantum Information and Many Body Quantum Systems*, edited by M. Ericsson and S. Montangero (Scuola Normale Superiore, Pisa).
- Schuch, N., M. M. Wolf, F. Verstraete, and J. I. Cirac, 2007, *Phys. Rev. Lett.* **98**, 140506.
- Schuch, N., M. M. Wolf, F. Verstraete, and J. I. Cirac, 2008, *Phys. Rev. Lett.* **100**, 030504.
- Shavitt, I., and R. J. Bartlett, 2009, *Many-Body Methods in Chemistry and Physics: MBPT and Coupled-Cluster Theory*, Cambridge Molecular Science (Cambridge University Press, Cambridge, England).
- Shi, Y.-Y., L.-M. Duan, and G. Vidal, 2006, *Phys. Rev. A* **74**, 022320.
- Shukla, S. K., M. Burak Şahinoğlu, F. Pollmann, and X. Chen, 2018, *Phys. Rev. B* **98**, 125112.
- Sierra, G., and M. Martin-Delgado, 1998, [arXiv:cond-mat/9811170](https://arxiv.org/abs/cond-mat/9811170).
- Silvi, P., V. Giovannetti, S. Montangero, M. Rizzi, J. I. Cirac, and R. Fazio, 2010, *Phys. Rev. A* **81**, 062335.
- Singh, S., R. N. C. Pfeifer, and G. Vidal, 2010, *Phys. Rev. A* **82**, 050301.
- Stinespring, W. F., 1955, *Proc. Am. Math. Soc.* **6**, 211.
- Stojevic, V., J. Haegeman, I. McCulloch, L. Tagliacozzo, and F. Verstraete, 2015, *Phys. Rev. B* **91**, 035120.
- Stoudenmire, E., and D. J. Schwab, 2016, in *Proceedings of the 30th Annual Conference on Neural Information Processing Systems (NIPS 2016), Barcelona*, edited by D. D. Lee, U. von Luxburg, R. Garnett, M. Sugiyama, and I. Guyon (Curran Associates, Red Hook, NY), pp. 4799–4807.
- Su, W., J. Schrieffer, and A. J. Heeger, 1979, *Phys. Rev. Lett.* **42**, 1698.
- Swingle, B., 2012, *Phys. Rev. D* **86**, 065007.
- Szalay, S., M. Pfeffer, V. Murg, G. Barcza, F. Verstraete, R. Schneider, and Ö. Legeza, 2015, *Int. J. Quantum Chem.* **115**, 1342.
- Szehr, O., and M. M. Wolf, 2015, *J. Stat. Phys.* **159**, 752.
- Szehr, O., and M. M. Wolf, 2016, *J. Math. Phys. (N.Y.)* **57**, 081901.
- Tagliacozzo, L., T. R. De Oliveira, S. Iblisdir, and J. Latorre, 2008, *Phys. Rev. B* **78**, 024410.
- Terhal, B. M., 2004, *IBM J. Res. Dev.* **48**, 71.
- Terhal, B. M., 2015, *Rev. Mod. Phys.* **87**, 307.
- Tilloy, A., and J. I. Cirac, 2019, *Phys. Rev. X* **9**, 021040.
- Tu, H.-H., A. E. Nielsen, J. I. Cirac, and G. Sierra, 2014, *New J. Phys.* **16**, 033025.
- Tuybens, B., J. De Nardis, J. Haegeman, and F. Verstraete, 2020, [arXiv:2006.01801](https://arxiv.org/abs/2006.01801).
- Van Acoleyen, K., A. Hallam, M. Bal, M. Hauru, J. Haegeman, and F. Verstraete, 2020, *Phys. Rev. B* **102**, 165131.
- Vanderstraeten, L., J. Haegeman, P. Corboz, and F. Verstraete, 2016, *Phys. Rev. B* **94**, 155123.
- Vanderstraeten, L., J. Haegeman, and F. Verstraete, 2018, [arXiv:1810.07006](https://arxiv.org/abs/1810.07006).
- Vanhecke, B., J. Haegeman, K. Van Acoleyen, L. Vanderstraeten, and F. Verstraete, 2019, *Phys. Rev. Lett.* **123**, 250604.
- Vanhecke, B., M. Van Damme, L. Vanderstraeten, and F. Verstraete, 2019, [arXiv:1912.10512](https://arxiv.org/abs/1912.10512).
- Vanhove, R., M. Bal, D. J. Williamson, N. Bultinck, J. Haegeman, and F. Verstraete, 2018, *Phys. Rev. Lett.* **121**, 177203.
- Verstraete, F., J. Cirac, J. Latorre, E. Rico, and M. Wolf, 2005, *Phys. Rev. Lett.* **94**, 140601.
- Verstraete, F., and J. I. Cirac, 2004a, [arXiv:cond-mat/0407066](https://arxiv.org/abs/cond-mat/0407066).
- Verstraete, F., and J. I. Cirac, 2004b, *Phys. Rev. A* **70**, 060302.
- Verstraete, F., and J. I. Cirac, 2006, *Phys. Rev. B* **73**, 094423.
- Verstraete, F., and J. I. Cirac, 2010, *Phys. Rev. Lett.* **104**, 190405.
- Verstraete, F., J. J. Garcia-Ripoll, and J. I. Cirac, 2004, *Phys. Rev. Lett.* **93**, 207204.
- Verstraete, F., M. A. Martin-Delgado, and J. I. Cirac, 2004, *Phys. Rev. Lett.* **92**, 087201.
- Verstraete, F., V. Murg, and J. I. Cirac, 2008, *Adv. Phys.* **57**, 143.
- Verstraete, F., M. Popp, and J. I. Cirac, 2004, *Phys. Rev. Lett.* **92**, 027901.
- Verstraete, F., D. Porras, and J. I. Cirac, 2004, *Phys. Rev. Lett.* **93**, 227205.
- Verstraete, F., M. M. Wolf, D. Perez-Garcia, and J. I. Cirac, 2006, *Phys. Rev. Lett.* **96**, 220601.
- Vidal, G., 2003, *Phys. Rev. Lett.* **91**, 147902.
- Vidal, G., 2007a, *Phys. Rev. Lett.* **98**, 070201.
- Vidal, G., 2007b, *Phys. Rev. Lett.* **99**, 220405.

- Vidal, G., 2008, *Phys. Rev. Lett.* **101**, 110501.
- Wahl, T. B., S. T. Haßler, H.-H. Tu, J. I. Cirac, and N. Schuch, 2014, *Phys. Rev. B* **90**, 115133.
- Wahl, T. B., A. Pal, and S. H. Simon, 2017, *Phys. Rev. X* **7**, 021018.
- Wahl, T. B., H.-H. Tu, N. Schuch, and J. I. Cirac, 2013, *Phys. Rev. Lett.* **111**, 236805.
- Weichselbaum, A., 2012, *Ann. Phys. (N.Y.)* **327**, 2972.
- Wen, X.-G., 2004, *Quantum Field Theory of Many Body Systems* (Oxford University Press, New York).
- Wen, X.-G., 2017, *Rev. Mod. Phys.* **89**, 041004.
- White, S. R., 1992, *Phys. Rev. Lett.* **69**, 2863.
- White, S. R., 1993, *Phys. Rev. B* **48**, 10345.
- White, S. R., and A. E. Feiguin, 2004, *Phys. Rev. Lett.* **93**, 076401.
- White, S. R., and R. L. Martin, 1999, *J. Chem. Phys.* **110**, 4127.
- Williamson, D. J., N. Bultinck, M. Marien, M. B. Sahinoglu, J. Haegeman, and F. Verstraete, 2016, *Phys. Rev. B* **94**, 205150.
- Williamson, D. J., N. Bultinck, and F. Verstraete, 2017, *arXiv*: 1711.07982.
- Wilson, K. G., 1975, *Rev. Mod. Phys.* **47**, 773.
- Witten, E., 1989, *Commun. Math. Phys.* **121**, 351.
- Wolf, M. M., 2006, *Phys. Rev. Lett.* **96**, 010404.
- Wolf, M. M., 2012, lecture notes, <https://www-m5.ma.tum.de/foswiki/pub/M5/Allgemeines/MichaelWolf/QChannelLecture.pdf>.
- Wolf, M. M., and J. I. Cirac, 2008, *Commun. Math. Phys.* **279**, 147.
- Wolf, M. M., F. Verstraete, M. B. Hastings, and J. I. Cirac, 2008, *Phys. Rev. Lett.* **100**, 070502.
- Xie, Z. Y., J. Chen, J. F. Yu, X. Kong, B. Normand, and T. Xiang, 2014, *Phys. Rev. X* **4**, 011025.
- Xie, Z.-Y., J. Chen, M.-P. Qin, J. W. Zhu, L.-P. Yang, and T. Xiang, 2012, *Phys. Rev. B* **86**, 045139.
- Xie, Z.-Y., H.-C. Jiang, Q. N. Chen, Z.-Y. Weng, and T. Xiang, 2009, *Phys. Rev. Lett.* **103**, 160601.
- Yang, S., Z.-C. Gu, and X.-G. Wen, 2017, *Phys. Rev. Lett.* **118**, 110504.
- Yang, S., L. Lehman, D. Poilblanc, K. V. Acoleyen, F. Verstraete, J. Cirac, and N. Schuch, 2014, *Phys. Rev. Lett.* **112**, 036402.
- Yang, S., T. B. Wahl, H.-H. Tu, N. Schuch, and J. I. Cirac, 2015, *Phys. Rev. Lett.* **114**, 106803.
- Zaletel, M. P., and R. S. Mong, 2012, *Phys. Rev. B* **86**, 245305.
- Zaletel, M. P., R. S. Mong, and F. Pollmann, 2013, *Phys. Rev. Lett.* **110**, 236801.
- Zaletel, M. P., R. S. Mong, F. Pollmann, and E. H. Rezayi, 2015, *Phys. Rev. B* **91**, 045115.
- Zauner, V., D. Draxler, L. Vanderstraeten, M. Degroote, J. Haegeman, M. M. Rams, V. Stojevic, N. Schuch, and F. Verstraete, 2015, *New J. Phys.* **17**, 053002.
- Zauner, V., D. Draxler, L. Vanderstraeten, J. Haegeman, and F. Verstraete, 2016, *New J. Phys.* **18**, 113033.
- Zauner-Stauber, V., L. Vanderstraeten, J. Haegeman, I. McCulloch, and F. Verstraete, 2018, *Phys. Rev. B* **97**, 235155.
- Zeng, B., X. Chen, D.-L. Zhou, and X.-G. Wen, 2019, *Quantum Information Meets Quantum Matter: From Quantum Entanglement to Topological Phases of Many-Body Systems* (Springer, New York).
- Zhang, Y., T. Grover, A. Turner, M. Oshikawa, and A. Vishwanath, 2012, *Phys. Rev. B* **85**, 235151.
- Zhang, Z., A. Ahmadain, and I. Klich, 2017, *Proc. Natl. Acad. Sci. U.S.A.* **114**, 5142.
- Zhao, H.-H., Z.-Y. Xie, Q. N. Chen, Z.-C. Wei, J. W. Cai, and T. Xiang, 2010, *Phys. Rev. B* **81**, 174411.
- Zhou, Z., J. Wildeboer, and A. Seidel, 2014, *Phys. Rev. B* **89**, 035123.
- Zou, Y., M. Ganahl, and G. Vidal, 2019, *arXiv*:1906.04218.
- Zou, Y., A. Milsted, and G. Vidal, 2018, *Phys. Rev. Lett.* **121**, 230402.
- Zwolak, M., and G. Vidal, 2004, *Phys. Rev. Lett.* **93**, 207205.